HUMAN SKIN DRUG DELIVERY USING BIODEGRADABLE PLGA – NANOPARTICLES

Dissertation
zur Erlangung des Grades
des Doktors der Naturwissenschaften
der Naturwissenschaftlich-Technischen Fakultät III
Chemie, Pharmazie, Bio- und Werkstoffwissenschaften
der Universität des Saarlandes

von

Javiana Elizabeth Luengo Contreras

Saarbrücken

2007

Tag des Kolloquiums : 30. April 2007

Dekan   : Prof. Dr. Uli Müller

Vorsitzender   : Prof. Dr. Hans H. Maurer

Berichterstatter   : Prof. Dr. Claus-Michael Lehr

                               Prof. Dr. Rolf Hempelmann

Akad. Mitarbeiter   : Dr. Ulrich F. Schäfer

TABLE OF CONTENTS

CHAPTER 3: MECHANISM OF IMPROVEMENT OF TRANSDERMAL
DELIVERY BY PLGA NANOPARTICLES 55

iv

SHORT SUMMARY

During the last years transdermal drug delivery has gained increasing interest due to the high acceptance of patients. However the major problem of drug delivery via the cutaneous route are the barrier properties of the skin which are located in the stratum corneum. To study the potential of polymeric biodegradable nanocarriers on drug delivery to and through the skin the well known biodegradable copolymer poly(D,L-lactide-*co*-glycolide) (PLGA 50:50) was used as main component of the carrier system. As model drug flufenamic acid, an antiinflamatory drug, was incorporated. Nanoparticles in the size range of 200 to 400 nm were prepared by means of a solvent extraction technique. *In vitro* skin transport experiments using Franz diffusion cell systems and the Saarbrücken model showed an enhancement effect for encapsulated flufenamic acid independent of particle size. Surprisingly, also the presence of drug-free nanoparticles in a preparation (hydrogel) with flufenamic acid in solution has also increased the permeated amount of drug. As mechanism of action an acidic nano-environment around the particles could be identified by confocal laser scanning microscopy and permeation experiments using buffered and non-buffered preparations. Other studies have shown that nanoparticles were able to penetrate into the hair follicles when massage was used. These results underscore the potential of polymeric biodegradable nanoparticles as carriers for transdermal drug delivery. Especially, the acidic pH of the nano-environment of the particles might be an advantage to develop special formulations designed for acidic drugs or might be used to re-establish the physiological acidic pH on the skin surface.

KURZZUSAMMENFASSUNG

Infolge der hohen Akzeptanz bei Patienten hat die transdermale Applikation von Arzneistoffen mittels Trägersystemen in den letzten Jahren zunehmend an Bedeutung gewonnen. Für die kutane Arzneistoffinvasion stellen jedoch die Barriereeigenschaften der Haut, welche im Stratum corneum lokalisiert sind, ein großes Problem dar. Um das Potential polymerer, bioabbaubarer und nano-partikulärer Trägersysteme auf die Arzneistoffinvasion in und durch die Haut zu untersuchen, wurde das schon ausführlich charakterisierte sowie bioabbaubare Copolymer Poly-(D,L-lactide-co-glycolide) (PLGA 50:50) als Trägermaterial eingesetzt. Als Modellarzneistoff wurde Flufenaminsäure, eine antiinflamatorisch wirksame Substanz, in die Nanopartikel inkoorperiert. Unter Verwendung der „Lösungsmittel Extraktions Technik" wurden Partikel im Größenbereich von 200 bis 400 nm hergestellt. Durch in vitro Experimente mit Franz-Diffusionszellen und dem Saarbruecker-Penetrationsmodell konnte gezeigt werden, dass, unabhängig von der Partikelgröße, der Arzneistofftransport verkapselter Flufenaminsäure in bzw. durch die Haut erhöht war. Überraschender Weise konnte bei Zugabe arzneistofffreier Nanopartikel in eine Zubereitung (Hydro-Gel) welche Flufenaminsäure in gelöster Form enthielt ebenfalls eine erhöhte Arzneistoffpermeation beobachtet werden. Mittels Konfokaler Mikroskopie und Permeationsexperimenten wurde als Wirkungsmechanismus, sowohl für gepufferte als auch für ungepufferte Präparationen, ein saurer pH-Wert im Nanometerbereich um die Partikel herum nachgewiesen. Des weiteren konnte gezeigt werden, daß Nanopartikel unter Anwendung einer Massage in Haarfollikel penetrieren. Die Ergebnisse unterstreichen das Potential polymerer, bioabbaubarer Nanopartikel als Trägersysteme für die transdermale Anwendung. Insbesondere der saure pH-Wert im Nanometerbereich um die Partikel könnte Vorteile für die Entwicklung spezieller Formulierungen für saure Arzneistoffe bieten. Weiterhin wäre auch eine mögliche Applikation zur Wiederherstellung des physiologischen, leicht sauren pH-Wertes der Hautoberfläche im Fall pathophysiologischer Veränderungen denkbar.

CHAPTER 1: GENERAL INTRODUCTION

Sections of this chapter:

- Have been submitted for publication as part of the book chapter entitled "Models for skin absorption and skin toxicity testing", Preclinical Biopharmaceutics - *in situ*, *in vitro*, and *in silico* tools for drug absorption studies, Springer (in preparation)

- Will be submitted as part of the review article entitled "Nanoparticles – present and future as drug delivery systems to the skin", European Journal of Pharmaceutics and Biopharmaceutics (in preparation).

1.1. THE DERMAL BARRIER

The skin, in Latin called *cutis*, is considered the largest organ of the body, accounting more than 10% of the body mass and having an average surface of approximately 2 m^2. This organ enables the body to interact most intimately and dynamically with the environment. The functions of the skin are considered essential for the survival of the human beings in a relatively aggressive environment, providing a multifunctional interface between the body and the surrounding media. These functions have been classified as protective, homeostatic, or sensorial. The first two mentioned are mainly function of its barrier properties, allowing the survival of humans among changes in environmental temperature, relative humidity, dangerous substances such as chemicals, bacteria, allergens, radiation, etc. To maintain its characteristics, this organ is in a continual renewing process [1]. Due to its barrier properties, the skin membrane is equally capable at limiting the molecular transport from and into the body. Overcoming this barrier function will be the purpose of transdermal drug delivery.

In order to understand the biopharmaceutical effects of dermatological formulations, it is necessary to know the anatomy, physiology and chemical composition of the skin.

Anatomically, the skin consists on 4 basic layers: the stratum corneum (nonviable epidermis), viable epidermis, dermis and subcutaneous tissues (Figure 1). In addition to these structures, there are also several associated appendages: hair follicles, sweat glands, apocrine glands, and nails.

The **subcutaneous tissues**, the innermost layer, is characterized by a fibrous connective structure, which is composed mainly by elastic fibres and fat. This layer acts as insulator, shock absorber, and reserve depot of calories and supplier of nutrients for the more superficial skin layers. On its domain are found the base of the hair follicles, the secretory portion of the sweat glands, the cutaneous nerves as well as networks of lymph and blood vessels.
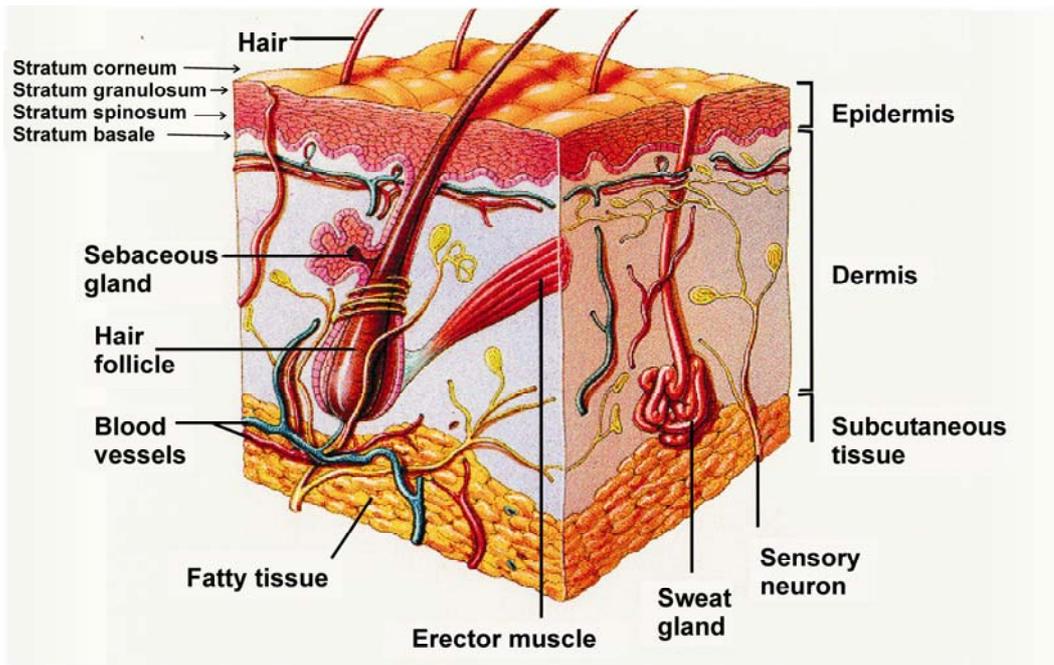
Figure 1: Structure of the human skin[1]

The **dermis** is a fibrous layer that supports and strengthens the epidermis. Its thickness varies from 2-3 mm. It consists of a matrix of loose connective tissue composed by collagen, a fibrous protein, embedded in a semigel matrix, which contains water, ions and mucopolysaccharides. This matrix helps to hold the cells and allows the oxygen and nutrients to diffuse to the epidermal cells. This layer contains an extensive blood vessel and nervous network, as well as hair follicles, sebum and sweat glands. The most adjacent layer of the dermis, called papillary layer, provides the nutritional support to the viable epidermis. The papillary layer plays no only a nutritional function but also a role in the temperature, pressure and pain regulation. In addition, it contains a sparse cell population: fibroblasts, responsible for the connective tissue synthesis; mast cells, which are involved in the immune and inflammatory responses; and melanocytes, involved in the production of melanin.

---

[1] Modified from the source http://www.agen.ufl.edu/~chyn/age2062/lect/lect_19/lect_19.htm, 14.02.2007

The **viable epidermis** consists of several cell strata varying in the differentiation level. From the bottom, the stratum basale is composed of two keratinocyte types, one that acts as stem cells having a proliferation capacity, and the second one which serves as anchor to the basement membrane. It contains as well: Merkel cells, Langerhans cells and melanocytes.

During the differentiation process the epidermal layers (stratum spinosum, granulosum, lucidum and corneum) are converted to corneocytes. Herein cellular changes includes the extrusion of lamellar bodies, loss of the nucleus and an increase in the keratin amount until the stratum corneum is formed [1, 2].

The **stratum corneum** (SC), the outermost layer of the epidermis, also called non viable epidermis, has an approximately thickness of 10 – 20 µm that can vary from one body site to the other. It consists, in a given cross-section, of 15 – 25 flattened, stacked, hexagonal, and cornified cells (corneocytes, also called horny cells) anchored in a mortar of highly organized intercellular lipids. This structure has been described as brick and mortar model (Figure 2) and is considered the rate controlling barrier in the transdermal absorption of substances. Each corneocyte is approximately 40 µm in diameter and 0.5 µm thick, and it is composed mainly of insoluble bundled keratins (approx. 70%) and lipid (~20%) located in the cell envelope. The intercellular matrix consists of lipids and desmosomes for the corneocyte cohesion [1]. The lipids of this area are distinctive in many respects: (i) they provide the only continuous phase (diffusion pathway) from the skin surface to the base of the SC; (ii) its composition (mainly ceramides, free fatty acids and cholesterol) is unique among biological membranes and particularly noteworthy is the absence of phospholipids; (iii) despite this deficit of phospholipids, polar bilayer-forming lipids, the SC lipids exist as multilamellar sheets; and (iv) the predominantly saturated, long-chain hydrocarbon tails facilitate a highly ordered, interdigitated configuration (Figure 2). The staggered corneocyte arrangement in a lipid matrix is suggested to provide a highly tortuous lipoidal diffusion pathway

rendering the membrane 1000 times less permeable to water relative to other biological

membranes Due to the continuous phase, the intercellular lipid layer is considered the

most important transdermal absorption pathway for small substances [3]. The turnover of

the complete SC layer occurs once every 2 – 3 weeks [1].
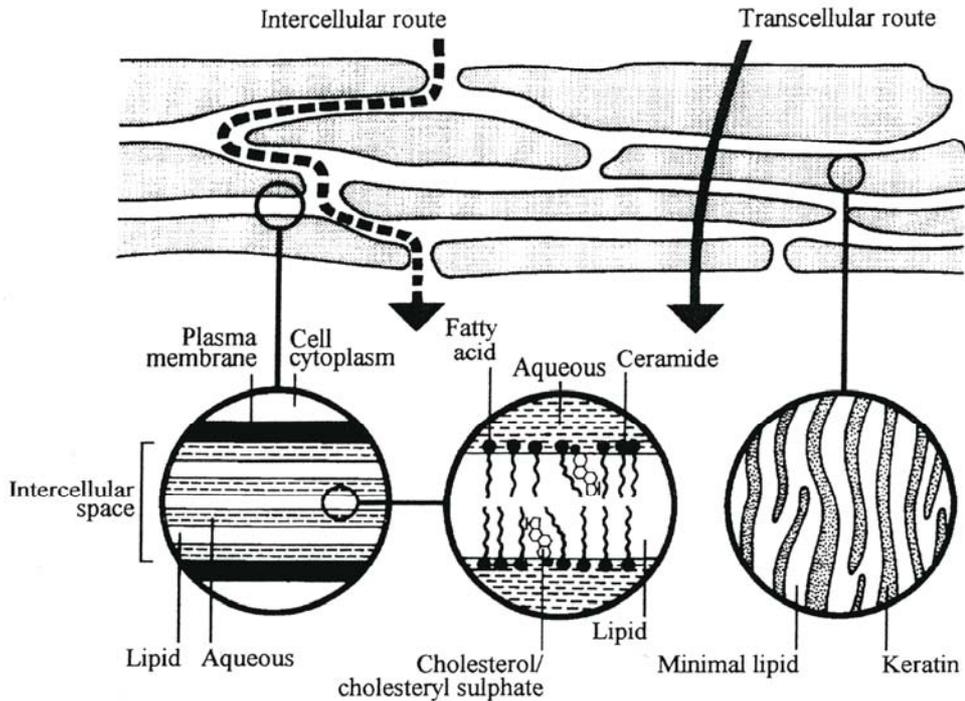
Figure 2: Schematic representation of the "brick and mortar" model of the stratum corneum, lipid bilayer organisation and possible pathways [2]

The SC by its composition and structure is considered to act as the main barrier

for the exchange of substances between the body and the environment. And therefore

became the real challenge on drug delivery into and through the skin. Moreover, this

anatomical barrier is accompanied by the intracutaneous metabolism, a high drainage

rate due to blood and lymph capillary present in the dermis and a peripheral immune

system [4].

---

[2] Reprinted from International Journal of Pharmaceutics, Vol. 131, Moghimi HR, Williams AC, Barry BW, A lamellar matrix model for stratum corneum intercellular lipids II. Effect of geometry of the stratum corneum on permeation of model drugs 5-fluorouracil and oestradiol, p119, Copyright 1996, with permission from Elsevier.

1.2. TRANSDERMAL DRUG DELIVERY

During the last years, developments in transdermal drug delivery have been incremented focusing mainly on overcoming problems associated with the skin barrier properties. Nevertheless, the transdermal delivery offers several advantages: the skin represents a relatively large and readily accessible surface area for absorption, the application is a non-invasive procedure that allows a continuous intervention, and it is possible to cease the absorption preventing overdose or undesirable effects. Compared with the traditional oral administration route, transdermal delivery shows additional advantages: it minimize the first-pass metabolism, it avoids drug degradation under the extreme acidity of the stomach, it prevents erratic delivery due to food interactions, and it provides more controlled delivery. Among its major disadvantages are: not all compounds are suitable for transport across the skin, there are different permeation rates depending on age, race, site of application and individuals, and also skin diseases can influence it [5, 6].

The goal of the transdermal administration of drugs is not to achieve a bolus-type drug input; rather, it is usually designed to offer a slow, sustained release of drug over long periods of time. Current transdermal delivery systems, as transdermal occlusive patches, are capable to deliver drugs in cases that oral administration is limited by poor bioavailability, side effects associated with high peak plasma concentrations or poor compliance due to the need of frequent administration [3, 7].

The criteria that merit consideration in transdermal delivery of drugs are: the nature of the barrier (discussed in the previous section), the balance between physicochemical properties of the membrane and the drug, and the technologies available to facilitate the transdermal transport.

Under normal conditions, there are three pathways postulated for the absorption of substances through the SC: transcellular, intercellular (paracellular) (Figure 2) and transappendageal [5]. The predominant route of transdermal penetration of the majority

of the applied drugs is through intercellular spaces; therefore, the transdermal pathway is much longer than the normal stratum corneum thickness (~20 μm) which was estimated as long as 500 μm. If the transcellular pathway is predominant, the diffusion involves several partitioning steps into the lipo- and hydrophilic domains of the corneocytes and the lipid layers before reaching the viable epidermis [8]. The transdermal absorption process requires drug characteristics or an appropriate carrier which should be able to deliver the drug to the desired skin deepness to reach topical or systemic effects.

In general the barrier limitations imposes that the drug chosen for transdermal delivery should be pharmacologically potent and has physicochemical characteristics which allow it to cross the main barrier, the stratum corneum. Among these requirements are: the drug must possess both lipoidal and aqueous solubility, which promote its permeation through the domains of the stratum corneum, i.e. and appropriate partition coefficient ($K_{O/W}$ ~ 1-3) to have an optimum absorption ; the drug mobility must be high, i.e. molecular weight and volume must be appropriate to facilitate its diffusion through the lipid bilayer. The permeation through the skin will also depend on the ionization degree of the drug at physiological and formulation pH, influencing as well its solubility and partition behaviour [3, 4, 8, 9].

A good transdermal delivery system must not only provide an adequate drug release from the formulation, but also allow considerable amounts of drug to overcome the skin barrier, ensure a non-irritancy of the skin, and also ensure that the drug will not be inactivated on the skin's surface or during the permeation process [10].

1.2.1. Strategies to overcome the epidermal barrier

Since several years, researchers have been working on the development of new strategies to improve the delivery of drugs through the skin. These could be separated in physical and chemical methods.

Physical enhancement methods

♦ *Iontophoresis*, which involves the use of low current via an electrode in contact with the skin, inducing the drug delivery promotion through ion repulsion, decrease on the resistance of the skin and electroosmosis in case of large molecules.

♦ *Electroporation* that uses the application of high voltage impulses during a very short time to create temporary pores on the skin, the driving force of the drug permeation is the ion repulsion or the electroosmosis.

♦ *Sonophoresis* uses low frequency ultrasonic energy to disrupt the lipid packing in the SC creating aqueous pores which improve the drug delivery.

♦ *Local thermal treatments* [4, 11].

♦ Mechanical perforation of the SC by *high-velocity particles* (ballistic) [11].

♦ *Micro-needles array* inducing the temporary loose of the barrier properties until the layer is recovered by the normal turnover cycle, as well as local thermal treatments have been used to deliver drugs [12].

Drug delivery systems

♦ Lipidic flexible particles as *liposomes, niosomes, ethosomes and transferosomes.*

♦ *Solid lipid nanoparticles and nanostructured lipid carriers*

♦ *Solid polymeric nanoparticles,* of biodegradable and non-biodegradable characteristics [11]

Chemical enhancement methods

♦ Increasing the *hydration* state of the SC by a high water content in the formulation or by occlusion (which prevents the trans-epidermal water loss from the tissue), some examples of this effect are given by patches and ointments, but tissue over-hydration is not a general rule for penetration enhancement;

♦ *enhancers* which disrupt the lipid organization in the SC such as azone, terpenes, fatty acids, dimethylsulphoxide (DMSO) and alcohols;

♦ compounds able to alter the protein organization in the SC, such as DMSO or urea;

♦ compounds which increase the solubility of the drug within the SC, e.g. Transcutol® P.

The enhancement effect can also act indirectly, for example:

♦ modifying the thermodynamic activity of the drug in the formulation at the moment of the application, e.g. ethanol;

♦ solubilizing the drug in the donor, in case of poor soluble substances, e.g. surfactants.

The main disadvantage of the chemical penetration enhancers is that most of them induce irritation or sensitation, cause damage and reduce the barrier function for a longer time. These conditions are not desirable in the process of transdermal drug administration [11, 13]

1.3. SELECTED DRUG CARRIER SYSTEMS FOR DERMAL DELIVERY

1.3.1. Solid nanocarriers in transdermal drug delivery

During the last decades, the study of inorganic and colloidal particles such as nanocapsules, nanospheres, nanostructured lipid carrier, etc. has been focused as dermal/transdermal drug delivery carriers. Some of them will be addressed in detail in the following section.

In general, solid colloidal nano-carriers systems have been extensively studied as drug delivery systems (DDS), mostly for oral and parenteral applications, and have shown to be one of the most promising strategies to achieve site-specific drug delivery [14]. To be considered as potential human drug delivery systems requires that the material has to be biocompatible, preferentially biodegradable, or at least should be able to be excreted [15]. This my be the reason why only a limited number of biodegradable polymeric nanoparticles [9, 16-20], solid lipid nanoparticles (SLN) and nanostructured lipid carriers (NLC) [21-30] have been studied with respect to their potential for drug systemic and topical administration. Nanoparticles can be used to deliver a wide variety of substances as hydrophilic or hydrophobic drugs, proteins, vaccines, biological macromolecules, etc., and they can be formulated for targeted delivery, e.g. to the brain, lungs, lymphatic system, or made for long term systemic circulation [16].

1.3.1.1 Lipid nanocarriers

Both, SLN and NLC, are composed of physiological and biodegradable lipids, which possess a low cytotoxicity and also low systemic toxicity [31]. SLN consist of pure solid lipid while NLC are made of a solid matrix entrapping liquid lipid compartment [25]. These carriers have been the most extensively studied for drug and cosmetic dermal applications.

There are two main preparation methods described for SLN, the high pressure homogenization methods, which can be performed under hot or cold conditions depending on the drug stability, and the microemulsion technique.

SLN posses some advantages when compared with liposomes (also lipid carriers but without a solid structure) and emulsions, e.g. the protection against chemical degradation of the drug and the modulating capacity of the active compound release. The main disadvantage of SLN is that during storage the drug entrapped is expulsed due to a change in the lipid conformation to a lower energy crystal state, a transformation from polymorphic to perfect crystals, which allow no guest molecules in the structure. To overcome this problem NLC were developed. In these nano-carriers, solid and liquid lipid are mixed in such a combination that the particle solidifies upon cooling but does not re-crystallize, remaining in amorphous state. This allows the drug to be accommodated in the particle for a longer time and will increase the drug loading capacity of the systems [24].

Several authors have studied the potential of SLN and NLC as topical delivery systems. Examples of the use of lipid solid nanocarriers are: Santos Maia et al (2000) have shown that the incorporation of prednicarbate into SLN increase the amount of drug which penetrated the human skin layers compared with a commercially available cream [27]; on the other hand, Wissing and Müller (2002) incorporating the sunscreen oxybenzone into SLN, reported a decrease of the SC penetration, characteristic desired when sunscreens are used [32].

The potential of these carriers are variable and must be studied specifically for the drug and delivery system.

1.3.1.2 Polymeric nanocarriers

Not as extensively as SLN the potential of polymeric nanocarriers have been studied for skin drug delivery.

Polymeric nanoparticles are particles of less than 1000 nm in diameter that can be prepared from natural or synthetic polymers. Natural polymers, such as protein and polysaccharides, have been not widely used since they vary in purity, and often require preparation processes which can lead to drug degradation. The most widely used polymers are synthetic polymers as polyalkylcyanoacrylates, poly(lactic acid), poly(glycolic acid) or their copolymers, poly(lactide-co-glycolide), etc. The last mentioned polymers have a very well known biocompatibility and resorbability through natural pathways, and their degradation and drug release rate can be regulated according to the polymer composition (monomers proportions and linkages) [16, 33].

Poly(D,L-lactide-co-glycolide) (PLGA) have been extensively studied for different therapeutic applications such as sustained drug, vaccine, and gene delivery [34-36]. PLGA microparticles were described as vehicles for topical drug delivery, providing a reservoir system for release into the skin [19, 36]. Other polymeric nanoparticles examples have been: poly(ε-caprolactone) NP, used by Alvarez-Román (2004) et al to increase the availability of octyl methoxycinnamate within the SC [9]; and chitosan NP, used by Cui and Mumper (2001) for vaccine delivery to the viable epidermis [17].

Despite of the apparent advantages compared with other DDS, polymeric nanoparticles appear rather unexplored for drug delivery to the skin.

1.3.2. Nanocarrier – skin interaction mechanism

Following the topical application of a dermatological formulation the absorption of the active compound could follow the transcellular, intercellular (paracellular) and transappendageal pathway through the epidermal barrier.

The mechanism of interaction of the nanoparticulated carrier systems and the skin and also the transport pathways within the membrane of the drug and/or the carrier, are required to establish the possibility of using such systems to optimize the drug transport process [9]. It has been described that SLN, due to its particle size, are able to ensure a high adhesion to the SC enhancing the amount of drug which penetrates into the viable skin. Furthermore, for SLN particles between 200 and 400 nm an occlusive effect has been described on artificial membranes [30], and reducing the trans-epidermal water loss and increasing the penetration of a occlusion sensitive drug into the skin layers [29, 37].

In another hand, *in vivo* studies indicated that NLC have been able to increase the anti-inflamatory effect of indomethacin on the time, correlated well with an increased permanence of the drug in the SC layers studied using tape stripping method [23].

The role of the hair follicles in the penetration process is often neglected based on the fact that the orifices of the hair follicles occupy only approximately 0.1% of the total skin surface area. However it is not considered that the hair follicles is an invagination of the epidermis extended deep into the dermis, increasing the absorption area below the skin surface [38, 39].

In the case of polymeric carriers, Rolland et al have demonstrated hair follicle targeting using 5 µm PLGA-adapalen-loaded microparticles [38], as well as de Jalon et al have shown PLGA-microparticles penetration into porcine skin [36]. In other studies, copolymer nanoparticles have been shown by Shim et al to deliver monoxidil through the skin in a size dependent form when hairy rats where used [20]. Using polystyrene nanoparticles of 20 and 200 nm in diameter and porcine ear skin, Alvarez-Román et al

have demonstrated that particles accumulate in the follicular opening and that smaller particles favour this localization [40]. Bigger particles of the same polymer (0.75 – 6 µm) were tested by Lademann's group showing *in vitro* and *in vivo* size dependent particle penetration that was independent of the hair type (terminal vs. vellus hairs). A massage increased the penetration into the hair follicle [41]. Finally, the same group have extensively studied the follicle penetration of particles using human skin and titanium dioxide microparticles which were found to reach only the outer layers of the SC as well as deep into the hair follicles. They stated out that particle penetration was dependent on the "activity" of the hair follicle, i.e. hair growth and sebum production will influence the particle penetration process [42-45]. As described before, follicular penetration of nanoparticles (see figure 3) appear to be a promising mechanism for drug delivery.
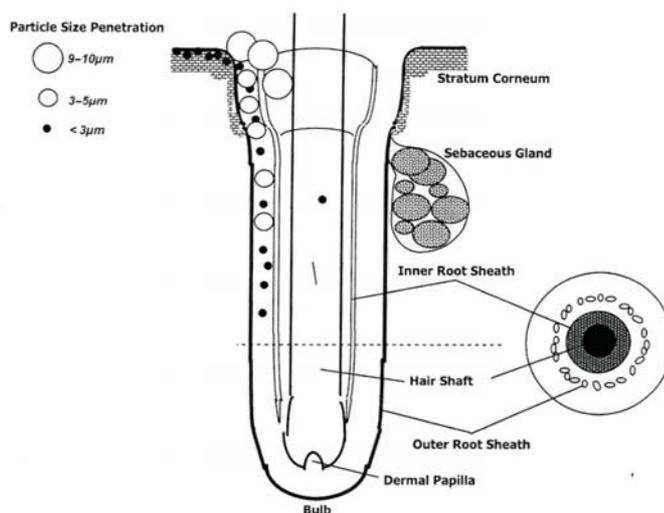
Figure 3: Size dependence of hair follicle particle penetration [3]

The hair follicle delivery has several pharmacokinetic advantages as a reduction or bypass of the tortuous pathway of the transepidermal absorption, decrease of the drug systemic toxicity when the follicle act as long term delivery reservoir and increasing

---

[3] Reprinted from Roberts M.S. et al, Dermatological and transdermal formulations, page 175, figure 35, Marcel Dekker , Inc., 2002, with permission from Taylor & Francis (UK).

additionally the therapeutic index of some drugs as well as reducing the applied dose or frequency of administration. Micro- as well as nanoparticles have been demonstrated to reach deep into the hair follicles, where the barrier posses only a few layers of differentiated corneocytes and can be considered highly permeable, and additionally the hair follicles can act as long-term reservoir, beneficial condition when transdermal delivery is intended.

Techniques as confocal laser scanning microscopy (CLSM) offer the possibility of visualizing the distribution of fluorescent probes in a skin sample by optical sectioning without previous cryofixation or embedding of the tissue, and it is considered as a valuable method for reporting the extent of penetration of molecules into the skin and for identifying the transport pathways [9]. Multi-photon fluorescence imaging can also be applied as technique for determinations *in vivo* tissue absorption/accumulation of dermatological and cosmetical preparations, such as interaction of nanoparticulated systems with the skin [46, 47].

1.3.3. Nanocarrier toxicology

Nanocarriers are present in different dermatological and cosmetic formulations. The most commonly used carriers are liposomes; solid poorly soluble materials as titanium dioxide and zinc oxide; polymer particles and SLN.

The small size of the carriers give them an increased ratio surface to total atoms or molecules exposed to the interaction with cellular systems, increasing its biological activity. This large activity can either positive (e.g. antioxidant, carrier capacity for therapeutics, penetration of cellular barriers for drug delivery) or negative (e.g. toxicity, induction of oxidative stress or of cellular disfunction), or a mixture of both. However, in strong contrast to the efforts to increasing its positive properties for improving the human health are the limited attempts to evaluate the potentially undesirable effects of nanoparticles when administered for medical or cosmetical purposes [48].

Some of the studies undertaken to evaluate the **toxicological potential** of dermatologically applied nanoparticles have reported the following results:

♦ Titanium dioxide nano- and microparticles have been studied by Lademann et al who report that micro-sized particles get through the human SC and into the hair follicles [44]; on other study, carried by Menzel et al, using commercially available sunscreen creams and pig skin has reported the penetration of nanoparticles (approximately 15 nm in diameter) in the SC and into the underlying stratum granulosum through the intercellular space [49]. Gamer et al studied the penetration of zinc oxide by tape-stripping method on porcine skin and found that approximately 100% of the applied amount remain in the uppermost layers of the SC, only a few samples showing the presence of particles in the deeper layers [50].

♦ PLGA microparticles (1-10 μm in diameter) have been studied by de Jalón et al using pig skin and were found to penetrate into the viable epidermis [36].

♦ Solid lipid nanoparticles have shown lower toxicity than poly(lactide-co-glycolide) or polyalkylcyanoacrylate nanoparticles when administered intravenously [31], but there are no studies performed when topically applied.

Limited literature or qualitative information about penetration and effect of nanoparticles during the skin transport is available, only in the case of liposomes, zinc oxide and titanium dioxide nanoparticles toxicological information is available. In general, only a few conclusions can be made about the toxicological potential of nanocarriers:

♦ Penetration of the skin layers is size dependent.

♦ Different type of particles have different behaviour with respect to the dermal membrane, and it is not possible to predict either its permeation or toxicological behaviour.

♦ Parts or materials which can dissolve or leach from the particles can possibly penetrate the skin.

♦ There are other studies, using particles not intended for dermatological use that have shown that particles can be phagocytized by macrophages or Langerhans cells, and this process can induce a sensitation response.

♦ There is no evidence that particle applied to the skin can penetrate and enter the systemic circulation when applied to normal skin [51].

The available data suggest that dematologically applied nanoparticles have a low human risk, but is necessary more information about the real effects under *in vivo* conditions.

1.4.   FLUFENAMIC ACID AS A MODEL DRUG

Flufenamic acid (FFA), a non-steroidal anti-inflammatory drug, is known as 2-[[3-(trifluoromethyl) phenyl] amino] benzoic acid (see figure 4). This drug is a weak acid soluble in organic solvents as methanol, ethanol, chloroform, and acetone, and it has a very low solubility in water at 22 °C 0.0067 mg/ml which can vary depending on the pH with a dissociation constant (pK$_a$) of 3.9. Its solubility is increased by non-ionic surfactants, and by urea and sodium citrate. Flufenamic acid 1-octanol/water partition coefficient (log P) have been estimated by Dunn with a value of 4.88, and Terada et al have determined it experimentally obtaining a log P equal to 5.62 [52, 53].
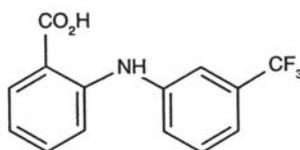
Figure 4: Chemical structure of flufenamic acid

From this drug exists several described modifications which differ on its crystal properties. The present work will be referred to FFA modification II that has a melting point of 128°C [52].

Human pharmacokinetics: FFA is intestinally absorbed in a pH dependent form, and in extent of 100% of the administered dose, from which 51% is eliminated as drug and its metabolites by renal way. The active undergoes metabolic transformations to FFA glucuronide, 5- and/or 4'-hydroxy FFA and its respective glucuronides. Due to its hydrophobicity it highly binds to proteins (have been studied using bovine and human serum albumin, BSA and HSA respectively), and FFA have shown a site specific binding when HSA is used, that is characteristic for drugs which contain aromatic carboxylic acid, as ibuprofen and flurbiprofen [52]. Skin pharmacokinetic behaviour has not been described, however, Wagner et al have shown that in the stratum corneum the concentration of drug increases with the incubation time, and have a good linear correlation among the *in vitro* test systems, e.g. Franz-diffusion cell system and Saarbrücken model, and the *in vivo* drug penetrated amount. In the same way the drug concentration rises in the deeper skin layer, but only *in vitro* information is available [54].

1.5. *IN VITRO* METHODS FOR TRANSDERMAL DRUG DELIVERY ASSESSMENT

1.5.1. *In vitro* permeation studies

The studies of *in vitro* skin permeation are the most common experimental set-ups for the control of dermatological formulations. It has been carried out using a wide variety of experimental protocols dependent on the research group, the substances in study and the purpose of the substance or formulation applied to the skin.

The *in vitro* methods involve the diffusion measurement of substances through the skin, bioengineered, various skin layers, or artificial membranes to a receptor fluid assembled in a diffusion cell, which can be static or flow-through (see figure 5). In Franz diffusion cell systems (FD-C), the formulation or substance in study is placed in the donor compartment, separated from the receptor compartment by a membrane, e.g. full thickness skin, epidermis or SC sheets, splitted skin from human or animal origin or bioengineered materials (keratinocyte cultures). The receptor compartment is usually a buffer solution, with a composition as close as possible to physiological conditions, normally pH 7.4. If the solubility of the substance is low, substances as ethanol, proteins, cyclodextrins or some surfactants can be added [55]. The sampling is performed either in a continuous form or at pre-determined time intervals. The system is maintained at constant temperature under conditions which simulate the skin surface temperature (32°C).
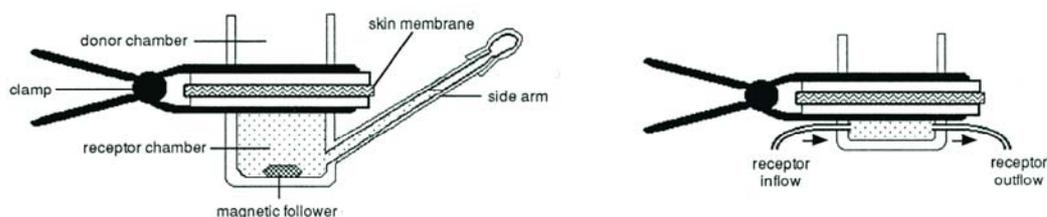
Figure 5: Schematic representation of Franz diffusion test systems: Horizontal static (left) and flow through (right) diffusion cell [4]

---

[4] Reprinted from Walters K.A. and Roberts M.S., Dermatological and transdermal formulations, page 200, Marcel Dekker , Inc., 2002

The dosage regime of the formulation in made under infinite (> 10 µl/cm^2 or mg/cm^2) or finite dose (≤10 µl/cm^2 or mg/cm^2) conditions and the donor compartment can be under occlusion or opened to the environment. In the first case, the occlusion of the system leads normally to an excessive hydration of the skin, and the second allows the evaporation of volatile substances.

Constant stirring of the system ensure the diffusion of the drug by homogenization of the receptor. The sink conditions are maintained along the experimental time under the following conditions: (i) in the receptor compartment only 10% of the saturation concentration is reached; (ii) the membrane is unaffected during the experimental time [56].

1.5.2. *In vitro* penetration studies

The Saarbrücken model (SB-M) was introduced in skin research by Loth and co-workers [57-61] and has been described in detail by Wagner et al [54]. Briefly, the skin is put onto a filter paper soaked with Ringer solution and placed into the cavity of a Teflon block. The drug preparation is filled into a cavity of a Teflon punch of 2 mm in depth, which is applied to the skin surface and a weight of 0.5 kg is placed on top of the punch for 2 min, to improve the contact between the skin and the drug preparation. After this time, the punch is fixed on its place and the gap between the two Teflon parts is sealed with Plastibase® to avoid the skin water loss. See a representation of the system on figure 6. The whole system is transferred into a plastic box and placed into a water bath, or into a forced air circulation oven, at (32 ±1) °C [54].
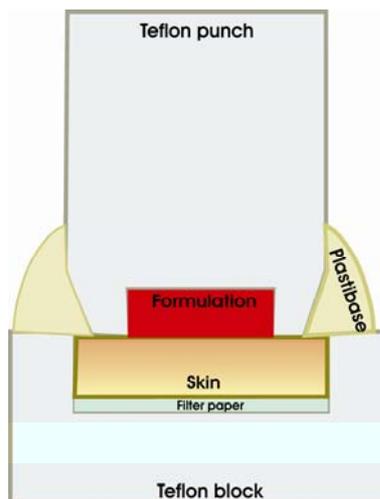
Figure 6: Schematic representation of the Saarbrücken penetration system.

If compared with FD-C, SB-M avoids the non-physiological hydration and changes of the skin due to the absence of liquid as receptor medium. This system, coupled to segmentation techniques, such as tape stripping or cyosectioning, allows the measurement of penetration profiles of the drug with respect to the depth of the tissue.

Under infinite dose conditions, a excessive amount of drug is applied to the skin, ensuring a reproducible way of application It is expected that the SC reach saturation and the effect of rubbing due to application procedure is avoided. Under finite dose conditions, only a limited amount of preparation is applied to the skin surface, and it is possible to observe the influence of other factors such as evaporation of excipients.

This model is suitable to study semisolid and liquid formulation (using porous holders), as well as patches. The experiments are carried out with different incubation time points. Consequently, the drug distribution in the skin layers or the formation of depots can be observed. At the end of the incubation time the preparation is removed from the skin surface, the thickness of the skin is measured and the tissue is segmented under standardized procedure.

1.6. CALCULATION OF PARAMETERS TO DESCRIBE TRANSDERMAL ABSORPTION

For practical reasons only the processes considered on the development of this thesis are mathematically described. Schematically, *in vitro* and *in vivo* processes are presented in the figure 7.
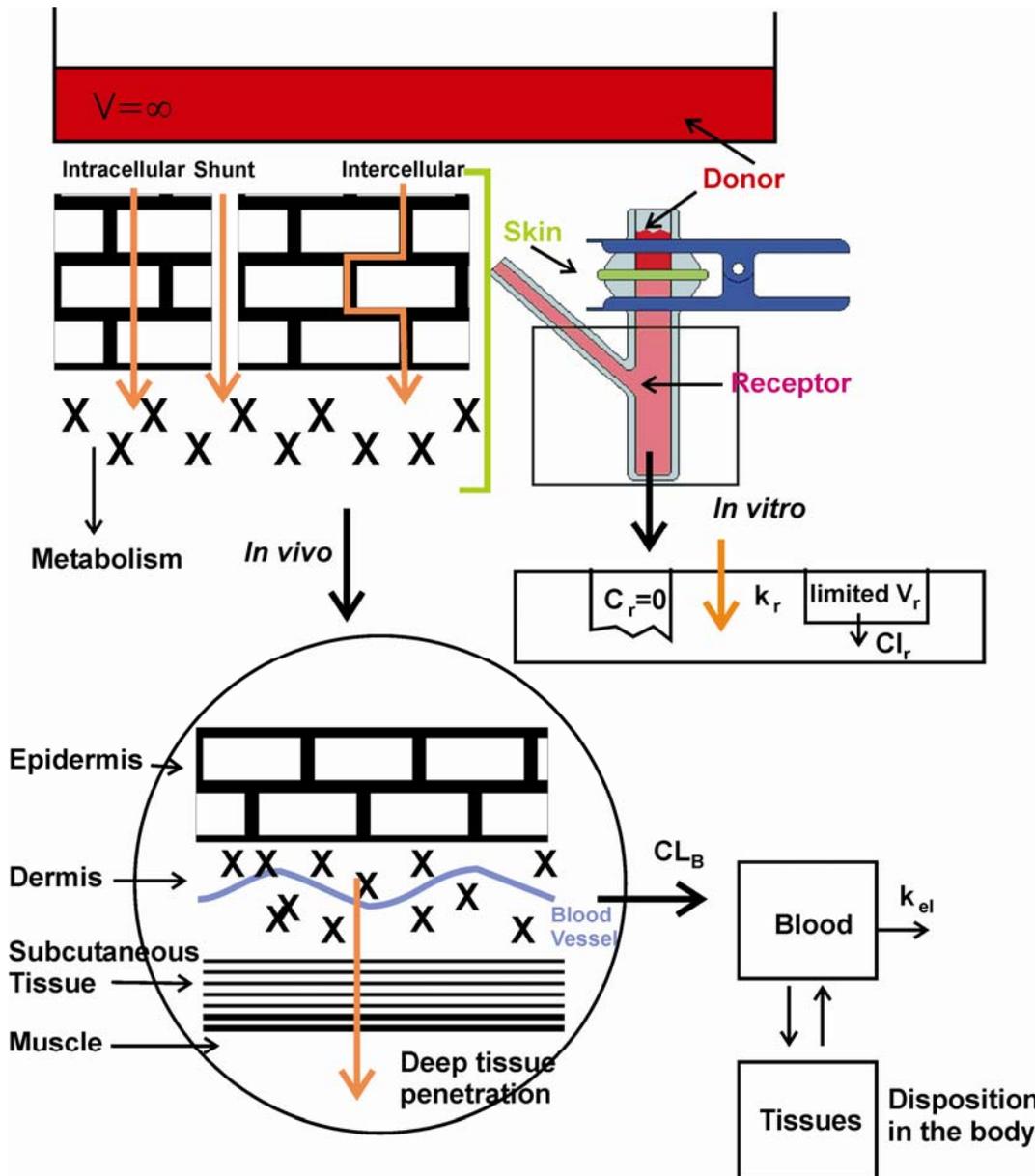
Figure 7: Diagrammatic representation of the processed involved on *in vitro* and *in vivo* percutaneous absorption [5]

---

[5] Adapted from Roberts and Anissimov, 2005 [62]

As shown in figure 7, under *in vitro* conditions, the volume (V) and the concentration of the donor compartment are considered to be constant over the experimental time, even though the receptor volume (V_r) and its clearance (Cl_r) are limited. On the other hand, under *in vivo* conditions, the concentration on the dermal tissue is conditioned to the clearance due to capillary network (Cl_B) and to the elimination/distribution from this fluid.

The data obtained from the *in vitro* permeation experiments can be plotted and several parameters can be calculated from them. Examples of the typical obtained curves with the different dosage regimes are shown in figure 8.
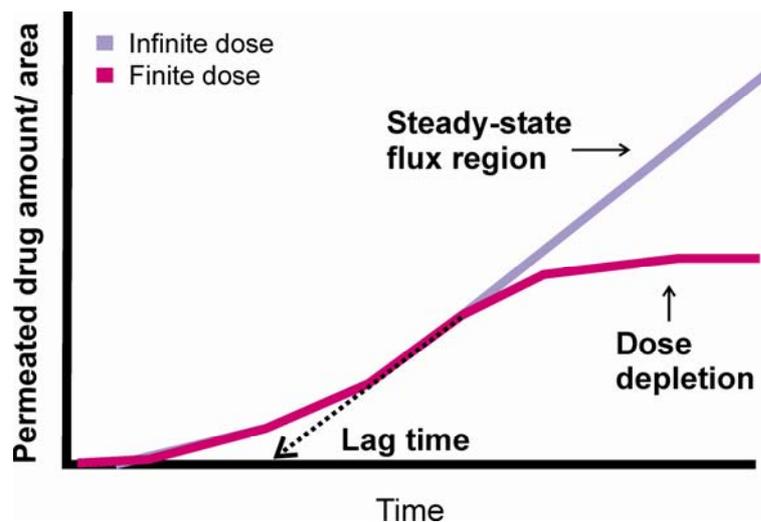
Figure 8: Cumulative permeation patterns following finite- and infinite-dosing regimes [6]

---

[6] from Walters K.A. and Roberts M.S., Dermatological and transdermal formulations, page 209, figure 4, Marcel Dekker , Inc., 2002

1.6.1. *In vitro* permeation studies using infinite dose regime

Most of the *in vitro* studies using infinite dose conditions are carried out assuming that:

- ♦ the concentration in the donor compartment (C_v), i.e. in the formulation applied, does not change considerably (change < 10%) during the experimental time;

- ♦ the drug concentration in the receptor compartment does not exceed 10% of the saturation concentration on the receptor media, i.e. the sink conditions, in the receptor compartment, are maintained during the experimental time;

- ♦ and the characteristics of the membrane does not change during the experimental time.

If the transport through the SC is the rate limiting process, the steady-state approximation of the amount of solute permeated (Q) with a apparent permeation constant (P_{app}) and a lag-time (t_{lag}) when the concentration of the donor (C_v) is applied to a determined area (A) during a exposure time (t) can be represented though the equation 1.

If the transport through SC is the rate limiting process, after a certain lag-time steady-state conditions will be achieved. Assuming a homogeneous membrane, the drug permeation can be described by diffusion and Fick's first law can be applied.

$$Q = P_{app} A C_v (t - t_{lag})$$

Equation 1: Steady-state permeated amount.

Rearranging equation 1 leads to:

$$P_{app}C_v = \frac{Q}{A(t - t_{lag})} = J_{ss}$$

Equation 2: Flux under steady-state conditions

With the flux at steady-state (**J**), which is represented by the slope of the linear part of a diagram of the permeated amount of drug per area versus time (figure 8) .

Then, the apparent permeability constant (**P_{app}**) represents the transport speed of the drug through the membrane, and can be calculated using the **J_{ss}** and **C_v**.

1.6.2. *In vitro* penetration experiments using infinite dose regime

Using the Saarbrücken model two types of data handling are possible:

1. Concentration – skin depth profile:

Plotting drug concentration in the different skin layers (mass of drug per thickness of the layer per area) versus skin depth (see figure 10). In this case, the formation of depots in the different layers can be observed.
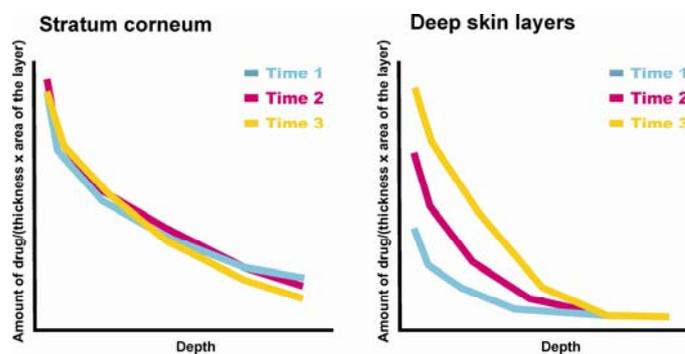
Figure 9: Example of penetration profiles of drug into the stratum corneum and deeper skin layers respect to the depth, using the same formulation (infinite dose regime) at different incubation time.

For detailed information concerning the calculation steps see Wagner et al (2000) [54]

Furthermore, area under the penetration curve can be calculated using the trapezoidal rule (see equation 3). Which may serve as surrogate for the bioavalability of the substance in each layer.

$$AUC(0 - t_n) = \frac{1}{2} \sum_{i=1}^{n} (C_{i-1} + C_i)(t_i - t_{i-1})$$

Equation 3: Area under the curve trapezoidal rule – General equation

2. The calculation of penetrated amount of drug in each layer, i.e. SC or deep skin layers, respect to the incubation time (see figure 9). In this case the influence of incubation time, drug concentration and excipients can be observed, as well as, saturation of the stratum corneum or the influence of different skin donors and anatomical regions.
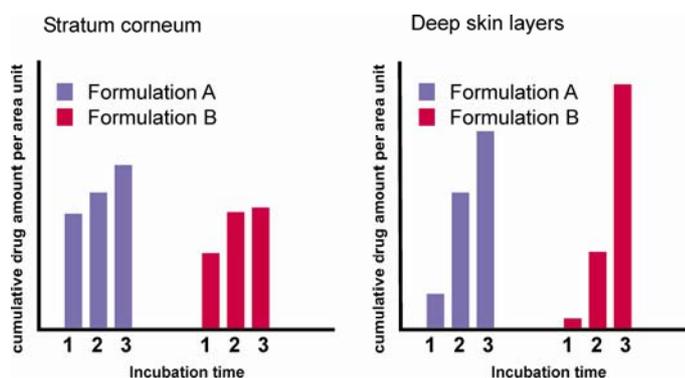
Figure 10: Example of cumulative amount of drug into the stratum corneum and deeper skin layers using different formulations (infinite dose regime) according to the incubation time

1.7.   MICRODIALYSIS AS *IN VIVO* DERMAL PHARMACOKINETIC TOOL

Born in neurosciences, the microdialysis as sampling technique have been used since several years to monitor the drug absorption and disposition from the extracellular space different organs, fluids and tissues, becoming used as technique in human research during the late 80's.

It consists of a microdialysis probe, a thin hollow tube made of a semi-permeable membrane, normally of around 200 – 500 µm in diameter, which is implanted into the skin and perfused with a receiver solution (perfusate) that recovers the unbound permeant from the local area (dialysate) which is collected and analysed. In principle, the dialysis driving force of the molecular moving is the diffusion down the concentration gradient existing between two compartments separated by a semi-permeable membrane (see figure 11), that for skin *in vivo* conditions these compartments are represented for the dermal or subcutaneous extracellular fluid and the artificial physiological solution in the microdialysis probe lumen. In essence, the principle of the microdialysis is to create an "artificial blood vessel" where the diffusion of compounds flows on the direction of lowest concentration [63-66].
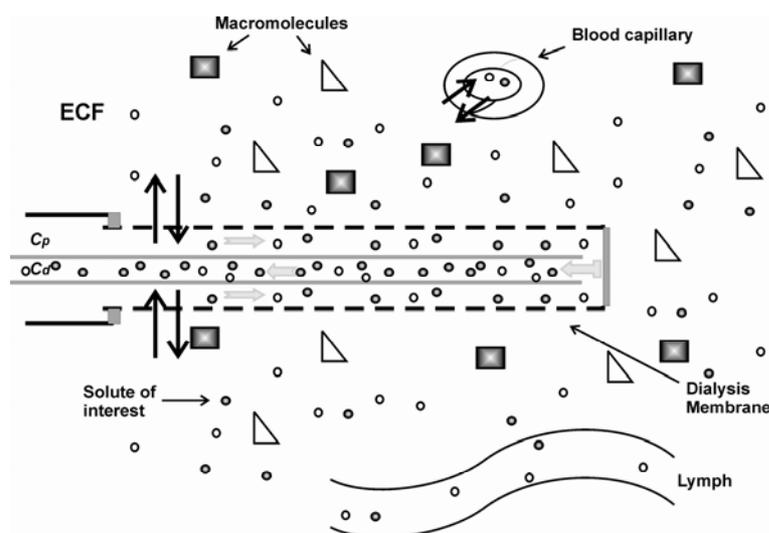
Figure 11: Microdialysis principle [7]

---

[7] adapted from Elmquist and Sawchuk, 1997 [66]

The material of the microdialysis membrane must be biocompatible and inert, respect to the substance in study and to the tissue components. The molecular weight cut-off [8] must be large enough to allow the free diffusion of the solute, but small enough to assure the exclusion of proteins and other macromolecules. The most commonly used materials have been: cellulose, cellulose-acetate, polycarbonate, polyarylethersulphone, etc.

For pharmacokinetic studies, different probe designs such as linear or concentric style were used.

Fick's second Law that considers the concentration gradient and diffusion rate of the substance from the medium and the surface area of the membrane mathematically describes diffusion microdialysis processes. One of the most important parameters to be considered is the flow rate of the perfusate (solution that comes into the probe), which is normally in the range of 0.1 – 5 µl/min, inversely related to the amount of drug recovered in the dialysate (solution that comes out of the probe). Other factors that strongly influence the drug recovery from the surrounding medium are: the lipophilicity of the substance, i.e. as more hydrophobic or protein bound substance as less recovered using an aqueous perfusate media, and the molecular weight and volume of the substance that will limit the pass through the dialysis membrane according to its molecular cut-off. To improve the recovery of lipophilic drugs strategies as addition of solvents (e.g., polyethylene glycol, cyclodextrins, proteins, or lipids) to the perfusate have been used [63, 65, 67].

The relative recovery (RR) of the probe, essential for data interpretation, is normally calculated using the retro-dialysis method, which assumes that the net transport

---

[8] Usually defined as the molecular weight in Daltons at which 80% of the molecules are prevented from passing through the membrane.

through the microdialysis membrane from the perfusate to the surrounding tissues equals the net transport from the tissues into the perfusate. The relative recovery is calculates using the equation 4 [67]:

$$RR = \left(\frac{C_{perfusate} - C_{dialysate}}{C_{perfusate}} \right)$$

Equation 4: Relative recovery of a microdialysis probe using retrodialysis method.

Among the techniques to determine cutaneous availability, such as tape stripping, biopsies or imaging procedures, microdialysis has shown to be promising having several advantages for the assessment of in-vivo drug pharmacokinetic profiles. The minimally invasive procedures ensures minor reversible trauma, allowing long term sampling under physiological conditions in awake individuals, that the individual itself is its own control, and the good temporal resolution of tissue concentration, make this technique, compared with the other above mentioned, require a lower number of volunteers. The obtained samples, due to the relatively low molecular cut-off of the membrane, are protein free allowing sample analysis without any further purification step and avoiding the enzymatic degradation of the sample. As the substance in study can be included on the perfusate, in situ metabolism can be acquired. Nevertheless, the small sample size is a disadvantage since it requires very sensitive analytical methods [56, 67, 68]

An increasing number of studies using microdialysis of a wide range of drugs in animal and human subjects were performed, supporting the potential of this technique for bioavailability and bioequivalence studies. Some examples of studies in-vitro as well as in-vivo, involving different delivery systems and species are: iontophoretic drug delivery in rats by Mathy et al [69]; oral delivery and skin pharmacokinetics by Bielecka-Grzela and Klimowicz [70]; determination of salicylic compounds on rat skin by Simonsen et al [71], and in human skin by Leveque et al [72]; anaesthetic extended release products in human skin by Kopacz et al [73]; among others.

OBJECTIVES

During the last years, the interest over the nanoparticles as drug delivery carrier system has increased due to its potential of controlled release, targeting, and stability advantages over other carrier systems. Several strategies, including physical and chemical methods, have been used to improve the delivery of drugs through the skin. During the last decades, the study of the potential of the nanotechnology for transdermal drug delivery have been mainly focused on the study of the use of solid lipid nanoparticles and nanostructured lipid carriers and only a few studies have been centred on the use of biodegradable polymeric nanoparticles.

The aim of this doctoral thesis is to study the potential of the biodegradable polymeric nanoparticles, made of poly(D,L-lactide-co-glycolide) (PLGA) , as transdermal delivery system. Following this general purpose, the specific objectives are:

- ♦ To study the effect of PLGA nanoparticles on the skin permeation using flufenamic acid as model drug

- ♦ To study the mechanism how PLGA nanoparticles enhance/retard the permeation of flufenamic acid through the skin

- ♦ To study the effect of PLGA nanoparticles on the skin absorption of flufenamic acid *in vivo*

CHAPTER 2: PLGA NANOPARTICLES AS TRANSDERMAL CARRIER

2.1. ABSTRACT

The effect of the inclusion of flufenamic acid in PLGA nanoparticles on the transport of flufenamic acid into excised human skin was investigated. Penetration and permeation data were acquired using two different *in vitro* test systems: the Saarbruecken penetration model (SB-M), where the skin acts as its own receptor medium, and the Franz diffusion cell (FD-C), where the receptor medium is a buffer solution. For the stratum corneum no differences were found between nanoencapsulated and free drug. Drug accumulation in the deeper skin layers and drug transport across human epidermis was slightly delayed for the nanoencapsulated drug compared to the free drug after shorter incubation times (< 12 h). In contrast, after longer incubation times (> 12 h) the nanoencapsulated drug showed a statistically significant enhanced transport and accumulation (P<0.05). Additionally, nanoencapsulated flufenamic acid was visualized by multiphoton fluorescence microscopy. Particles homogeneously distributed on the skin surface and within the dermatoglyphs were found, but no nanoparticles within or between the corneocytes were detected.

2.2.   INTRODUCTION

Due to its special structure, the skin provides the main barrier between the body and the environment, at the same time it limits the drug delivery along this route [1, 6, 8, 74, 75]. Many strategies have been employed to improve the dermal and transdermal delivery of drugs, e.g. increasing the effective concentration of the drug in the vehicle, improving the partitioning between the formulation and the skin, the use of chemical penetration enhancers and different physical enhancement methods [6, 76]. Furthermore, carrier systems like liposomes, microparticles or nanoparticles (NP) [11, 77, 78] have been explored. For microparticles, some targeting to the hair follicles has been shown by Toll et al. [41], using polystyrene microspheres in a range of 0.75–6 μm, and Lademann et al. [79], using titanium dioxide particles in a range of 0.1–0.3 μm also resulting in an enhanced delivery to the deeper skin layers. Studies on solid lipid NP [27, 29, 30] also showed increased transdermal drug delivery induced by their occlusive effects. Alvarez-Román et al. [40] reported preferential accumulation of non-biodegradable drug-free polymeric NP in the hair follicle opening of pig skin. In addition, the same authors reported an increased level within the stratum corneum of the pig ear of the highly lipophilic sun-protecting agent, octylmethoxycinnamate, when nanoencapsulated in the biodegradable polymer poly(ε-caprolactone) [9].

Some of the most widely used polymers in the NP formulation are poly(lactic acid), poly(glycolic acid), and their co-polymer, poly(lactide- co -glycolide) (PLGA), which are known for their good biocompatibility and resorbability through natural pathways [33]. In oral and parenteral applications, solid biodegradable polymeric NP based on PLGA have shown their advantage over liposomes by their increased stability [16, 80, 81], but in the field of dermal delivery their potential appears to be rather unexplored.

The objective on this chapter was to investigate the influence of nanoencapsulation on the permeation and penetration of the lipophilic model drug flufenamic acid (FFA) into skin using PLGA as carrier polymer. In order to monitor drug

penetration, the Saarbrücken model [54] (SB-M) was used in which the skin itself acts as a receptor compartment. A tape stripping technique followed by cryosectioning of the deeper skin layers allows the quantification of the penetrated drug amount. Drug release from the formulation and drug permeation through the epidermis were studied using the static Franz diffusion cell (FD-C) technique.

Due to the size differences between the hair follicles of pig skin and of human skin [82], which may play an important role in the results, we decided to use excised human skin from abdominal plastic surgery instead of pig skin. As polymer, PLGA was chosen in view of its excellent biocompatibility and the availability of various methods to prepare drug-loaded NP from this polymer. To verify the presence and to visualize the distribution of the applied NP on the skin, multiphoton fluorescence imaging was used. This technique allows to excite the natural fluorescence of the FFA in non-polar surroundings (λ max = 420 nm) by a two-photon absorption process. Two-photon excitation induced with femtosecond near infrared laser pulses offers the possibility of high-resolution 3-dimensional imaging of the skin [83].

2.3.   MATERIALS AND METHODS

2.3.1. Materials

Natrosol® 250 M (Aqualon, Hercules Inc., DE, USA), Flufenamic acid, modification II (Kali-Chemie Pharma, Hannover, D), Poly(D,L-lactide-co-glycolide) (50:50) with a molecular weight of 40000 to 75000 Da (Sigma Chemical Co., St. Louis, MO, USA), Polyvinyl alcohol (PVA) Mowiol® 4-88 (Kuraray Specialities Europe GmbH, Frankfurt, D), Ringer solution, McIlvaine citric acid phosphate buffer (pH 2.2), Sodium hydroxide solution (0.05 M) (all components from Merck, Darmstadt, D), Plastibase® (Heiden GmbH, Muenchen, D), Methanol Chromasolv® (Sigma-Aldrich GmbH, Seelze, D), Tesa Film Kristall-klar 19 mm (Tesa AG, Hamburg, D), Ethyl acetate (Fluka Chemie GmbH, Bucks, Switzerland), Cellulose membrane MWCO 12000 – 14000 Da (Medicell International Ltd., London, LX, USA) were used as obtained from the suppliers.

2.3.2. Equipment

HPLC System: Chromeleon™ Version 6,5 SP2, build 968; P580 Pump; ASI-100 automated sample injector; STH 585 Column oven; UVD 170S Detector (Dionex Softro GmbH, Germering, D); Franz diffusion cell type 6G-01-00-15 (Perme Gear, Riegelsville, PA, USA); Cryomicrotome HR Mark II, model 1978 (Slee, Mainz, D); Centrifuge Sigma 3E-1 (Sigma, Aichach, D); High-speed homogenizer Ultra-Turrax® T25 (Jahnke & Kunkel GmbH & Co. KG, Staufen, D); Atomic Force Microscope Nanoscope IV Bioscope™ (Veeco Instruments, Santa Barbara, CA, USA); Freeze-drier Alpha 2-4 LSC (Christ, Osterode, D); Rotavapor® R-205 (Büchi, Flawil, CH); Zetasizer® 3000 HS A (Malvern Instruments GmbH, Herrenberg, D); for multiphoton fluorescence imaging the femtosecond laser imaging system DermaInspect® (JenLab GmbH, Jena, D), equipped with a Chameleon laser system (Coherent Inc., Santa Clara, CA, USA) and a Hamamatsu PMT(H7732) detector (Hamamatsu Photonics Deutschland GmbH, Herrsching am Ammersee, D) was used.

2.3.3. Nanoparticle preparation and characterization

PLGA nanoparticles loaded with flufenamic acid (FFA NP) were prepared using a solvent extraction method. 30 mg of flufenamic acid were dissolved in a solution of 600 mg of PLGA in 20 ml of ethyl acetate. This organic phase was added dropwise into 20 ml of an aqueous phase, containing 1% of PVA as a quasi-emulsifier, under stirring with a magnetic stirring bar. The resulting O/W emulsion was homogenized with a high-speed homogenizer at 13500 rpm for 10 minutes. To complete the precipitation, water was added up to 200 ml under stirring with a magnetic bar. Organic solvent was then removed using a rotating evaporator. The resulting nanoparticles suspension was freeze-dried and stored until use.

For reference, standard drug-free nanoparticles were prepared in the same way.

Size and surface morphology of the FFA NP were determined using photon correlation spectroscopy (PCS) and atomic force microscopy (AFM). For the AFM measurements, a drop of the nanoparticles suspension and hydrogel, respectively, were air-dried on a silica wafer. Imaging was done using a silicon cantilever with a spring constant of approximately 40 N/m and a resonance frequency of about 170 kHz. The scan speed applied was 0.2 Hz. The resolution was 512 × 512 pixels. In order to avoid generating sample artefacts the tip loading force was minimized.

The content of FFA in the particles was determined using the following equation:

Whereas FFA Free was determined in the supernatant obtained from a centrifuged suspension (23147×g), FFA Total was obtained after a proper extraction of the NP suspension using 0.05 M sodium hydroxide solution. The obtained drug entrapment was 63.6 % w/w that was calculated using the following equation:

$$E(\%) = \left(\frac{m_{id} - m_{fd}}{m_{id}} \right) \times 100$$

Equation 5: Entrapment percentage of drug into nanoparticles

Where m_{id} is the mass of the initial drug used and m_{fd} the mass of the free drug detected in the supernatant after centrifugation of the nanoparticle suspension.

2.3.4. Gel preparation

Flufenamic acid Natrosol® hydrogel (FFA HG) was prepared with flufenamic acid dissolved in water under vigorous stirring. Afterwards, Natrosol® was added in a proportion equivalent to 1.5 % (w/w) and stirred overnight until the polymer was completely swollen. The absence of crystals was determined by microscopic inspection of the gels.

To prepare a flufenamic acid nanoparticles hydrogel (FFA NP HG) a Natrosol® gel (3% w/w) was mixed with an aqueous suspension of the nanoparticles in a 1:1 ratio to obtain the same concentration as in FFA HG. The presence and integrity of the particles in the gel was confirmed by AFM (see figure 1). In addition, the FFA concentration in each gel was verified by HPLC.

In the same way, a hydrogel containing drug-free nanoparticles was prepared.

Penetration and permeation experiments were carried out using FFA HG and FFA NP HG, each with a drug concentration of 0.12 mg/g.

2.3.5. Skin preparation

Excised human skin from Caucasian female patients, who had undergone abdominal plastic surgery, was used. The Ethical Committee of the Caritas-Traegergesellschaft (6th July 1998), Trier, Germany, approved the procedure used. Adequate health and no medical history of dermatological disease were required. After excision, the skin was cut into 10×10 cm^2 pieces and the subcutaneous fatty tissue was removed from the skin specimen using a scalpel. Afterwards the surface of each specimen was cleaned with water, wrapped in aluminium foil and stored in polyethylene bags at –26°C until use. Previous investigations have shown that no change in the penetration characteristics occurs during the storage time of 6 months [77, 84].

Disks of 25 mm in diameter were punched out from frozen skin, thawed, cleaned with Ringer solution, and either transferred directly into the Saarbrücken model or used to prepare heat separated epidermis sheets for the Franz diffusion cell experiment.

2.3.6. Heat separated epidermis preparation

The epidermis was separated placing the thawed and cleaned skin disk in water at 60°C for 90 seconds. After that, the skin was removed from the water and placed, dermal side down, on a filter paper. The epidermal layer was peeled off from the skin using forceps. Before use in the FD-C, the epidermal membrane was pre-hydrated for 1 h.

2.3.7. Permeation experiments

Using a FD-C, experiments were carried out using heat-separated epidermis mounted on a cellulose membrane disk. The membrane was positioned between the donor and acceptor compartment. As donor 750 μl of preparation and as receptor 12.1 ml of Soerensen phosphate buffer (pH 7.4) were used. The donor compartment was

sealed with aluminium foil and the system was maintained at (32 ± 1) °C in a water bath. The acceptor fluid was stirred using magnetic bars at 500 rpm. At predetermined time intervals, samples of 1.0 ml were collected from the acceptor medium and replaced immediately with fresh buffer solution. Samples were collected until 29 h and analysed by HPLC.

Release experiments were done in the same way but using a cellulose membrane to separate donor and receptor compartment.

2.3.8. Penetration experiments

Using a SB-M apparatus, a full thickness skin disk was transferred into the cavity of a Teflon block on filter paper soaked with Ringer solution to prevent any change in the hydration state of the skin. The cavity of the upper Teflon punch was filled with the drug preparation and fixed in position. The gap between the two Teflon parts was sealed with Plastibase® to avoid water loss from the skin. The whole apparatus was transferred into an oven at (32 ± 1) °C for a predetermined incubation time. For details see [54].

2.3.9. Skin segmentation

After the incubation time all the skin specimens investigated with SB-M were segmented using tape stripping and cryosectioning method.

Tape stripping method: At the end of the experiment, the formulation was wiped off from the skin surface using cotton. Then the skin piece was transferred to a special apparatus where it was mounted using small pins to stretch the tissue. After, the skin was covered with a Teflon mask with a central hole of 15 mm in diameter and successively stripped with 20 pieces of adhesive tape placed on the central hole. Each tape was charged with a weight of 2 kg per 10 seconds and rapidly removed. The

samples obtained were pooled according to the following scheme: #1= 1 strip, #2= 1 strip #3= 3 strips and #4-6= 5 strips.

Cryosectioning: After tape stripping, the skin was rapidly frozen in a stream of expanding carbon dioxide. A specimen of 13 mm in diameter was punched out from the stripped area and transferred into a cryomicrotome. The sections were pooled using the following scheme: #1= incomplete cuts, #2-5= 2*25 μm, #6-10= 4*25 μm, #11-15= 6*25 μm, #16= 8*25 μm, #17= Rest of skin.

2.3.10. Sample extraction

The pooled samples were extracted with 0.05 M sodium hydroxide solution and shaken during 2 h at room temperature. After that, tape-stripping samples were separated from the solid content and directly transferred to the HPLC system. The samples of cryosectioning were centrifuged at 456×g for 30 min; afterwards the supernatant was separated and transferred to the HPLC system.

2.3.11. HPLC method

All the samples were analyzed using the following HPLC conditions: Column LiChrospher 100 RP-18, 5 μm, 125*4 mm (Merck, Darmstadt, D); Mobile Phase: McIlvaine buffer pH 2.2: Methanol (20:80); Flow rate: 1.2 ml/min; Wavelength: 284 nm; Injection volume: 20 μl; Retention time: (3.5 ± 0.2) min. This method has been previously validated by Wagner et al [54].

2.3.12. Area under the penetration curve (AUPC)

The AUPC was calculated from the curves of penetrated amount per cubic centimetre of skin (C = µg/cm3) versus depth (d = µm) obtained from the SB-M experiments, using the following equation:

$$AUPC(d_i) = \sum_{i=1}^{n} C_i(d_i - d_{i-1})$$

Equation 6: Area under the permeation curve calculation

2.3.13. Statistical evaluation analysis

For statistical evaluation, SigmaStat 3.0.1 was used.

2.3.14. Multiphoton fluorescence imaging

Skin samples were punched out, thawed and cleaned before gel application and image acquisition. Plain Natrosol® hydrogel, hydrogel containing not loaded nanoparticles or containing flufenamic acid loaded nanoparticles respectively, were applied to the skin and imaged using multiphoton fluorescence imaging with an 40×/ NA 1.3 (oil) objective, at excitation wavelength of λ = 720 nm (pulse length 170 fs, repetition rate 90 MHz) and an average power of 13 mW. Images were acquired in a time less than 30 minutes after application of the gel onto the skin. Acquisition time was chosen to be 25s for a 512×512 pixel image. Starting at the skin surface (z = 0 µm) every 2.3 µm an image was recorded to finally obtain a $200×200×46\ \mu m^3$ stack. The focal plane was varied by a piezo driven objective, allowing to survey the entire epidermis down to the stratum basale.

2.4. RESULTS

To avoid any inter-individual variability of human skin, all penetration and permeation experiments were carried out with skin from the same donor and repeated 6 times. Only for visualization studies skin from a different donor was used.

As shown by atomic force microscopy (AFM) in figure 12, the incorporation of NP (mean size 328.2 nm, PI 0.16) into a hydroxyethyl cellulose gel has no influence on shape and size distribution of the particles, confirming that the hydrogel contained undamaged nanoparticles.
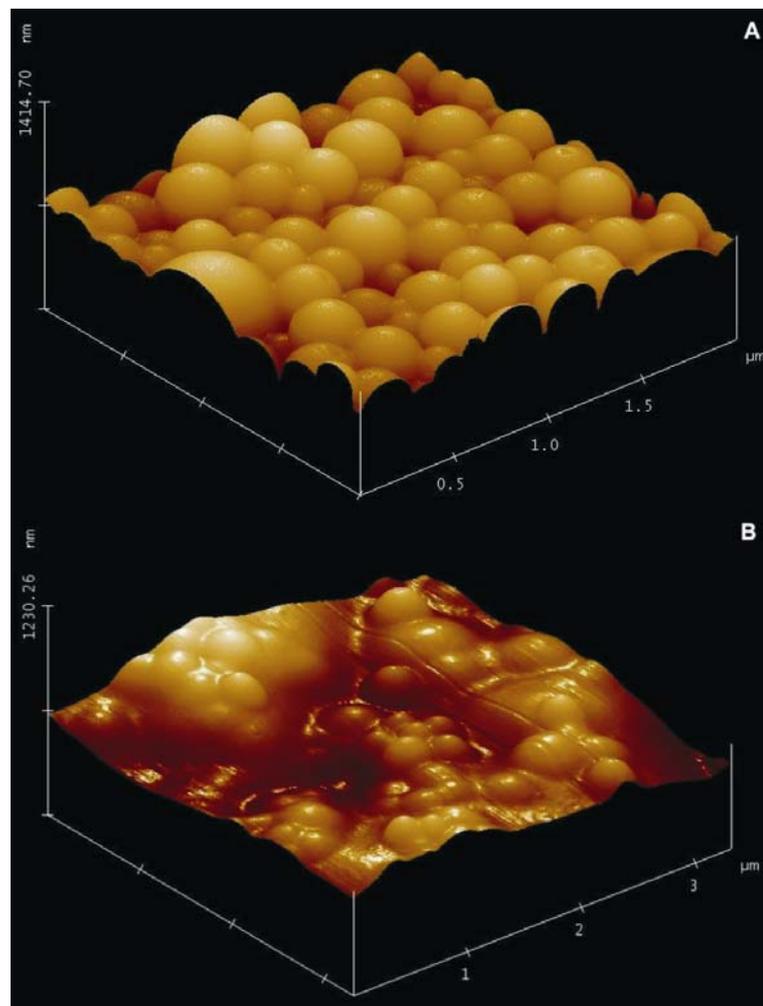

Figure 12: Atomic force microscopy images of flufenamic acid containing nanoparticles: A) aqueous suspension; B) incorporated into Natrosol® a hydrogel

2.4.1. Release experiments

Release experiments have shown very similar profiles for free and nanoencapsulated drug. At approximately 6 hours all the drug content in each formulation have been released See figure 13.
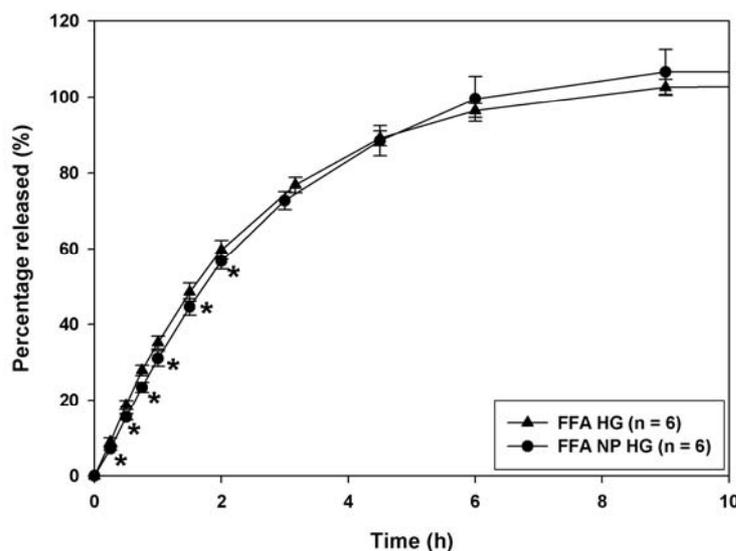

Figure 13: Percentage of flufenamic acid released from FFA HG and FFA NP HG.

2.4.2. Human skin penetration experiments using Saarbrücken model

Stratum corneum: Between the free and the nanoencapsulated drug no statistical significant difference in the amount of flufenamic acid accumulated in the SC, expressed as AUPC, was detected at any incubation time. Furthermore, it is remarkable that there was a slight decrease of the AUPC for both formulations with increasing incubation time (figure 14a).

Deeper skin layers (viable epidermis and dermis): For these layers statistical significant differences in the flufenamic acid amounts between the 2 formulations (t-test, $P < 0.05$) were observed at 3 h and 24 h of incubation time respectively. Interestingly, after 3h higher levels were found for the preparation containing the free drug than for the NP formulation. In contrast, after 24 h this relation was inverted, i.e. a considerably

higher amount of drug has penetrated from nanoparticles compared to the free drug (figure 14b). In addition, a decrease compared with the 6 h values for both preparations was observed, although the same preparations were used. The reason for these results may be addressed to a radial diffusion in the SB-M. Considering that the drug was extracted only from samples obtained from a disk of 13 mm (in diameter) of the stripped area, not all the drug can be detected. For both preparations FFA was detected in the filter paper under the skin, indicative that the sink conditions, which favour the vertical diffusion of the drug, were not maintained completely and therefore could influence the obtained results. However, one can assume that for both experimental series the effect occurs in the same magnitude. Therefore, direct comparison of the nanoencapsulated drug preparation and the free drug preparation at this incubation time is still justified.

2.4.3. Human skin permeation experiments using Franz diffusion cell system

For better comparison, the same time points as chosen in the penetration studies (SB-M) were used in the permeation experiments (FD-C). At shorter incubation times (< 12 h) there were no significant differences in the permeated amount of drug. The levels of the free drug formulation tended to be slightly increased, but the differences were statistically not significant (figure 15). However, for longer incubation times (24 h and later) there was a statistically significant inversion of the drug amount permeated, i.e. more drug had permeated from the nanoencapsulated drug formulation compared to the free drug formulation.
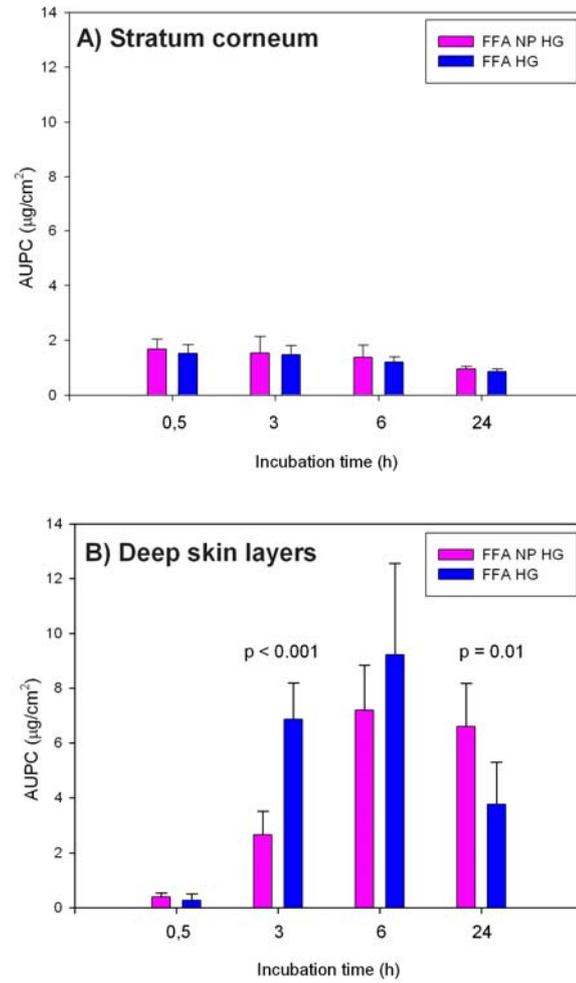
Figure 14: Area under the penetration curve (AUPC) of flufenamic acid penetrated into human skin using a Saarbruecken model at different incubation time (n=6).
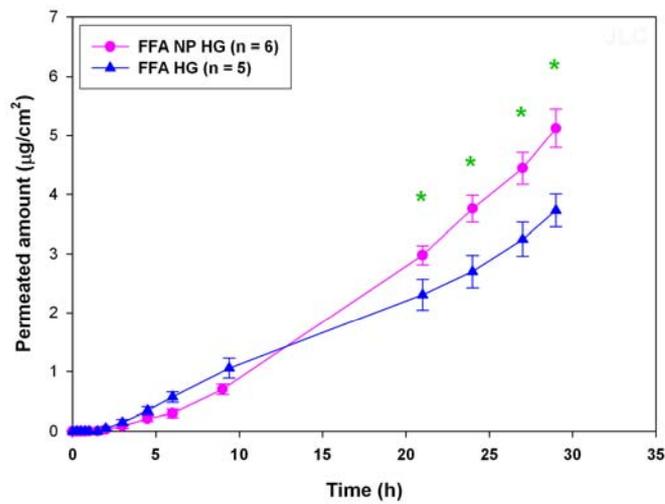

Figure 15: Permeation of flufenamic acid amount through heat-separated human epidermis using Franz diffusion cell system (starred points indicate statistically significant difference).

2.4.4. Visualisation experiments

Multiphoton fluorescence imaging experiments were carried out using a particle-free hydrogel, a hydrogel containing drug-free nanoparticles and a hydrogel with FFA nanoparticles. As expected, the skin shows an auto-fluorescence and structure corresponding to published data [85]. In preliminary studies, it was found that neither FFA in solution nor FFA crystals could be visualised in the hydrogel by this technique. However, nanoencapsulated FFA yielded a fluorescence signal probably due to the fact that the fluorescence of the drug is favoured by the non polar and acidic environment of the polymer (figure 5) [52]. The ostensive size of some of the nanoparticles in the multiphoton images on the order of a few microns is due to (1) the system resolution (dx = dy ≈ 0.4µm, dz ≈ 1µm), (2) partly aggregation and (3) the Brownian motion of the sub-diffraction-limit-sized particles during image acquisition. Transversal drift of the particles led to stretched shapes of their fluorescence spots.

The multiphoton sections taken at different relative depth to the surface (0 to 50 µm) of the human epidermis after treatment with the flufenamic acid nanoparticles formulation showed a consistent lateral and normal uniform distribution of particles on the skin surface and within the dermatoglyphs. But no particles were detected within and between the corneocytes (figure 16 E and F). The particle distribution was not indicative of accumulation in any skin structure at least after 30 minutes of incubation. See figure 16.
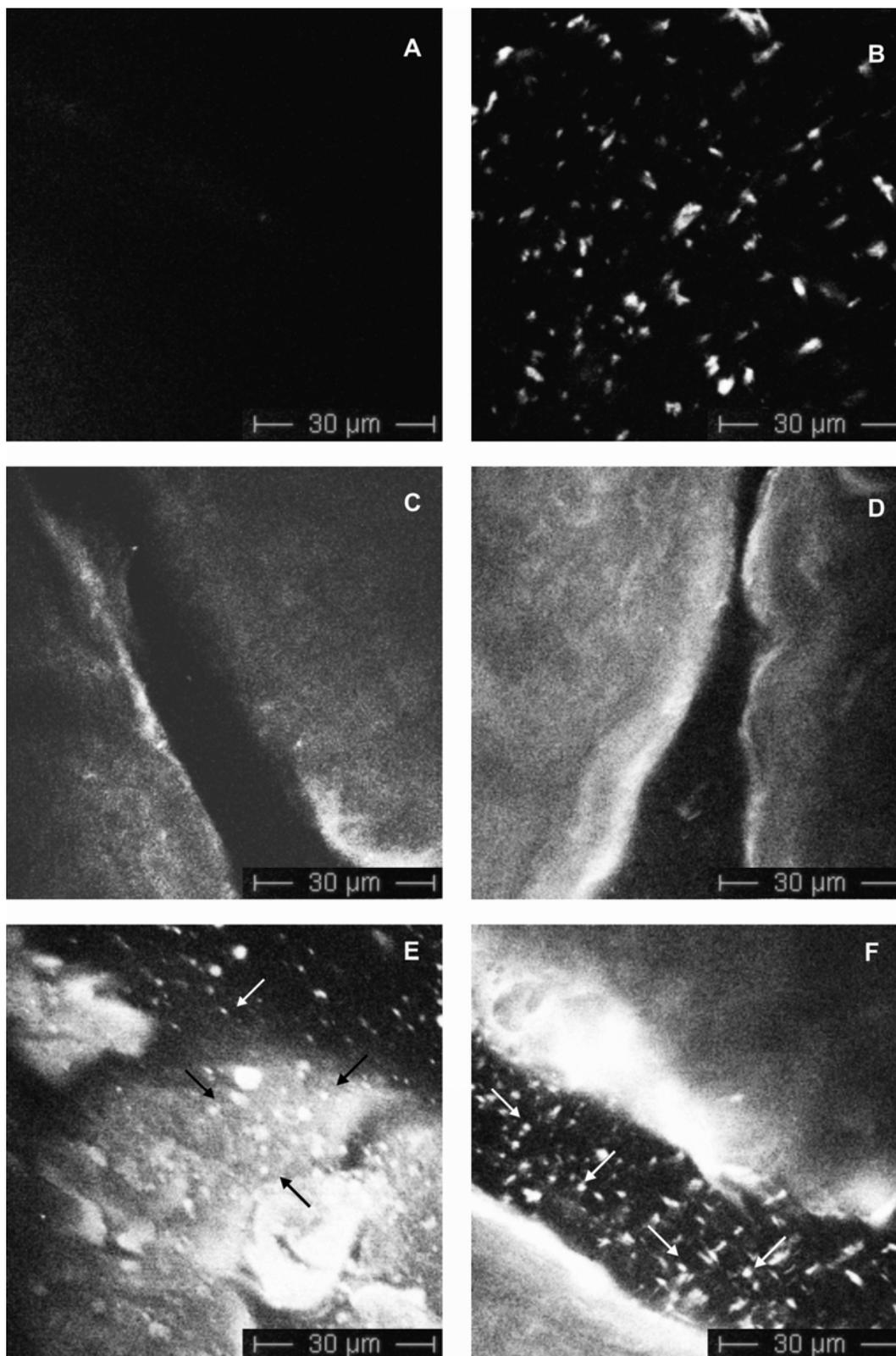
Figure 16: Multiphoton fluorescence imaging of A) plain hydrogel, B) FFA NP HG, C) skin with plain hydrogel, D) skin with drug-free nanoparticles hydrogel, E) skin with FFA NP HG distributed on the surface and F) skin with FFA NP HG in the dermatoglyphs at a depth of 16 μm.

2.5. DISCUSSION

Using the Saarbruecken penetration model no differences in drug transport into the stratum corneum could be detected for the nanoencapsulated compared to the free drug (figure 14). Normally for infinite dose experiments would be expected that the drug amount in the SC reaches a plateau while in the DSL the drug amount increases. In our experiments it is remarkable that a slight decrease of drug amounts for both preparations is visible for the SC. The reason might be a radial spreading of the preparation on the skin specimen surface.

For the DSL the permeation of the drug appeared lower when delivered by nanoparticles in comparison to the free drug preparation in both test systems for relatively short incubation times (<12 h).

In contrast to the results obtained at short incubation times, the proportion of drug transported into the DSL was inverted after longer incubation times (>12 h). A statistically significant higher level of drug was found for the nanoencapsulated drug compared to the free drug with both techniques, the FD-C and SB-M (figure 14 and 15). The mechanisms how nanoparticles increase the amount of FFA at longer incubation times in the DSL remains unclear. Since the overall concentration of the flufenamic acid in the FFA HG and in FFA NP HG is equal, this should not affect the drug transport. However, it may be speculated that the degradation of the particles leads to some release of acidic compounds (lactic and glycolic acid). This acidification of the particles and their surroundings favours the non-ionised form of FFA which penetrates the SC better. pH changes of the PLGA particles due to the degradation has been reported by Fu et al [86] earlier. Furthermore, if particles were able to cross the stratum corneum [80] after a certain incubation time, this could also increase the amount taken up. However, multiphoton fluorescence imaging does not give any hint to this mechanism at least not after short incubation time (30 min).

Our attempts to visualise drug transport into the skin by multiphoton fluorescence microscopy were restricted to the nanoencapsulated drug, while the free flufenamic acid did not yield any fluorescence signal. The distribution of nanoparticles applied to the skin appeared to be homogeneous within the hydrogel and followed the structure of the skin surface and the dermatoglyphs. No hair follicles or sweat glands were observed, so that possible transport of nanoparticles along these structures such as previously reported by others [40, 41, 79] could not be confirmed by this study. At least after the relatively short incubation time of 30 minutes, no particles were detected within or in between the corneocytes. The visualization of drug transport processes for nanoparticles after longer incubation times (>12 h) is still ongoing and subject of further investigations.

In summary, while there were no differences in the SC between free and nanoencapsulated drug, such differences became visible at the level of the DSL. After shorter incubation times (< 12 h), a significantly higher penetration was obtained with the free drug preparation, suggesting that nanoencapsulation causes a slight delay of drug transport, whereas, for longer incubation times (> 12 h) the result was inverted and up to 50% more of drug was transported into the DSL by the nanoparticles compared to the free drug formulation.

2.6. CONCLUSIONS

In this study the effect of the nanoencapsulated flufenamic acid on the skin transport was investigated at different incubation times using permeation and penetration systems (FD-C and SB-M, respectively). For shorter incubation time (< 12 h) a slight delay in the skin transport was observed. In contrast, for longer incubation times (> 12 h) the drug transport was enhanced for nanoencapsulated drug compared to the free drug. Although not yet fully understood, such observation underscores the potential of nanotechnology for transdermal drug delivery.

CHAPTER 3: MECHANISM OF IMPROVEMENT OF TRANSDERMAL DELIVERY BY PLGA NANOPARTICLES

3.1. ABSTRACT

The aim of this chapter was to investigate the pH influence due to the presence of poly(lactide-co-glycolide) (PLGA) nanoparticles in semisolid as well as liquid formulations on the epidermal permeation of the anti-inflammatory drug flufenamic acid (FFA). For this purpose different vehicles, under non-buffered and buffered conditions, and different membranes (human heat separated epidermis and a commercially available reconstituted human epidermal model) were tested. Permeation experiments were performed using static Franz diffusion cells under occlusion.

It was observed that the presence of nanoparticles increased drug permeation across the skin barrier. This effect was stronger applying drug-loaded nanoparticles.

Under different temperature storage conditions it has been observed that suspensions and not gels containing nanoparticles shown a drop on the total pH of the preparations, being time and temperature dependent. The same preparations have shown physical evidence of degradation.

The use of buffered vehicles with different pH values showed the influence of the pH on the permeation behaviour of the FFA. An increased permeated amount with lower pH was determined suggesting an impact on the environmental pH of the biodegradable nanoparticulate carrier system. This drop of pH on the nano-environment of the carrier system was demonstrated and visualized using pH sensitive fluorescent probes.

Having tested the formulations under buffered and non-buffered conditions, it can be concluded that the drop of pH due to the presence of PLGA nanoparticles is the reason for the observed enhanced permeation of FFA through the epidermal barrier, even increasing it more than 10 folds.

3.2.   INTRODUCTION

The stratum corneum have been widely acknowledge as the main barrier to percutaneous absorption of substances, limiting the drug characteristics only to small, moderate lipophilic and highly potent molecules, it is also regarded as the main pathway for penetration through the skin. Although several strategies to improve the cutaneous delivery of active pharmacological ingredients have been investigated (e.g. ionto- and sonophoresis, electroporation, microneedles, supersaturated formulations, micro-emulsions, liposomes, colloidal polymeric suspensions, penetration enhancers, etc.) the cutaneous penetration of highly lipo- and hydrophilic drugs remains a big issue.

Biodegradable polymers have long been of interest in the controlled release technology because of their biocompatibility and bioresorbability by natural pathways, and without the need of the removal of the release device. Polymers derived from lactic and glycolic acid have the property that when degrading in the body their end-products take part in the Krebs cycle, generating atoxic compounds [87, 88]. For this reason they are products of high interest in the drug delivery field. Their degradability can be regulated according to the proportions of the units of lactic and glycolic acid present in every polymer chain, although by the isomers used, as well as, the molecular weight of the latter mentioned. The dissolution conditions of the polymeric device could accelerate or retard the degradation process.

Nanoparticles for pharmaceutical use are in a size range between 10 to 1000 nm. Their small particle sizes determine a large interfacial area, increasing the number of molecules able to be exchanged. Polymeric nanoparticles consist of macromolecular materials and can be used as drug carriers [89]. In various applications nanoparticles have shown advantages over liposomes on their physical increased stability, drug loading capacity, and a controlled release of the active compound [16]. In these devices the drug can be entrapped, dissolved, encapsulated or simply attached to the matrix [80]. During the last years polymeric nanoparticles have attracted considerable attention as

drug delivery devices but only limited biodegradable nanoparticulate systems have been investigated to be used on dermal and transdermal delivery.

The aim of the present work was to elucidate the mechanism how poly(lactide-co-glycolide) (PLGA) nanoparticles improve the permeation of the anti-inflammatory drug, flufenamic acid through the epidermal membrane, considering the results presented in the previous chapter which have shown this effect using PLGA nanoparticles. Following this objective, permeation experiments using loaded and not loaded nanoparticles were performed to examine if the drug must be incorporated into the particle to have the enhancing effect; also the influence of the particle size of loaded nanoparticles was studied. To investigate the effect of the nanoparticles-containing formulations under normal application conditions, finite dose regime was used. The influence of the presence of hair follicles was studied using human heat-separated epidermis and a hair follicle-free reconstituted human epidermal barrier. To investigate the pH effect of the nanoparticles on the permeation improvement through the epidermal barrier, formulations were tested under buffered or non-buffered conditions.

3.3. MATERIALS AND METHODS

3.3.1. Materials

Hydroxy ethyl cellulose (HEC) Natrosol® 250 M (Aqualon, Hercules Inc., DE, USA), Flufenamic acid, modification II (Kali-Chemie Pharma, Hannover, D), Poly(D,L-lactide-co-glycolide) (50:50) with a molecular weight of 40000 to 75000 Da (Sigma Chemical Co., St. Louis, MO, USA), Polyvinyl alcohol (PVA) Mowiol® 4-88 (Kuraray Specialities Europe GmbH, Frankfurt, D), Ringer solution, McIlvaine citric acid phosphate buffer at different pH values, Phosphate buffer (pH 6) (all components from Merck, Darmstadt, D), Sodium hydroxide solution (0.1 M) , Hydrochloric acid (0.1M) (Grüssing GmbH, Filsum, D), Methanol Chromasolv® (Sigma-Aldrich GmbH, Seelze, D), Ethyl acetate (Fluka Chemie GmbH, Bucks, Switzerland), Cellulose membrane MWCO 12000 – 14000 Da (Medicell International Ltd., London, LX, USA) were used as obtained from the suppliers, Arabic gum (Caeser & Lorentz, Hilden, D), Gelatine A (Dt. Gelatine Fabriken, Eberbach, D), n-Octanol and Propanol (Merck, Darmstadt, D), LysoSensor™ Green DND-189 (Invitrogen GmbH, Karlsruhe, D) were used as obtained from the suppliers.

3.3.2. Equipment

HPLC System: Chromeleon™ Version 6,5 SP2, build 968; P580 Pump; ASI-100 automated sample injector; STH 585 Column oven; UVD 170S Detector (Dionex Softro GmbH, Germering, D); Franz diffusion cell type 6G-01-00-15 (Perme Gear, Riegelsville, PA, USA); High-speed homogenizer Ultra-Turrax® T25 (Jahnke & Kunkel GmbH & Co. KG, Staufen, D); Rotavapor® R-205 (Büchi, Flawil,CH); Zetasizer® 3000 HS A (Malvern Instruments GmbH, Herrenberg, D), Confocal laser scanning microscope (CLSM) MRC 1024 (BioRad/Carl Zeiss AG, Jena, D), Atomic Force Microscope Nanoscope IV Bioscope™ (Veeco Instruments, Santa Barbara, CA, USA).

3.3.3. Nanoparticles preparation and characterization

PLGA loaded and drug-free nanoparticles were prepared by solvent extraction method, and characterized using photon correlation spectroscopy (PCS) and atomic force microscopy (AFM), for further details please refer to Section 2.3.3.

3.3.4. Microparticles from PLGA and arabic gum/gelatine A

The PLGA microparticles were prepared using the same composition like the nanoparticles but modifying the homogenization conditions (speed: 8000 rpm and time: 2 minutes).

In brief, the preparation of the arabic gum/gelatine A microparticles was done by dissolving homogenously gelatine A in distilled water. Then n-octanol (several drops) and the dissolved arabic gum were added. Afterwards, distilled water at 50°C was added and the pH adjusted to 4 using acetic acid. After a cooling step over night, the particles are re-dispersed in isopropanol for post-curing and dried.

3.3.5. Non-buffered gel preparations

Flufenamic acid HEC hydrogel (FFA HG) was prepared with flufenamic acid dissolved in water and a minimal amount of sodium hydroxide solution to accelerate the dissolution (that was neutralized later on using hydrochloric acid solution) under vigorous stirring. Afterwards, HEC was added in a proportion equivalent to 1.5% (w/w) and stirred overnight until the polymer was completely swollen. The absence of crystals was determined by microscopic inspection of the gels.

For the preparation of the NP containing gels, the original NP suspension was concentrated by centrifugation as follows: volumes of 20 ml of fresh prepared nanoparticles suspension were centrifuged at 2468xg per 5 min, 15 ml of the supernatant

were removed and the particles re-suspended, and the suspension drug content determined and adjusted.

To prepare a flufenamic acid nanoparticles hydrogel (FFA NP HG) a HEC gel (3% w/w) was mixed with a concentrated aqueous suspension of the nanoparticles in a 1:1 ratio to obtain the same concentration as in FFA HG.

A hydrogel containing drug-free nanoparticles (FFA HG + DF-NP) was prepared using a doubled flufenamic acid and HEC concentration, prepared as described for FFA HG and mixed with a concentrated drug-free nanoparticles suspension in a proportion 1:1.

To the nanoparticles-containing-gels, the same amounts of NaOH and HCl solutions as in FFA HG were added. The presence and integrity of the particles in the gel was confirmed by AFM.

Permeation experiments were carried out in quadruplicate using FFA HG, FFA NP HG and FFA HG + DF-NP, each with a drug concentration of 0.125 ± 0.006 mg/g. The pH of the preparations was 5.4 ± 0.1.

3.3.6. Flufenamic acid saturation concentration in different solutions

The studies regarding the concentration of saturation in varying vehicles were performed as follows: 500 mg of flufenamic acid were placed in a 500 ml volumetric flask and Soerensen phosphate buffer (pH 6.0) and McIlvaine buffer solutions at pH values between 3.4 and 7.4 (for composition, please refer to [90]) were added. Every mixture was stirred at 500 rpm during 48 h at 32 ± 1°C and left sediment during 12 h at the same temperature. Three samples of 10 ml each were taken from each flask and filtered through OptiFlow-PTFE filter (0.2 μm) at the same temperature. The first 7.5 ml were discarded and the last 2.5 ml collected in a separate flask. One millilitre of the filtrated solution was diluted to 100 ml with NaOH 0.05 M and analysed by HPLC.

3.3.7. Buffered gels preparation

Buffered gels were prepared as described above using HEC and buffer solution at different pH (Soerensen phosphate buffer pH 6.0) instead of water, and the respective flufenamic acid, additional drug-free nanoparticles or loaded nanoparticles.

Permeation experiments were carried out by quadruplicate using FFA HG, FFA NP HG and FFA HG + DF-NP, each with a drug concentration of 0.125 ± 0.006 mg/g. The pH of the preparations was those of the respective buffer solution with an error of ± 0.1 unit.

3.3.8. Flufenamic acid solutions and NP suspensions

Non-buffered formulations

A concentrated solution of flufenamic acid of 98.85 µg/ml was prepared in NaOH 0.04 M.

Flufenamic acid non buffered solution (FFA sol), loaded nanoparticles non buffered suspension (FFA NP), and solution containing drug-free nanoparticles non buffered suspension (FFA + DF-NP) were prepared mixing the components described in table 1:

	FFA sol	*FFA NP suspension*	*FFA solution + DF-NP suspension*
FFA concentrated solution	40.464 ml	--	40.464 ml
HCl 0.1 M	1.480 ml	1.480 ml	1.480 ml
NaOH 0.04 M	--	40.464 ml	--
FFA NP concentrated suspension[9]	--	25.536 ml	--
DF-NP concentrated suspension [9]	--	--	25.536 ml
Deionised water to	100 ml	100 ml	100 ml

Table 1: Compositions of flufenamic acid non-buffered formulations.

---

[9] Prepared as described in section 3.3.5

3.3.9. Buffered formulations

One hundred millilitres of McIlvaine concentrated buffers were prepared by the composition describe in table 2:

	pH 5.4	*pH 6.4*	*pH 7.4*
Citric acid monohydrate 0.2 M	44.7	31.4	9.8
Disodium phosphate dihydrate 0.4 M	55.3	68.6	90.2

Table 2: Composition of McIlvaine buffer solutions for flufenamic acid buffered preparations

Flufenamic acid solution (FFA sol), loaded nanoparticles suspension (FFA NP) and containing drug free nanoparticles buffered formulations were prepared as follows: Buffer solution and water were mixed with the drug and stirred overnight to allow the drug to be dissolved, afterwards nanoparticles concentrated suspension was added to the mixture (when corresponds). See composition in table 3.

	FFA sol	*FFA NP suspension*	*FFA solution + DF-NP suspension*
	FFA sol	**FFA NP**	**FFA + DF-NP**
Concentrated buffer	50.000 ml	50.000 ml	50.000 ml
Flufenamic acid	4000 µg		4000 µg
FFA NP concentrated suspension[10]		25.536 ml	
DF-NP concentrated suspension[10]			25.536 ml
Deionized water to	100.000 ml	100.000 ml	100.000 ml

Table 3: Composition of flufenamic acid buffered preparations.

For determination of the drug concentration all preparations were extracted and diluted with NaOH 0.05 M and samples were analysed by HPLC. The concentration of all liquid formulations was in the range of 37.6 ± 1.9 µg/ml.

---

[10] Prepared as described in section 3.3.5

3.3.10. Skin preparation

See method described in section 2.3.5.

3.3.11. Heat separated epidermis preparation

See method described in section 2.3.6.

3.3.12. Degradation of nanoparticles hydrogels and suspension

Degradation of particles was studied in hydrogels and suspension by visualization using atomic force microscopy (AFM) and at the same time pH of the preparations was measured using an electrode pHmeter. The later mentioned formulations were stored at different conditions: 4°C, room temperature and 32°C, protected from the light. Samples at different time points were collected during several weeks and analysed.

3.3.13. Permeation experiments

Using static Franz diffusion cells (FD-C), experiments were carried out using heat-separated epidermis mounted on a cellulose membrane disk, or reconstituted epidermis, as membrane. The membrane was positioned between the donor and acceptor compartment. As donor 0.75 ml of the gel or 1 ml of solution or NP suspension for infinite dose experiments, and approx. 18 mg of gel for finite dose experiment (exact weight was noticed and used for the calculations). As receptor 12.1 ml of Soerensen phosphate buffer (pH 7.4) were used. The donor compartment was sealed with aluminium foil and the system was maintained at (32 ± 1) °C in a water bath. The acceptor fluid was stirred using a magnetic bar at 500 rpm. At predetermined time intervals, samples of 0.3 ml were collected from the acceptor medium and replaced immediately with fresh buffer solution. Samples were collected until 30 h and analysed by HPLC.

3.3.14. HPLC method

See method described in section 2.3.11.

3.3.15. Determination of apparent permeation coefficient

Apparent permeation coefficient (P_{app}) values were calculated from an equation derived from the Fick's first law assuming perfect sink conditions in the system (i.e. the FFA concentration does not exceed the 10% of its saturation concentration in the receptor compartment), see equation 1. The flux at steady state (J_{ss}) was calculated from the slope of the linear portion of the cumulative amount per area unit versus time plots (for HSE the points between 3 and 9 hours and for SkinEthic[®] points between 2 and 6 hours were considered). C_v parameter corresponds to the concentration of the donor.

$$P_{app} = \frac{J_{ss}}{C_v}$$

Equation 7: Apparent permeation coefficient of the epidermal barrier using infinite dose under steady state conditions

3.3.16. Enhancement factor calculation

Enhancement factor (E) was calculated using the P_{app} values of the different preparations (n) respect to the dissolved drug containing formulation (FFA HG or FFA sol as reference (ref) when corresponds).

$$E = \frac{P_{app}^{n}}{P_{app}^{ref}}$$

Equation 8: Enhancement factor calculation using the apparent permeation coefficient of the different formulations respect to that containing dissolved drug

3.3.17. Local pH measurements using confocal laser scanning microscopy measurements

For the measurement of the local pH the particle suspensions' pH were adjusted roughly to pH = 7 using sodium hydroxide. Hereafter, 10 µl of the suspension were mixed with 10 µl of a 0.1 mM LysoSensor™ solution. The mixture was given on a microscope slide and sealed with a cover slip using nail polish. The fluorescence measurements were performed using the 488 nm line of the argon/krypton laser line and a band pass filter (522/35) for each of the particle suspensions. Transmission light images were taken using a conventional light bulb with the red channel of the CLSM.

3.3.18. Statistical evaluation

For statistical evaluation, SigmaStat 3.0.1 was used. ANOVA test were run using "all pairwise comparison procedure" (Holm-Sidak method). Significance level $p < 0.05$.

3.4.   RESULTS AND DISCUSSION

3.4.1. Infinite dose permeation experiments using hydrogels and heat separated human epidermis

Infinite dose permeation experiments using FFA hydrogels containing the drug as dissolved form, either in the presence or in the absence of drug-free NP, or as drug loaded NP, were performed to investigate the influence of nanoparticles on the dermal permeation of the highly lipophilic drug, flufenamic acid. The high lipophilicity of the drug (log P = 4.88) [52] and its ability to dissociate under dermal physiological conditions (pK_a = 3.9) [53] makes it a good candidate to be absorbed through the skin.

As shown in figure 17 an increase in the permeation of flufenamic acid from a hydrogel through the complete epidermis into an aqueous medium was observed when the drug was loaded into PLGA nanoparticles. When drug-free nanoparticles were co-administered an intermediate effect, between dissolved drug and loaded nanoparticles, was observed. At the same time, the particle size seemed to have a minor influence in the permeation profile of the drug when loaded nanoparticles were used.
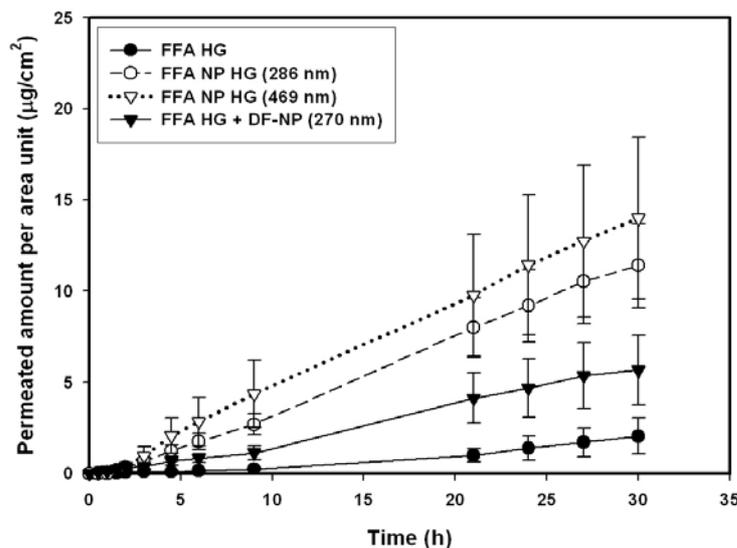

Figure 17: Heat separated human epidermis permeation profiles of flufenamic acid using infinite dose regime of non buffered hydrogels containing: dissolved drug (FFA HG), loaded nanoparticles of different size (FFA NP HG), and dissolved drug with drug-free nanoparticles (FFA HG + DF-NP).

Several explanations for the increased permeation might be possible: (i) the nanoparticles are able to cross the epidermis through the hair follicles (27 ± 3 μm in diameter), inducing a higher permeated amount of FFA in the receptor medium. Hair follicle targeting using inorganic and polymeric nanoparticles, has been demonstrated by several authors, as Lademann and Toll [41, 44], as one of the mechanisms how nanoparticulate carriers could increase the drug delivery into the deeper skin layers. In the case of the drug-free nanoparticles, their more lipophilic nature compared with the hydrogel might lead to an adsorption of drug on the surface of the nanoparticles. In this form they could cross the epidermal barrier using the same pathway than the loaded ones; (ii) on the other hand, particles could release some degradation products (lactic and glycolic acid) to the hydrogel that could change the ionization state of the drug or modify the permeability characteristics of the stratum corneum, improving the permeation of FFA through the epidermal barrier. To evaluate those hypothesis further additional experiments were carried out.

3.4.2. Infinite dose permeation experiments using hydrogels and reconstituted human epidermis (Skinethic®)

Trying to elucidate the mechanism how the PLGA nanoparticles increased the permeation through heat separated epidermis, experiments were carried out using a reconstituted human epidermal equivalent, SkinEthic®, as barrier and the same hydrogels containing different sized FFA NP, dissolved drug and the latter mentioned containing drug-free nanoparticles. SkinEthic® is a human reconstructed epidermal model, highly permeable [91-93] and devoid of hairs and hair follicles. If the penetration enhancement of FFA in the presence of NP as observed in natural human HSE involves hair follicles, lower or no differences among the formulations were expected for the reconstituted human epidermis. But in contrast to these considerations, FFA permeation differences were accentuated with respect to those observed using human HSE when nanoparticle-containing formulations were used (see figure 18). Now FFA permeation

reached almost 100% of the applied dose permeated. The described results suggested that the mechanism proposed by Lademann and Toll was not exclusively responsible for the increased permeation using nanoparticles.
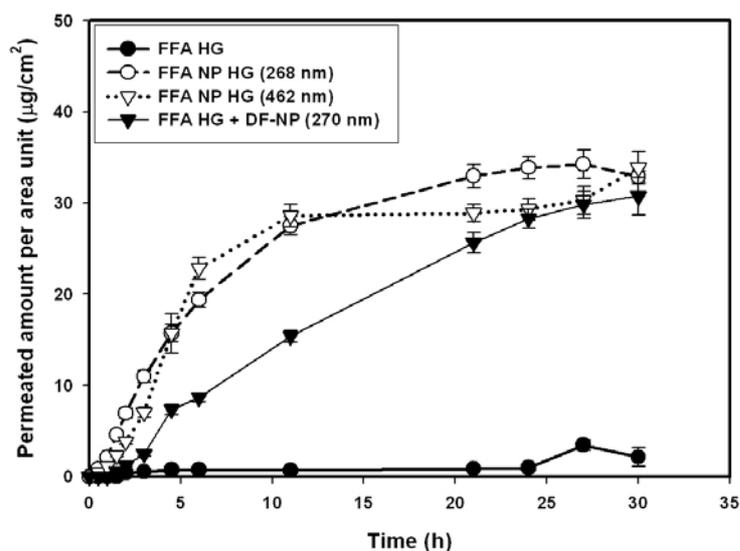

Figure 18: Reconstructed human epidermis (SkinEthic[®]) permeation profiles of flufenamic acid using infinite dose regime of: dissolved drug hydrogel (FFA HG), loaded nanoparticles hydrogel of different size (FFA NP HG), and dissolved drug with drug-free nanoparticles hydrogel (FFA HG + DF-NP)

3.4.3. Finite dose permeation experiments using hydrogels and heat separated human epidermis

Finite dose permeation experiments were performed using different sized FFA NP HG compared with free drug containing HG. Again the same trend as in infinite dose experiments was found, i.e. a higher permeation for the nanoparticle-containing formulation. However, the differences failed to reach statistical significance (see figure 19).

Only weak differences might be a result of the rapid depletion of the donor phase due to the small amount applied.

In view of the fact that some similar penetration enhancement was observed both for natural and reconstituted (i.e. follicle free) epidermis, as well as under infinite and finite dose conditions, led us to the following hypothesis. The degradation of the nanoparticles generates a lower pH microenvironment around the particles, favouring the non-ionized form of the drug, which is able to cross the barrier easier than the ionic form. This idea is supported by the results obtained by different research groups during the last years, detailed as follows: (i) PLGA microparticles develop a strongly acidic core when particles are incubated in a buffered medium over several days [86]; (ii) the smaller the size of the carrier is (e.g. 15 ↔ 40 nm), the faster the diffusion of degradation products (lactic and glycolic acid) to the medium become [94, 95]; (iii) PLGA 50:50 has a very fast degradation rate which can be influenced by the medium conditions (e.g. pH, temperature) [87, 88, 96]; (iv) the degradation products (lactic and glycolic acid) are able to modify the permeation characteristics of the epidermal barrier [97, 98]. To substantiate this hypothesis, the following experiments were carried out to elucidate if the pH generated by the nanoparticles has any influence on the permeation through the epidermal barrier.
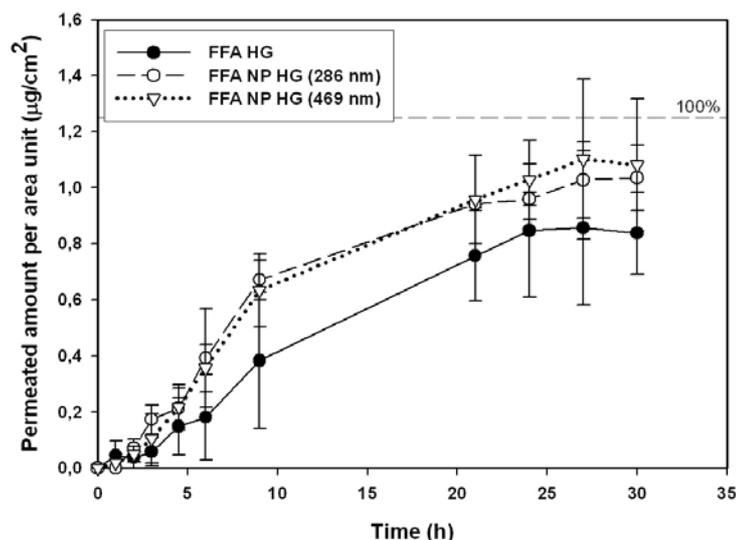

Figure 19: Human heat separated epidermis permeation profiles using finite dose regime of dissolved drug (FFA HG), different size loaded nanoparticles (FFA NP HG), and dissolved drug with drug-free nanoparticles (FFA HG + DF-NP) containing hydrogels.

3.4.4. Flufenamic acid saturation concentration in different solutions

Solvent		Saturation concentration (µg/ml)	Ionized percentage (%)
Water		5.8 ± 0.8	
Soerensen buffer	pH 6.0	29.4 ± 0.4	99.21
Mc Ilvaine buffer	pH 3.4	1.8 ± 0.2	24.00
	pH 4.4	5.6 ± 0.5	75.97
	pH 5.4	43.1 ± 1.8	96.93
	pH 6.4	383.4 ± 14.2	99.68
	pH 7.4	2896.1 ± 55.9	99.97
Soerensen buffer	pH 7.4[11]	2059.5 ± 21.6	99.97

Table 4: Saturation concentration and ionized percentage of flufenamic acid in different solvents at 32 °C (mean ± SD)

The saturation concentrations in different solutions at different pH values were determined, and the theoretical percentages of ionized drug at every pH were calculated. The results are described in table 4:

It can be seen that at different pH values the solubility of the drug changes as well as its thermodynamic activity, a fact that will influence the drug transport through the epidermis.

3.4.5. Formulation pH and particle degradation

The pH values were measured in non-buffered suspension and gel during two weeks after preparation to determine the influence of the storage temperature on the stability of the preparation. It was noticed that in suspensions the pH values dropped of one unit when the formulation was stored at 32°C, an intermediate effect was observed

---

[11] Data obtained from Henning, A. 2005

at room temperature, and only a slight drop of the pH of 0.1 units when stored at 4°C (see figure 20A) was found.

When pH was measured in the gels, stored under the same conditions, it was noticed that the decrease on pH was not as evident as has been observed with the suspension (see figure 20B).This could be due to the reduced mobility of the hydrogen ions in the gel that cannot be detected by the electrode or that the degradation of the polymer is not so fast as in suspension.

Visualization studies using AFM has shown that the degradation process in gels is not as fast as in the suspension at 32 °C (Figure 21)[12]. At 4 °C the rate of degradation is much slower and at the end of the experience particles have the same appearance than at week 1 (data not shown). At week 4, also pore formation and fusion of the particles appeared as has been observed before by Panyam et al using protein loaded PLGA nanoparticles. Finally at week 6, no particles were found in the suspension, and in the gel there were still some particles in the last degradation stages. Panyam et al have demonstrated that an increase in the particle size results in a decrease in the degradation rate of the particles. Moreover, and a biphasic degradation profile with a higher initial degradation rate followed by a second slower phase, were pores and fusion of the particles was observed, probably due to the easier diffusion of the degradation products out of the particles [99]. It may be speculated that particularly the initial fast degradation could influence the permeation of flufenamic acid through the epidermal barrier.

---

[12] Mrs. Noha Nafee (Department of Biopharmaceutics and Pharmaceutical Technology, Saarland University) is thanked for the atomic force microscopy pictures
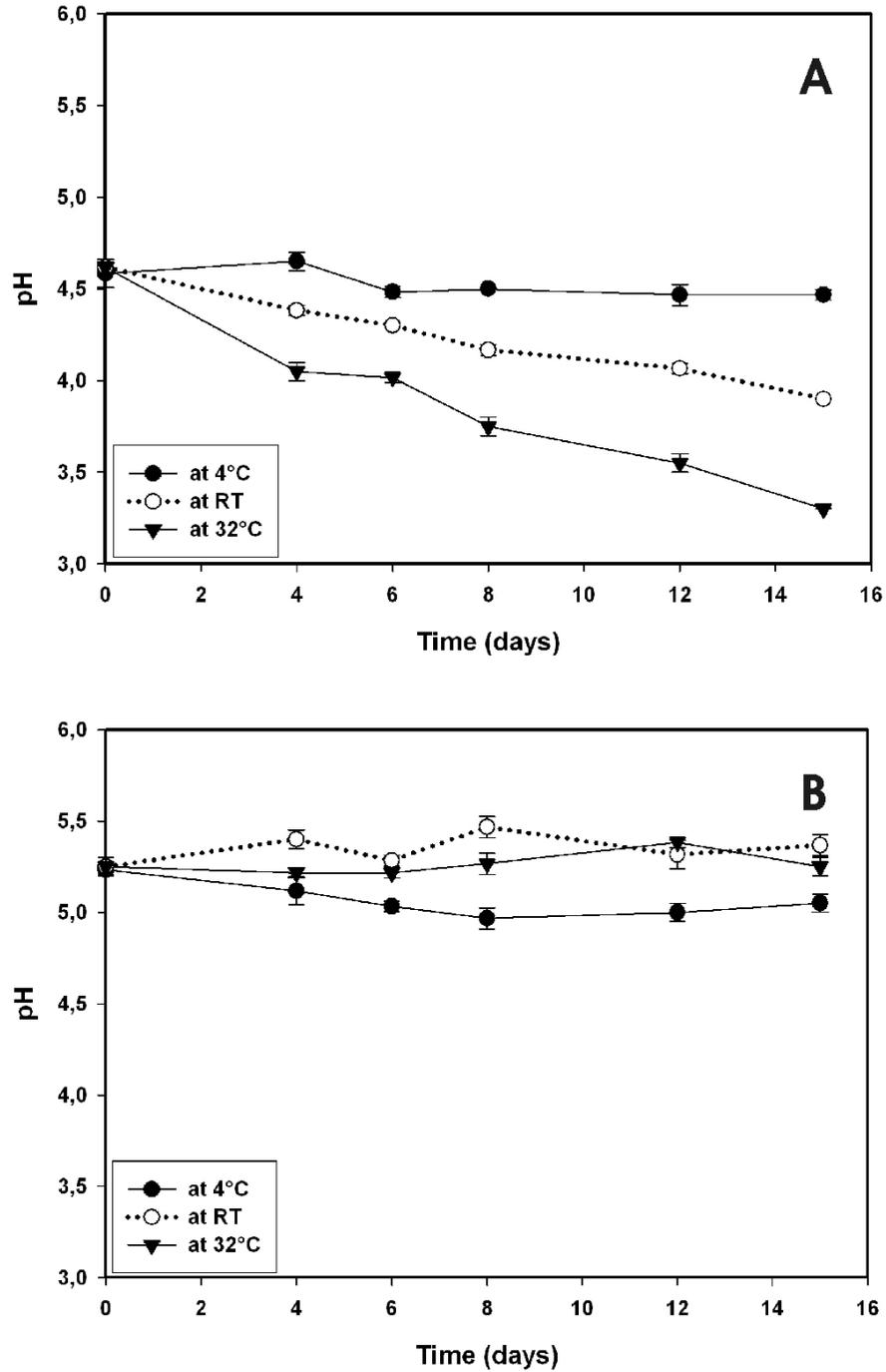
Figure 20: pH variation according to the storage temperature versus time of FFA NP suspension (A) and FFA NP containing hydrogel (B)
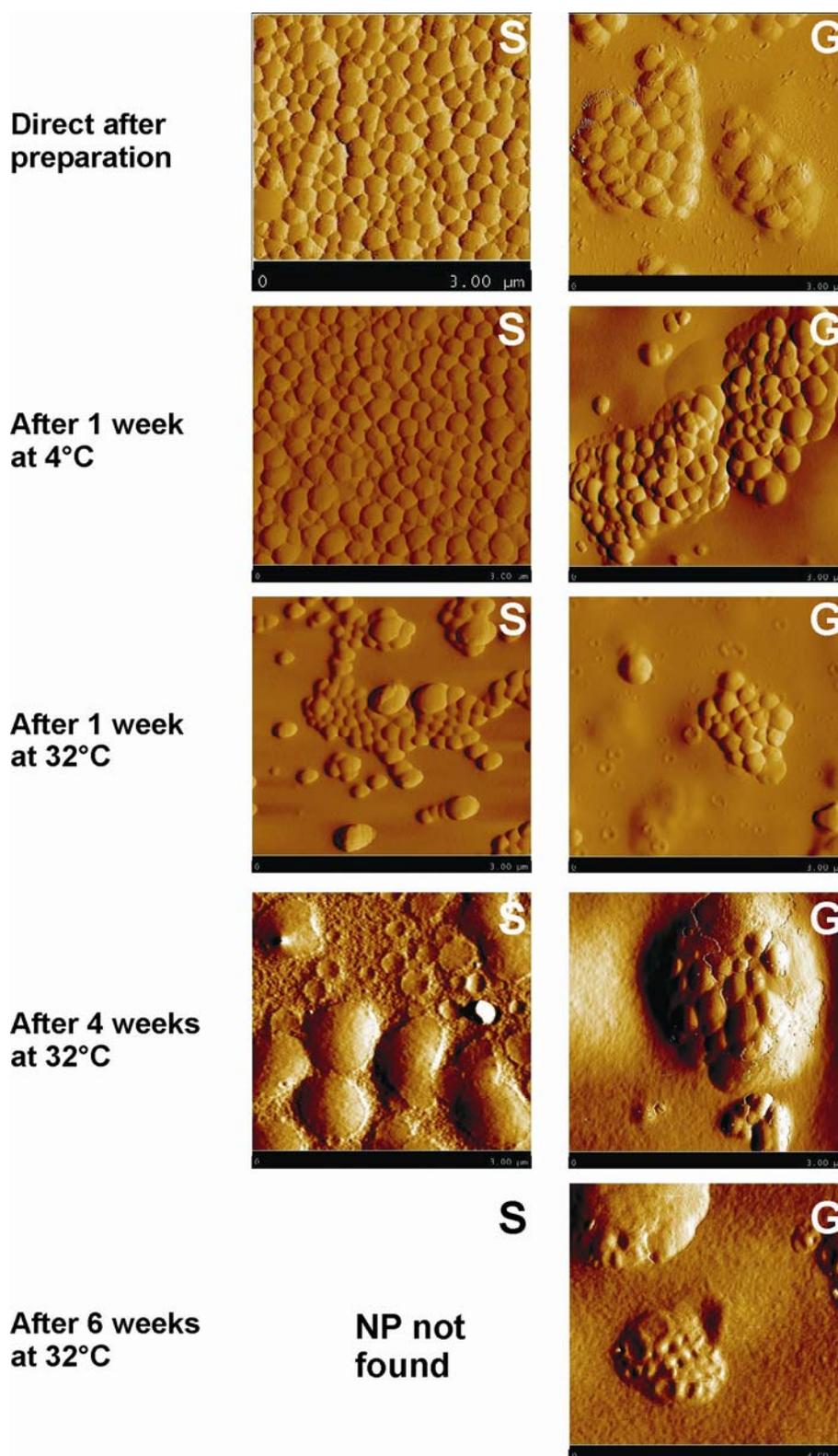
Figure 21: Atomic force microscopic pictures of nanoparticles degradation in suspension (S) and hydrogel (G) media at different time and temperature conditions

3.4.6. Infinite dose permeation studies using buffered hydrogels and heat separated human epidermis

To examine the influence of the pH and buffered systems, permeation experiments were carried out using buffered gels containing the same amount of drug but with adjusted pH values. When hydrogels containing Soerensen phosphate buffer at pH 6.0 were investigated an extremely high increase in the permeation, especially using the formulation containing the dissolved drug (see figure 22) was found. Two possibilities could be responsible for those results: the buffer compensated the effect of the nanoparticles on the skin or the buffer system influenced the barrier properties of the skin, inducing a higher permeation of the dissolved drug.

Under steady state conditions apparent permeation coefficient values (P_{app}) were calculated from the above mentioned infinite dose experiments (see table 5). Comparing the P_{app} values it was possible to observe that: non-buffered conditions, the use of HSE and the application of loaded nanoparticles increased the permeation approximately 8 fold compared to the administration of dissolved drug while the application of non loaded nanoparticles increased it only 3 fold. When reconstituted human epidermis was used the increase in flux was approximately 50 fold with loaded nanoparticles and almost 30 fold with non-loaded ones. When a buffered system and HSE was used an unclear tendency (pH 6) of the effect of the particles presence was observed. These results suggest that buffer systems are able to compensate the effect of the nanoparticles on the skin permeation of the drug.
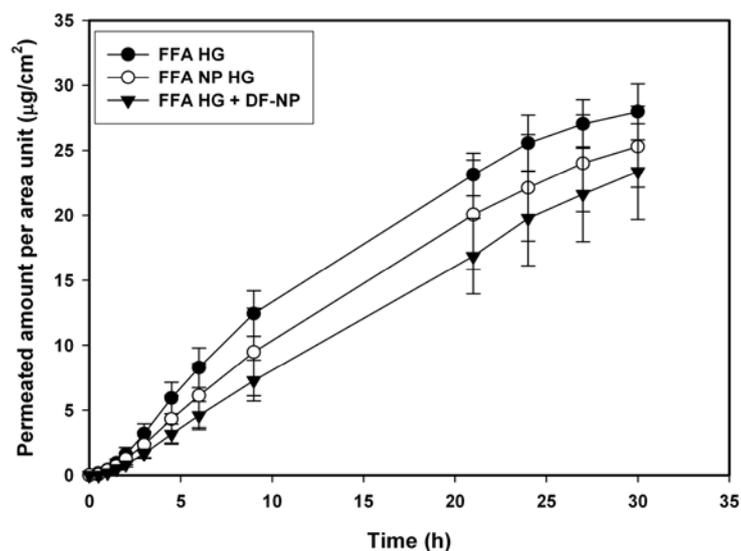
Figure 22: Human heat separated epidermis permeation profiles of a pH 6.0 buffered hydrogel using infinite dose regime of preparations containing flufenamic acid as dissolved drug (FFA HG), loaded nanoparticles (FFA NP HG), and dissolved drug with drug-free nanoparticles (FFA HG + DF-NP)

		FFA HG	*FFA NP HG (286 nm)*		*FFA NP HG (486 nm)*		*FFA HG + DF-NP*	
		P_{app}	P_{app}	E	P_{app}	E	P_{app}	E
HSE	Non buffered pH 5.4	0.6 ± 0.3	4.7 ± 0.9*	8	7.6 ± 3.0*	13	1.8 ± 0.6	3
SE		1.1 ± 1.2	48.5± 1.8*	44	77.0 ± 3.7*	70	31.2 ± 1.6*	28
HSE	Buffered pH 6.0	24.4 ± 2.7	18.3 ± 6.0	0.8	----	---	14.7 ± 3.1*	0.6

Table 5: Apparent permeation coefficient (P_{app}) of flufenamic acid through human heat separated epidermis (HSE) and reconstituted human epidermal model, SkinEthic® (SE), and enhancement factor (E) respect to the dissolved drug containing formulation (FFA HG), using hydrogels in infinite dose regime. P_{app} values are expressed as 10^{-6} cm/s (mean ± SD). Statistical significant difference is marked with a star.

3.4.7. Permeation studies using non-buffered and buffered solutions and nanoparticles suspensions

To rule out the influence of the gel forming agent over the skin permeation it was decided to apply a solution and/or nanoparticles in suspension in a non-buffered and buffered form at different pH values.

Similar results to those observed using non-buffered hydrogels where obtained when non-buffered solution or NP suspension were tested (see figure 23 NB): a higher permeation using loaded nanoparticles, an intermediate effect when non-loaded particles were added to a drug solution and the lowest permeation was obtained with the drug in dissolved form. These results confirmed that the gel forming agent has no influence on the permeation of FFA through the epidermal barrier.
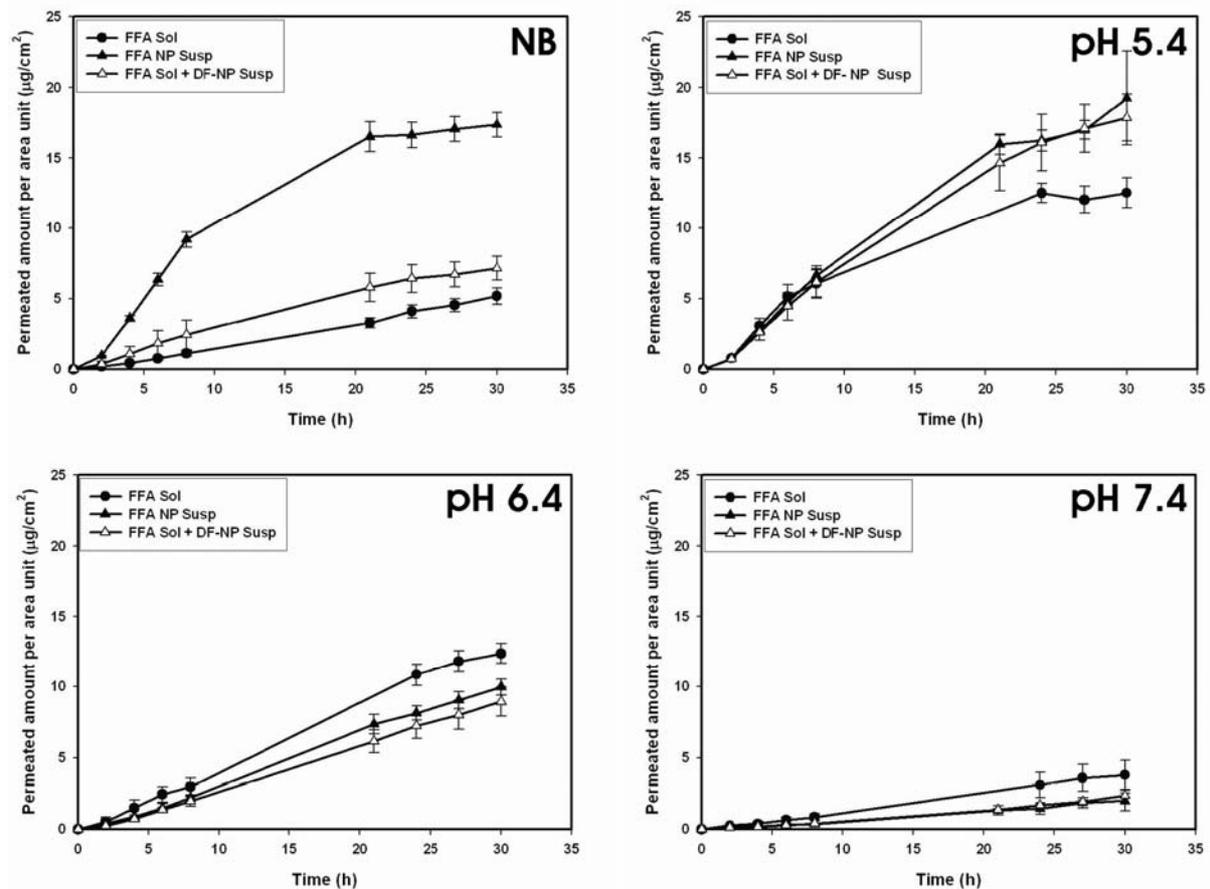
Figure 23: Human heat separated epidermis permeation profiles using flufenamic acid solution (FFA sol), FFA solution containing drug-free nanoparticles suspension (FFA sol + DF-NP susp) and loaded nanoparticles suspension (FFA NP susp) as non-buffered preparations (NB) and buffered at different pH values

The summarized results were compared with those obtained using the same above mentioned preparations at different pH values (see figure 23). In all cases, a decrease of the permeation in combination with an increase of the pH value was observed. Additionally it was found that when non-buffered preparations were used, permeation of the flufenamic acid solution show a similar permeation to the higher pH value (pH 7.4), the solution containing drug-free nanoparticles to the intermediate pH value (pH 6.4) and the loaded nanoparticles to those with the lower pH value (pH 5.4).

Considering that the measured pH of the non-buffered preparations was in the range of 5.8 ± 0.2 these results confirmed the hypothesis that the nanoparticles have an influence on the pH and hence modify/influence the permeation behaviour of the drug. As proved by Fu et al, PLGA particles suspended in a buffered medium are able to create an inner acidic environment due to the polymer degradation which is more pronounced for smaller than larger particles [86]. Additionally, a change of the acidity was demonstrated for non-buffered systems over a time period of several days. Therefore, these carriers might be able to create an external micro-surrounding acidic environment that could increase the amount of non-ionized drug available for the permeation through the epidermal membrane when the nanoparticles are in contact with it.

The P_{app} of flufenamic acid through the HSE using non buffered solutions and suspensions have approximately the same magnitude than with the hydrogel preparations (see table 6), increasing approx. 8 and 3 folds, respectively, when loaded nanoparticles and drug-free nanoparticles were used (values relative to the flux obtained with flufenamic acid solution). When buffered preparations were used no differences among them at one determined pH were observed. When the same preparation at different pH values was compared in all cases, i.e. flufenamic acid solutions, loaded nanoparticles suspensions and solutions containing drug-free nanoparticles, an increase of approx. 4 and 10 or more folds was observed when pH decrease around 1 or 2 pH

units. These findings indicate that the pH which was generated by the presence of the particles in the non-buffered systems induces a low pH region only in the interior of the particle or the close surrounding.

Some authors investigated the mechanism how α-hydroxy acids can reduce the stratum corneum cohesion, favouring the increase of permeation of drugs across the skin. E.g. Sebastiani et al have studied the effects of lactic acid on the skin permeation using rabbit skin. Three drugs with different physicochemical characteristics were examined proving that only the passive permeation of ibuprofen, an anionic drug (characteristic present also in flufenamic acid), was affected by the presence of lactic acid, increasing its permeation by several-fold, suggesting an increase in the partitioning from the formulation to the skin, and assuming that the diffusion pathway remained unchanged [98].

		FFA solution	*FFA NP suspension*		*FFA solution + DF-NP suspension*	
		P_{app}	P_{app}	E	P_{app}	E
Non Buffered	**pH 5.8**	1.1 ± 0.2	10.0 ± 0.7*	9	2.4± 1.1*	2
Buffered	**pH 5.4**	11.2 ± 2.0	7.4 ± 0.5*	0.7	6.6 ± 1.3*	0.6
	pH 6.4	2.9 ± 0.5	2.2 ± 0.3	0.8	2.0 ± 0.4*	0.7
	pH 7.4	0.7 ± 0.2	0.6 ± 0.8	0.9	0.3 ± 0.1	0.4

Table 6: Apparent permeability coefficient (P_{app}) of flufenamic acid through human heat separated epidermis using a solution, a suspension of loaded NP or a solution containing drug-free NP, and enhancement factor (E) respect to the dissolved drug containing formulation (FFA solution). P_{app} values are expressed as 10^{-6} cm/s (mean ± SD). Statistical significant difference is marked with a star.

3.4.8. Investigation of the nanoparticles surface pH changes

To investigate the possible micro-surrounding acidic environment experiments using confocal scanning microscopy were performed. The pH change might take place only in the very close (nano-) environment of the particles. However, the resolution is limited because the optical transfer function will depict objects smaller than the resolution at a dimension which equals the so-called "Airy disc". For the application of fluorescence-based methods such as pH-sensitive dyes the local resolution is therefore also limited and will exceed the extension of the area where the pH change might take place. To overcome these problems regarding the particles, we used PLGA microparticles in the range of several micrometers. This facilitated the investigation of the pH on the surface only. As a negative control arabic gum/gelatine A microparticles were deployed. The use of a dye like the LysoSensor® enables one at least to visualize if different pH values are established even though the precise local determination is not accessible. The LysoSensor® dyes are known as acidotropic compounds. For pH-values above the pK_a the dye is unprotonated and the fluorescence is quenched. Therefore, the dye chosen exhibits practically no fluorescence in neutral surrounding. In acidic environment the molecules are protonated and the fluorescence quenching is relieved; light emission is strongly increased. The images depicted in figure 6 reveal a strong fluorescence around the microparticles and indicate that our assumption regarding the particles' pH is correct. Image 24A) reveals the presence of the arabic gum/gelatine A particles in transmission light whereas in 24B) no fluorescence can be seen e.g. the particles do not change the pH of the dye solution. For the PLGA micro- and nanoparticles testing the background fluorescence was reduced, pre-setting the pH to approximately 7 (The situation is sketched in fig. 24C: particles in a slightly fluorescent solvent). The result changes completely exposing the PLGA particles to the same surrounding and measuring conditions as described before. An intense fluorescent signal (fig. 24 D and E) was observed. Due to the resolution limits, PLGA microparticles were used to demonstrate the location where the fluorescence is originated from. The microparticle fluorescence

discloses that the light is emitted from/or close to the surface of the particles. The inner particle shows fading fluorescence indicating the absence of fluorescent molecules and due the optical transfer function of the microscope. For the PLGA nanoparticles used throughout the other experiments the fluorescence is observed as well but due to their size only fluorescent spots are visible (fig. 24E). The results indicate clearly the different pH values at the particles' surface or close environment compared to other particles[13].
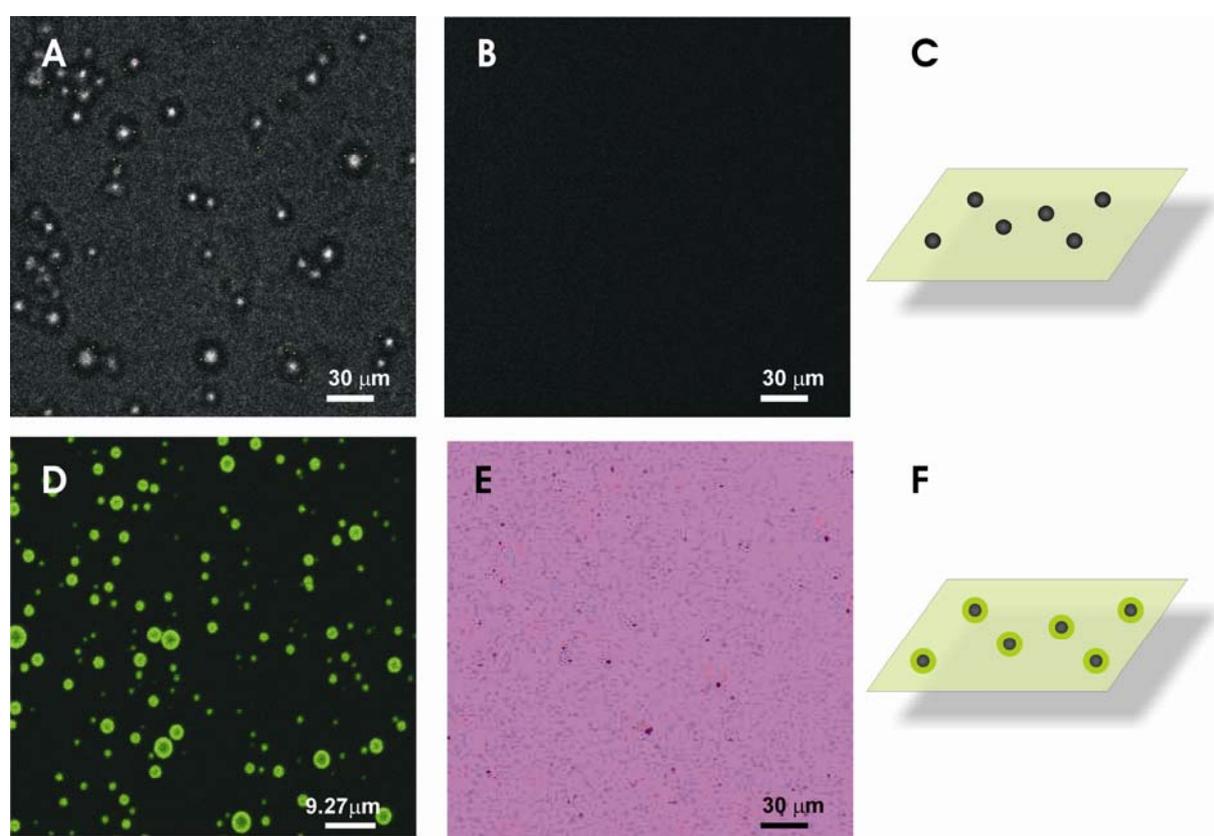
Figure 24: Fluorescence images obtained immersing different particle fractions into the pH sensor solution. Transmission light image to detect the presence of the arabic gut/gelatine A paricles (A) and the corresponding fluorescence image (B). PLGA microparticles show green fluorescence localized at the surface of the particles or the close surrounding (D). In the case of nanoparticles fluorescent spots were observed (E). To highlight the particles the color coding was changed so that the particles appear as black spots on a pink background. The situation was sketched to illustrate the experimental condition (C, F)

3.5. CONCLUSIONS

The increased permeation of flufenamic acid through the epidermal layer under different conditions indicated that PLGA nanoparticles improve its transdermal delivery. The results suggest that these carriers have a pH effect that influence the ionization state of the drug and could improve the concentration gradient from the stratum corneum to the dermal side of the barrier as well as have a penetration enhancing effect due to the degradation products.

CHAPTER 4: *IN VIVO* ABSORPTION OF FLUFENAMIC ACID USING DERMAL MICRODIALYSIS: THE EFFECT OF PLGA NANOPARTICLES - PRELIMINARY STUDY

The experiments presented on this chapter were made in collaboration with Prof. Dr. Carlos von Plessing (Departamento de Farmacia) and Prof. Dr. Jacqueline Sepúlveda (Departamento de Farmacología) from Universidad de Concepción, Chile.

4.1. ABSTRACT

It has been demonstrated *in vitro* that PLGA nanoparticles are able to improve the permeation and penetration of drug through the skin. In order to obtain a first insight in the pharmacokinetic profile *in vivo*, skin microdialysis experiments were carried out. Rats were chosen as model to get a first approach of the absorption of flufenamic acid using non-buffered hydrogel containing: dissolved drug, loaded nanoparticles or a mixture of dissolved drug and drug-free nanoparticles.

Unfortunately, no concluding results were obtained from the experiments performed, indicating that many of the experimental parameters must be adjusted to get more information about the flufenamic acid pharmacokinetic using PLGA nanoparticles as transdermal carrier.

4.2.   INTRODUCTION

As shown in chapters 2 and 3, *in vitro* experiments the permeation through heat separated epidermis, using two-compartment static Franz-type diffusion cells (FD-C), and the penetration into full thickness skin, using Saarbruecken model (SB-M), of the model drug flufenamic acid, a highly lipophilic drug, was improved by the use of loaded and drug free nanoparticles. Therefore, arises the question to what extent this effects will persist under *in vivo* conditions.

Among the most critical limitations of the last mentioned *in vitro* methods is the lack of elimination routes in terms of vascular system and viable metabolising enzymes, alterations of the stratum corneum (SC) due to the water uptake and the determination of permeation instead of penetration, last two apply in case of FD-C.

In another hand, to obtain clinically relevant information about the pharmacokinetics profiles in the skin, *in vivo* techniques must be applied. One of the most used techniques has been tape stripping, technique which removes the SC cell layers by consecutive adhesion of tape peaces. Another techniques such as, suction blisters, tissue biopsy and dermal imaging techniques such as confocal laser scanning microscopy have been also used. Their main disadvantages are that only assesses the penetration of the drug into the SC, which normally is not the target of dermal drug delivery, and only determine a single concentration-time point. Additionally they need a large number of sampling sites on a particular subject, therefore increasing the invasiveness involved [67, 100].

During the last decade microdialysis has been successfully applied to assess cutaneous drug delivery of numerous substances. This technique has been shown to be minimally invasive and supply pharmacokinetic information directly in the target organ for cutaneous drug delivery with high temporal resolution without further intervention with the tissue after implantation. This technique uniquely enables the assessment of drug levels directly in the dermis and appears as a very sensitive method to investigate minor

differences in cutaneous drug delivery. It has been indicated that cutaneous microdialysis in rats may be useful for prediction of dermal pharmacokinetic properties of novel drugs/topical formulations in man. In the assessment of bioequivalence in terms of absorption rate by *in vivo* microdialysis appears to correlate well with the established *in vitro* FD-C assessment of permeation rates for formulations with the same drug. Assessment of systemic levels has been demonstrated to not always adequately estimate relative dermal absorption rates, and *in vivo* microdialysis is currently the only technique to assess directly unbound drug levels in the dermis [67].

4.3.   MATERIALS AND METHODS

4.3.1. Materials

Natrosol® 250 M (Aqualon, Hercules Inc., DE, USA), Flufenamic acid, modification II (Kali-Chemie Pharma, Hannover, D), Poly(D,L-lactide-co-glycolide) (50:50) with a molecular weight of 40000 to 75000 Da (Sigma Chemical Co., St. Louis, MO, USA), Polyvinyl alcohol (PVA) Mowiol® 4-88 (Kuraray Specialities Europe GmbH, Frankfurt, D), Soerensen phosphate buffer (pH 7.4), McIlvaine citric acid phosphate buffer (pH 2.2), Sodium hydroxide (all components from Merck, Darmstadt, D), Hypodermic stainless steel tubes type 304W, Stay-Clean soldering flux and Super Solder Wire (Small Parts Inc. Miami Lakes, FL), Cuprophan® membrane (type RC 55 8/200) of MWCO 10000 Da, approx. o.d. 200 µm, Loctite® Quick set™ Epoxy (Henkel Consumer Adhesives, Inc, Avon, OH), silica capilar tube with plastic cover (Polymicro Technologies Inc, Phoenix, AZ), Flo-texx® (Lerner Laboratories, Pittsburgh, PA), Veet depilatory cream (Reckitt Benckiser Inc., Berks, UK), Ketamin hydrochloride Ketamil® (Agrovet Ltda., Chile), chloral hydrate (Sigma- Aldrich Co., St. Louis, MO, USA), Introcan® 22G 1" (B. Braun Melsungen AG, Melsungen, D), Hematoxylin and Eosin Y (Sigma- Aldrich Co., St. Louis, MO, USA), Micro Test Tube 3810X (Eppendorf AG, Hamburg, D)

4.3.2. Equipment

HPLC system: Autosampler LaChrom L-7200, Pump LaChrom L-7100, Diode array detector LaChrom L-7450, Interface D-7000 and Multi HPLC System Manager Software LaChrom D-7000 (Merck Hitachi, Japan); 74900-15 Infusion pump Cole Palmer Instrument Company (Vernon Hills, IL, USA); Probes for dermal microdialysis were manufactured and provided by Departmento de Farmacología, Facultad de Ciencias Biológicas, Universidad de Concepción – Chile. Leica TP1020 and Leica EG1150 H (Leica Microsystems GmbH, Wetzlar, D); Reichert-Jung microtome (Reichert-Jung, D)

4.3.3. Microdialysis probes

The probes were assembled using of cellulose tubing (12.000 MWCO) of 200 μm outer diameter and 10 μm wall thickness, sealed at one end with an epoxy plug. The open end was attached to the probe body composed by 26 Ga, 21 Ga and 30 Ga stainless steel hypodermic tubes as described in figure 25. A silica capillary tube with polyimide cover (150 μm o.d. and 75 μm i.d) was inserted into a stainless steel and cellulose tube. The efficient dialysis length was 30 mm.
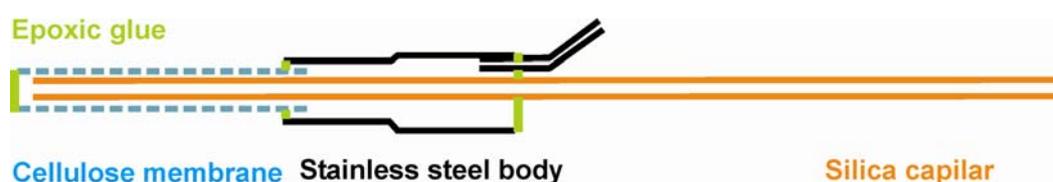
Figure 25: Diagram of concentric microdialysis probe.

4.3.4. Specimens

Sprague-Dawley strain female rats, weighing 250–350 g, were obtained from the animal facility of Departmento de Farmacología, Facultad de Ciencias Biológicas, Universidad de Concepción – Chile. All the animal used were individually housed and maintained on a 12/12-h light–dark cycle at constant room temperature (22°C) with food and water *ad libitum*.

All experiments were performed in accordance with the institutional guidelines and with the National Institutes of Health Guide for the Care and Use of Laboratory Animals.

The abdominal skin of the rats was prepared 18 h before the experiment under anesthesia. The abdominal hair was cut using a electrical machine. Subsequently, depilatory cream was applied (3 min) and gently washed off using cotton wipes and distilled water. The rat was returned to the animal facility overnight.

4.3.5. Anaesthesia

Previous to the microdialysis probe implantation, the animals were pre-anesthetized using ketamine hydrochloride (100 mg/kg) administered intraperitoneally. After this the animals were anesthetized using chloral hydrate (300 mg/kg) administered intraperitoneally. This dose that was re-administered as required every 2 -3 h [101].

4.3.6. Probe implantation

The microdialysis probes were implanted into the abdominal region of the rat under anaesthesia, as shown by the arrows in figure 26. The arrows indicate the flow direction of the perfusate. Dashed circles indicate the delimited application area of the formulation.
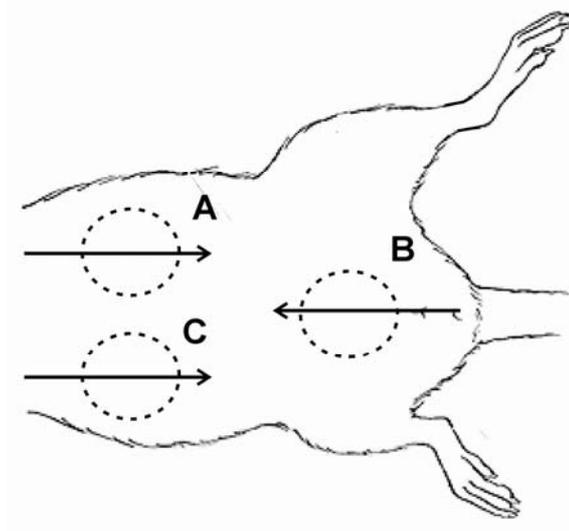
Figure 26: Microdialysis probe implantation diagram and formulation application area in the rat abdominal region.

4.3.7. Retrodialysis probes recovery

In vivo retrodialysis experiments were carried out using as perfusate solutions of 2.5, 4 and 8 µg/ml flufenamic acid dissolved in Soerensen buffer pH 7.4. Ten samples were collected every 30 minutes (n = 8). The percentage of relative recovery was

calculated using equation 4 (Chapter 1) . In all cases the relative recovery was > 90% and therefore in an acceptable range.

4.3.8. *In vivo* transdermal absorption experiments

The non-buffered formulations (FFA HG, FFA NP HG and FFA HG + DF-NP), prepared as described in section 3.3.5 were used.

The microdialysis probes have a perfusion flow of 1 µl/min. After the probe implantation, Teflon chambers (see figure 27) to delimit a circular application area of 15 mm in diameter were stuck on the skin using a double side tape ring.
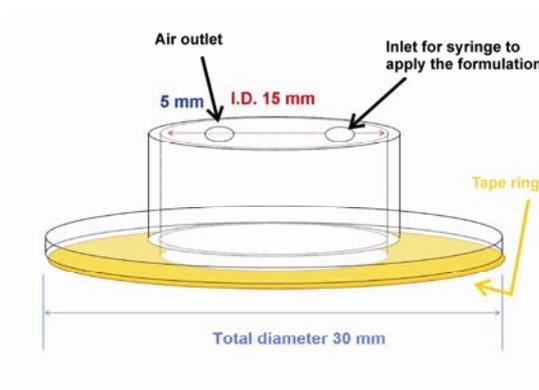
Figure 27: Teflon chamber for *in vivo* applications.

After 90 min (equilibrium time) the blank sample was collected. Subsequently, the Teflon piece was filled with approximately 1 ml of the corresponding formulation using a syringe, and samples of dialysate were collected every 30 min over a period of 6 hours after the formulation application. To avoid inter-individual differences, the three preparation were tested simultaneously in each rat. To exclude differences due to the application site, each formulation was alternated among the positions A, B and C for consecutive animals (see figure 26).

4.3.9. Tape-stripping

After 6 h of dialysate sample collection the animal was sacrificed and the skin from the application site, including the Teflon chamber and implanted section of the microdialysis probe, was removed and fixed over cork plates using pins. Subsequently, the Teflon chamber was take out from its place and the preparation wiped off from the surface using cotton swabs. A Teflon mask with a hole of 15 mm in diameter was placed over the application area. The tape stripping procedure and sample pooling was made as described in section 2.3.9. The remaining skin (15 mm in diameter) was punched out with the same diameter and collected in a separate flask.

4.3.10. Sample extraction and HPLC analysis

The samples obtained from the tape stripping and deep skin layers were extracted by using 6 ml of 0.05 M NaOH, under stirring during 2 h at room temperature. One millilitre from this extract was transferred into Micro Test Tube (1.5 ml) and centrifugued at 12000 rpm for 1 min. The supernatant was analysed by HPLC using the method described in 2.3.11.

4.3.11. Histological sectioning

This sample treatment was made under the standardized procedure at the Departamento de Anatomía Patológica (Universidad de Concepción). The skin samples were fixed in formalin (10% v/v) and afterwards treated using a Leica tissue processor using the following steps: 4 h in formalin, 1 h in ethanol 99% (3 times), 1 h in xylol (3 times), and finally 1 h in paraffin at 60°C (2 times). After this process the tissue was transferred to a Leica embedding system where the tissue samples were embedded in a paraffin block (2 x 2 x 2 cm) to proceed with the histological transversal sectioning using a microtome. The sections of the skin are placed in glass slides and dried on a forced air circulation oven at 60°C. The sections were stained as follows: the samples were

immersed 5 min in xylol (3 times), 1 min in ethanol 99%, 30 seconds in ethanol 70% and 50% successively, and finally washed with water. Afterwards, the samples were immersed successively in a hematoxylin solution (1 - 5 min), in water (10 min), and eosin solution (30 sec – 2 min). The samples were passed through water, 30 seconds in alcohol 99% (6 times), and 30 seconds in xylol (3 times). After this process the samples were covered using a cover slide and sealed with Flo-texx®.

4.4.   RESULTS AND DISCUSSION

4.4.1. *In vivo* microdialysis

In all experiments performed the dialysate samples analysed were under the detection limit (0.05 µg/ml) , n = 12 for each preparation. The high amount of hair follicles and close proximity of the capillary network to the probes [39] must be considered as important factors to explain the results obtained with the *in vivo* microdialysis experiments. The high clearance from the absorption site, considering that nanoparticles can also penetrate the hair follicle and act as on-site drug reservoir in deeper skin regions reduce the amount of drug able to reach the microdialysis probe, and therefore no drug could be detected in the dialysate. Another possible explanation of these results may be that flufenamic can bind in a high extent to plasma proteins [52], and it may bind also in a high extent to the proteins present in the epidermal and dermal environment (i.e. keratin, elastin, collagen), making the drug not available to be recovered in the dialysate.

4.4.2. Microdialysis probe intradermal location

Microscopic evaluation of the microdialysis probe location have shown the following distribution (Figure 28):
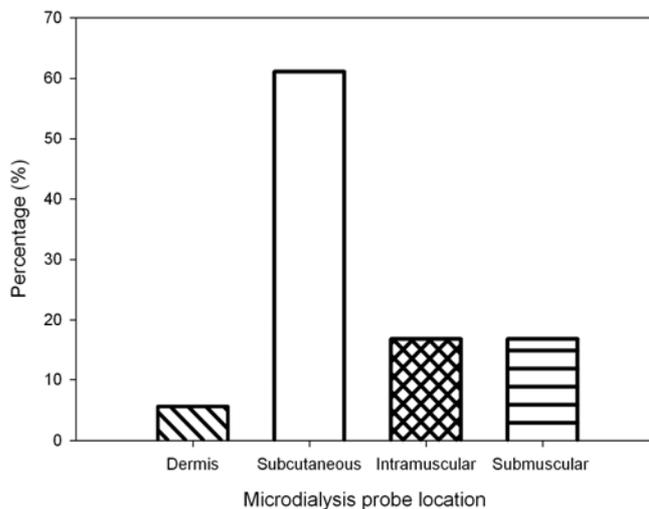
Figure 28: Microdialysis probe intradermal location (n = 18)

Its clear to see that most pf the probes were placed in the subcutaneous tissue and even in deeper tissue regions. However, to properly collect the drug permeated through the epidermis the optimal location would have been just beneath this layer. This non-optimal placement of the probe may explain the lack of drug detection in the dialysate due to tissue clearance, protein binding or enrichment of the highly lipophilic drug, flufenamic acid, in the subcutaneous fatty tissue.

4.4.3. Tape-stripping and deep skin layers

The result obtained from the tape stripping and the deep skin layers are shown in figure 29. These results shown a high variability of the content of drug in the stratum corneum as well as in the deep skin layers.
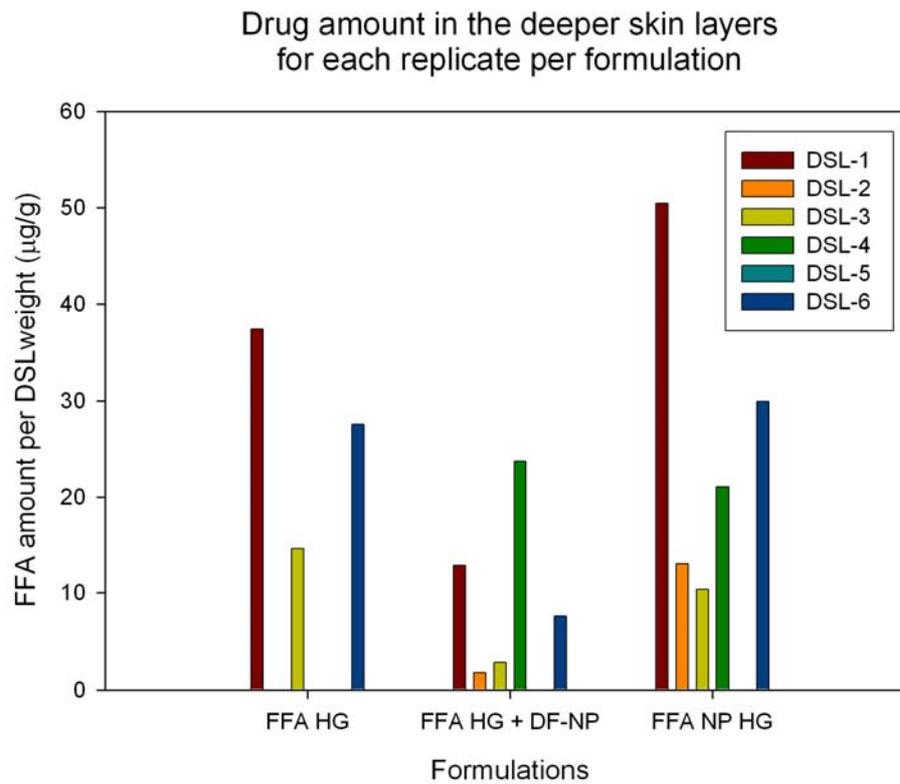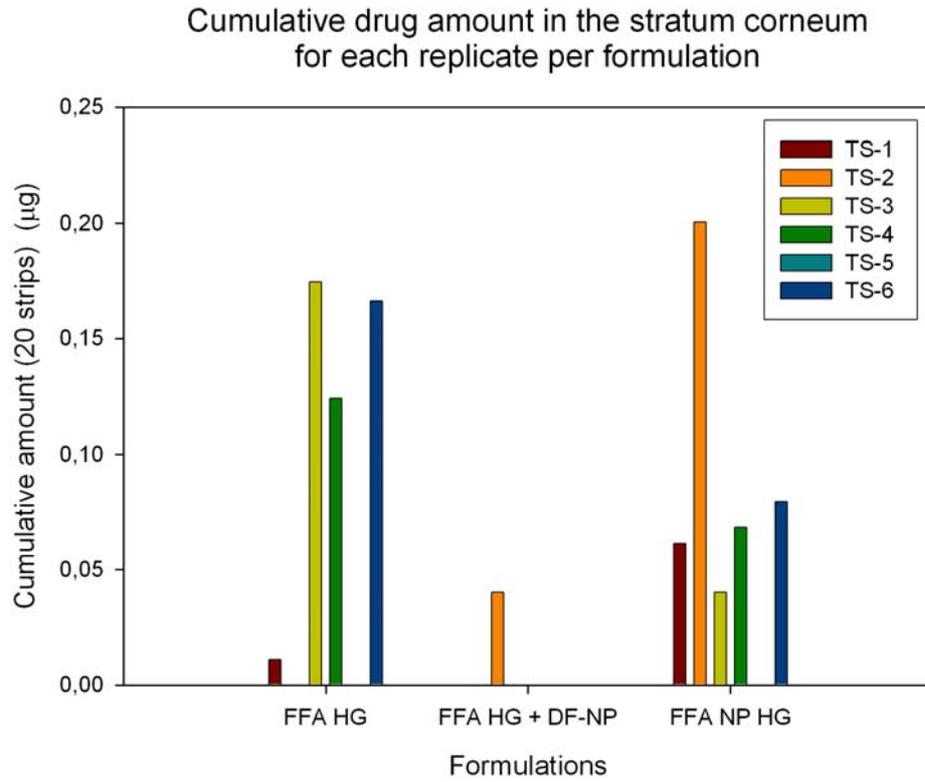
Figure 29: Drug content per replicate found on stratum corneum and deep skin layers per replicate per formulation

One explanation for the stratum corneum may be that due to the presence of the microdialysis probe, the contact between the tape and the skin, even using the 2 kg weight, was not optimal and the removed stratum corneum layers were different in each tape application. In addition, the influence of the depilation cream could be not excluded.

It can be speculated that in the deeper skin layer a strong binding to proteins and to the fatty tissue may occur. Moreover, a high clearance of the drug may occur *in vivo* due to the reach capillary network and the metabolic activity of the dermal tissue must be considered. Altogether, these different factors may influence the results and may be responsible for the high scattering of the data, making suitable conclusions impossible.

4.5. OVERVIEW

There are many parameters that must be considered to optimize this *in vivo* microdialysis experimental work:

1. Experiments performed between human and animal skin are difficult be representative from each other;

2. Metabolic activity, clearance from the application site, and binding to different structures of the skin *in vivo* must be studied;

3. A better placement of the microdialysis probe and study the different parameter which influence the drug recovery during the process are required.

CHAPTER 5: ADDITIONAL EXPERIMENTS

5.1. COLLABORATION WORK WITH OTHER RESEARCH GROUP

The contribution to this work involved to establish a suitable semisolid preparation for nanoparticles and the preparation of the hydrogels containing sodium fluorescein or fluoresceinamine labelled PLGA nanoparticles.

5.1.1. Methods

5.1.1.1 Preparation of the fluoresceinamine labelled nanoparticles containing hydrogel

Biefly, a 1% suspension of fluorescein labeled nanoparticles (average diameter 320 nm, PI 0.06) was prepared in water. A 3% hydroxyethylcellulose hydrogel (Natrosol® type 250 M pharma, Aqualon, Duesseldorf, D) was prepared separately. The polymer was dispersed in water under vigorous stirring (800 rpm) until it was homogeneously distributed; later on, the polymer was allowed to swell under low speed stirring (100 rpm) overnight. Both preparations were mixed at a proportion 1:1 and shaken until a homogeneous distribution of the particles in the gel was obtained, resulting in a nanoparticle content of 0.5% w/w.

5.1.1.2 Preparation of sodium fluorescein containing hydrogel

Briefly, a 0.003% sodium fluorescein-containing hydrogel (equivalent to the fluoresceinamine amount linked to the polymer) was prepared by dissolution of the dye in water and addition of the 1.5% hydroxyethylcellulose under stirring. Again, the preparation was stirred overnight at low speed (100 rpm) to allow swelling of the polymer.

Both gels showed similar viscosities.

5.1.2. Results

The follicular penetration depth of the topically applied fluorescein in particle (A) and non-particle form (B), applied by massage of the skin, was determined by analyzing biopsies of porcine skin (Figure 30). Significant differences were observed: the particles penetrate much deeper into the hair follicles than the non-particle form if massage is applied.
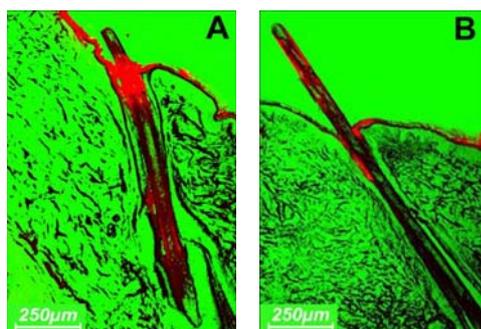
Figure 30: Examples of *in vitro* penetration of the dye-containing formulation into the hair follicles of porcine skin after application of a massage. (A) Dye in particle form. (B) Dye in non-particle form [14]

The same two formulations were gently applied to the skin without massage (Figure 31), resulting in penetration depth of the two formulations nearly identical.
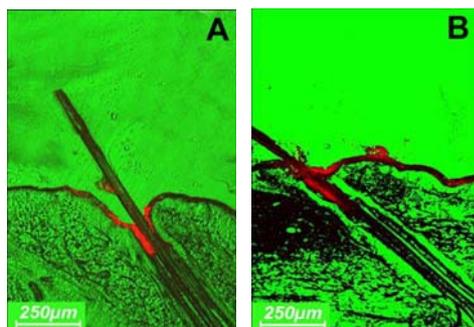
Figure 31: Examples of *in vitro* penetration of the dye-containing formulation into the hair follicles of porcine skin without massage. (A) Dye in particle form, (B) Dye in non-particle form [14].

---

[14]   Reprinted from European Journal of Pharmaceutics and Biopharmaceutics, *doi:10.1016/j.ejpb.2006.10.019*, Lademann J et al, Nanoparticles – An efficient carrier for drug delivery into the hair follicles, p4, Copyright 2006, with permission from Elsevier.

Penetration of particle-containing formulations was enhanced by mechanical massage, reaching significant deeper penetration depths than without massage. However, without any mechanical manipulation on the skin surface, no significant differences between the two formulations were observed.

It may be expected that the small amounts of non-particle substances, with their relatively small size, penetrate better into the small hair follicles than the much larger particles. The results obtained show the opposite effect, but only in the case of a massage being applied. From the structure analysis of hair surface and hair follicles, it is known that the cuticle produced by keratinocyte desquamation forms a structured surface, which can be approximated by a zigzag relief [102]. This relief is determined by the thickness of the keratin cells, which is between 500 and 800 nm. If the hairs are moved by massage, the cuticle cells may act as a geared pump. Particles, comparable in size to the surface structure of the hairs and hair follicles, are probably pushed into the follicles by means of the pump movement of the hairs. These findings are in agreement with the results obtained by Toll et al. [41], the microparticles with a diameter of 750 nm penetrated better into the hair follicles of excised human skin than larger particles, when a massage had been applied.

5.2. INFLUENCE OF DIFFERENT PARAMETERS ON NANOPARTICLE PREPARATION

5.2.1. Variation of the polymer/quasi-emulsifier ratio

Experiments were carrier out using the standard preparation method described in section 2.3.3. Additionally to the PLGA: PVA 6:2 ratio, also ratios of 6:1 and 6:4 were tested.

Variations of the particle size of about 100 nm were obtained using different proportions of polymer and quasi emulsifier (see figure 32). Two different batches of each composition were prepared and measured three times each. Furthermore, it can be clearly seen that an increase in the PVA concentration results in a decrease in the particle size. Although the polydispersity index is influenced, the values lower than 0.1 indicate a monodisperse size distribution.
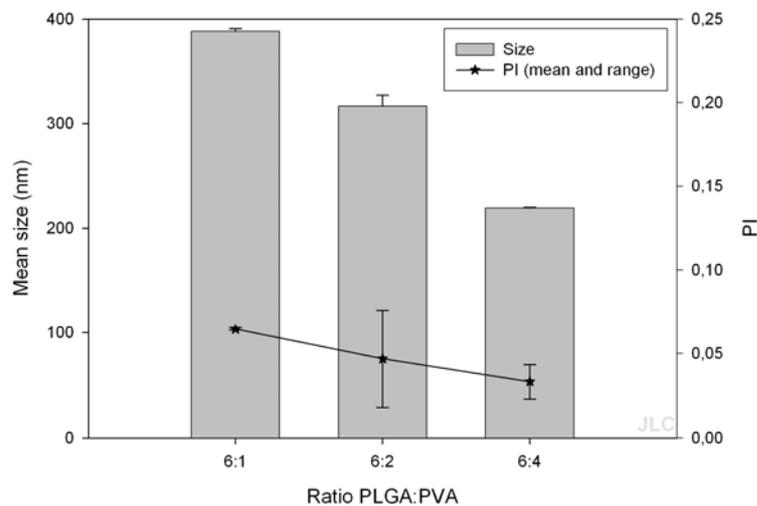
Figure 32: Effect of the ratio polymer/quasi-emulsifier used on the particle size

5.2.2. Variation of the homogenization speed or time

Changes on the homogenization speed using the same nanoparticles composition described in section 2.3.3 were tested. Instead of 13500 rpm, speeds of 8500 and 20500 rpm were used while the homogenization time remain constant.

Moreover, changes in the homogenization time using the formulation composition described in section 2.3.3 were tested. Instead of 10 min, 5 and 20 minutes were used.

With an homogenization speed of 8500 rpm no nanoparticles could be obtained. No differences were observed with the further homogenization speed concerning the particle size. Only the polydispersity of the batches was altered, however the polydispersity index was in the same range indicating a monodisperse distribution (Figure 33).
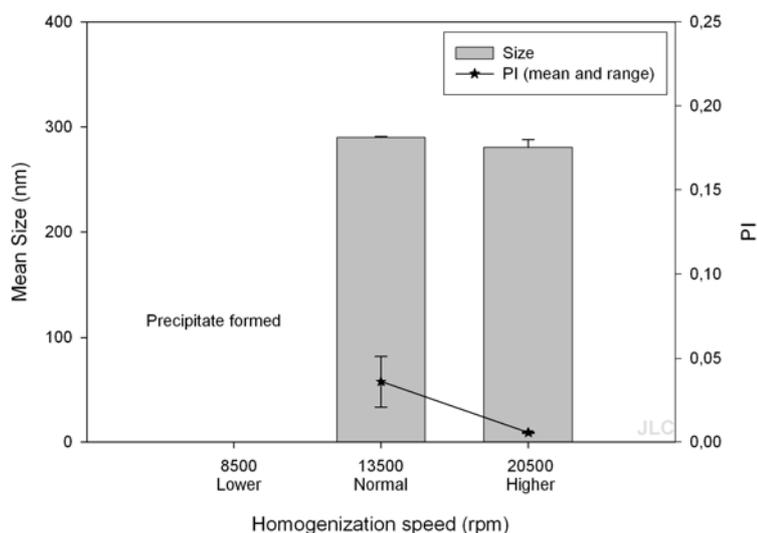
Figure 33: Effect of the homogenization speed on the particle size (homogenization time 10 min)

Variations of the homogenization time between 5 and 20 minutes does not influence the particle size nor the polydispersity index.
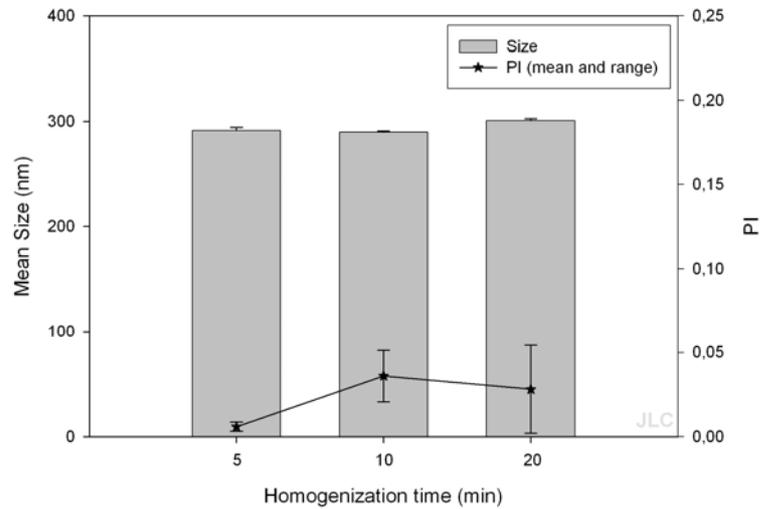
Figure 34: Effect of the homogenization time on the particle size (homogenization speed 13500 rpm)

In conclusion: The ratio PLGA:PVA does affect the particle size therefore this is crucial manufacturing parameter. However, if exceeding a critical homogenization speed and modifying the homogenization time do not seem to be crucial parameters.

5.3. NANOPARTICLE FREEZE-DRYING AND CRYOPROTECTION

5.3.1. Method

Nanoparticles were prepared as described in section 2.3.3. Separately a saccharose [Saccharose (EU-Categorie)] saturated solution in water was prepared in a concentration of 64% w/w under vigorous stirring at room temperature. The amount of solution added was calculated according to the percentage in weight of saccharose per polymer weight present in the nanoparticles suspension. The amount of sugar used was in the range between 10 – 200 % related to the polymer content. One sample was collected from each concentration and the size measured by photon correlation spectroscopy. Afterwards, the nanoparticles were freeze-dried [Freeze-dryer Alpha 2-4 LSC (Christ, Osterode, D)], re-suspended in water and the size of the particles measured.

5.3.2. Results

A ratio 1:1 between polymer and saccharose was observed to be the lowest amount of cryoprotectant that produces no change on the particle diameter before and after the freeze drying process (see figure 35).
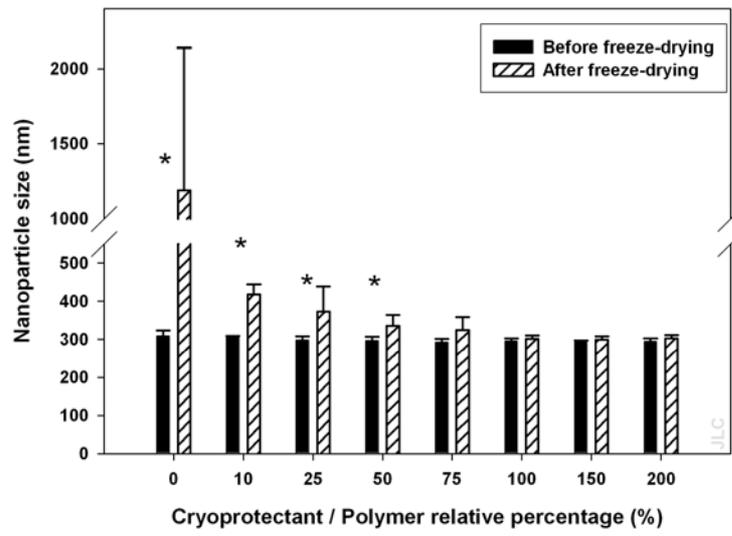
Figure 35: Effect of the cryoprotectant amount on particle size before and after freeze-drying

CHAPTER 6: SUMMARY

6.1. SUMMARY

The skin, due to its structure, is considered a complex organ for drug delivery. Although composed by four main layers, only the stratum corneum is considered the most important barrier for the drug absorption through the skin.

During the last years the transdermal drug delivery studies have been focused on overcoming the problems associated with the skin barrier properties. Following this objective, several physical and chemical enhancement methods have been studied to improve the drug transport through the skin, such as iontophoresis, electroporation, microneedles, chemical penetration enhancers, carriers as liposomes, solid lipid nanoparticles, among others.

The use of polymeric nanoparticles has been extensively studied for peroral and parenteral applications however their use in the field of dermal application is rare and the mechanisms which affect skin absorption are almost unknown. Therefore, the interest of this research project was to study the potential of polymeric biodegradable nanocarriers on drug delivery to and through the skin. To prepare the nanoparticles, the well known biodegradable polymer PLGA 50:50 polymer was chosen, and to study the drug transport, flufenamic acid, an antiinflamatory, ionisable lipophilic drug was used.

Using the solvent evaporation technique PLGA nanoparticles, with or without the incorporation of flufenamic acid, in the size range of 250 nm and a polydispersity index of less than 0.2 could be obtained. For these particles it has been shown, that, particularly for longer experimental times, PLGA nanoparticles improve the dermal drug permeation in vitro, using heat separated human epidermis in Franz diffusion cell systems. This result was confirmed by skin penetration studies with full-thickness human skin in the Saarbrücken model showing higher amounts of flufenamic acid in the viable epidermis and dermis when encapsulated flufenamic acid was applied. Moreover, for various incubation times constant concentrations in the stratum

corneum were found, indicating that the system has reached steady-state conditions. When permeation experiments were performed, the results have shown that enhancement effect is reached using loaded nanoparticles independent of particle size. Surprisingly the presence of drug-free nanoparticles in a preparation with flufenamic acid in solution has also increased the permeated amount of drug. Therefore the question arose which mechanistic effects are responsible for the enhancement effects of PLGA nanoparticles in combination with flufenamic acid.

For the first time, it was demonstrated by confocal laser scanning microscopy and permeation experiments using buffered and non-buffered preparations that one of the mechanisms how PLGA nanoparticles increase the delivery of drug to the skin is due to an acidic nano-environment around the particles. This induces an increased concentration of the non-ionized form of the drug at the skin surface and therefore the concentration gradient between the stratum corneum surface and the dermal side of the epidermal membrane becomes steeped. Due to the local effect the total pH of the formulation is not affected.

Other studies, developed in collaboration with Prof. Lademann's research group, have shown that nanoparticles were able to penetrate into the hair follicles when massage was used. Such conditions must be considered for *in vivo* applications.

In a preliminary *in vivo* study, using dermal microdialysis in rats, the effect of the nanoparticles could not be demonstrated due to methodological problems.

The results presented in this thesis underscore the potential of polymeric biodegradable nanoparticles to be used as vehicles for transdermal drug delivery. Especially, the acidic pH of the nano-environment of the particles might be an advantage to develop special formulations designed for acidic drugs or might be used to re-establish the normal pH on the skin surface.

6.2. ZUSAMMENFASSUNG

Auf Grund des strukturellen Aufbaus unserer Haut ist eine dermale Arneistoffinvasion als schwierig anzusehen. Obwohl die Haut aus vier verschiedenen Schichten aufgebaut ist, ist lediglich das Stratum corneum als Hauptbarriere für die Arzneistoffaufnahme durch die Haut anzusehen.

Während der letzten Jahren wurden Studien zur transdermal Arzneistoffapplikation vor allem auf Problemstellungen fokussiert, die auf die Überwindung der Barriereeigenschaften der Haut ausgerichtet waren. So wurden verschiedene physikalische und chemische Methoden zur Erhöhung der Arzneistoffabsorption durch die Haut untersucht, wie zum Beispiel Iontophorese, Elektroporation, Microneedles, und chemische Penetrationsenhancer aber auch Trägersysteme wie Liposome und Solid Lipid Nanoparticles.

Polymernanopartikel wurden sehr intensiv hinsichtlich ihrer Anwendung im peroralen und parenteralen Bereich untersucht. Zur dermalen Anwendung jedoch findet man für diese Präparate kaum Untersuchungen und der Mechanismus, wie die Hautabsorption beeinflußt wird, ist weitgehend unbekannt. Hieraus ergibt sich dann auch das Thema dieser Doktorarbeit in der das Potential bioabbaubarer Polymernanopartikel zur Erhöhung der dermalen Arzneistoffinvasion untersucht werden sollte. Zur Herstellung der Nanopartikel wurde das gut beschriebene Polymer PLGA 50:50 ausgewählt und Fufenaminsäure, eine antiinflamatorisch wirksame, ionisierbare, lipophile Substanz wurde benutzt um Effekte auf die dermale Arzneistoffinvasion aufzeigen zu können,.

Durch Anwendung der sogenannten „Solvent-Evaporation-Technik" konnten PLGA Nanopartikel sowohl mit als auch ohne Flufenaminsäure erhalten werden deren Partikelgröße bei etwa bei 250 nm lag und die einen Polydispersitätsindex unter 0.2 aufwiesen. Für diese Partikel konnte in Franz-Zellen Experimente mit humaner Epidermis gezeigt werden, daß vor allem bei längeren Anwendungszeiten

die Arzneistoffpermeation *in vitro* erhöht war. Dieses Ergebnis wurde durch Experimente mit humaner Vollhaut im Saarbrücker-Penetration-Modell bestätigt bei denen größere Mengen an Flufenaminsäure in der lebenden Epidermis und Dermis gefunden wurden, wenn Flufenaminsäure in der nanopartikulären Form eingesetzt wurde. Des weiteren wurden bei verschiedenen Versuchszeiten für das Stratum corneum konstante Flufenaminsäurekonzentrationen gefunden, die darauf hindeuten, daß sich ein sogenannter „steady state Zustand" ausgebildet hat. Des weiteren konnte mittels Permeationsexperimente gezeigt werden, daß der penetrationsverstärkende Effekt unabhängig von der Partikelgröße durch mit Flufenaminsäure beladene Nanopartikel erreicht werden kann. Überrachenderweise führte jedoch die Anwesenheit von reinen PLGA-Nanopartikel in Präparationen, die Flufenaminsäure lediglich gelöst enthielten, ebenfalls zu einer erhöhten Permeation. Daher ergab sich die Frage welche Mechanismen für die penetrationsverstärkende Effekte von PLGA-Nanopartikel in Kombination mit Flufenaminsäure verantwortlich sind.

Zum ersten Mal konnte mittels confokaler Laser Mikroskopie und Permeationsversuchen mit gepufferten und nicht gepufferten Formulierung aufgezeigt werden, daß einer der Mechanismen, wie PLGA Nanopartikel die dermale Arzneistoffinvasion beeinflussen, durch das Ausbildend einer sauren Umgebung im Nanobereich um die Nanopartikel herum zu Stande kommt. Dies führt zu einer erhöhten Konzentration der undisoziierten Form des sauren Arzneistoffs an der Hautoberfläche was wiederum einen steileren Konzentrationsgradient zwischen der Oberfläche des Stratum corneum und der Grenzschicht Stratum corneum zu lebender Epidermis bedingt. Auf Grund des räumlich begrenzten Effektes wird der pH-Wert der Formulierung nicht beeinflußt.

Weitere Versuche, die in Zusammenarbeit mit der Forschungsgruppe von Prof. J. Lademann, Charié Berlin, durchgeführt wurden haben gezeigt, daß

Nanopartikel bevorzugt dann in die Haarfollikel eindringen wenn sie mechanisch einmassiert werden. Dies entsprich durchaus den in vivo Anwendungsbedingungen.

In einer ersten in vivo Studie, bei der das Verfahren der dermalen Mikrodialyse bei Ratten eingesetzt wurde, konnte auf Grund experimenteller Schwierigkeiten der Einfluß von Nanopartikeln auf die dermale Invasion nicht aufgezeigt werden.

Die Ergebnisse, die im Rahmen dieser Doktorarbeit ermittelt wurden, unterstreichen das Potential von biologisch abbaubaren Polymernanopartikel als Träger zur dermalen Arzneistoffinvasion. Besonders könnte der saure pH-Wert des Nanobereichs der Nanopartikel für saure Substanzen von Vorteil sein, um hier spezielle Formulierungen zu entwickeln, oder dieses Phänomen könnte dazu ausgenutzt werden den normalen leicht sauren pH-Wert auf der Hautoberfläche wieder herzustellen.

CHAPTER 7: APPENDICES

REFERENCES

[1] Walters, K. A. and Roberts, M. S. (2002) The structure and function of skin, in K. A. Walters, ed., Dermatological and Transdermal Formulations: Drugs and the Pharmaceutical Sciences, v. 119: New York, Marcel Dekker, Inc., p. 1-39.

[2] Washington, N.*, et al.* (2001) Transdermal Drug Delivery, in N. Washington, ed., Physiological Pharmaceutics, Taylor and Francis, Inc., p. 181-198.

[3] Naik, A.*, et al.* (2000) Transdermal drug delivery: overcoming the skin's barrier function, Pharmaceutical Science & Technology Today, 3 (9): 318-326.

[4] Cevc, G. (2004) Lipid vesicles and other colloids as drug carriers on the skin, Advanced Drug Delivery Reviews, 56 (5): 675-711.

[5] Roberts, M. S. and Cross, S. E. (2002) Skin transport, in K. A. Walters, ed., Dermatological and transdermal formulations: Drugs and the Pharmaceutical Sciences, v. 119: New York, Marcel Dekker, Inc., p. 89 - 195.

[6] Cleary, G. W. (2003) Transdermal and transdermal-like delivery system opportunities: today and the future, Drug Delivery Technology, 3 (5): 35-40.

[7] Thomas, B. J. and Finnin, B. C. (2004) The transdermal revolution, Drug Discovery Today, 9 (16): 697-703.

[8] Hadgraft, J. (2004) Skin deep, European Journal of Pharmaceutics and Biopharmaceutics, 58 (2): 291-299.

[9] Alvarez-Román, R.*, et al.* (2004) Enhancement of topical delivery from biodegradable nanoparticles, Pharmaceutical Research, 21 (10): 1818-1825.

[10] Langer, R. (2004) Transdermal drug delivery: past, progress, current status and future prospects, Advanced Drug Delivery Reviews, 56 (5): 557-558.

[11] Barry, B. W. (2006) Penetration enhancer classification, in E. W. Smith and H. I. Maibach, eds., Percutaneous Penetration Enhancers: Boca Raton, Taylor & Francis Group, p. 3-15.

[12] Prausnitz, M. R. (2004) Microneedles for transdermal drug delivery, Advanced Drug Delivery Reviews, 56 (5): 581-587.

[13] Williams, A. C. and Barry, B. W. (2004) Penetration enhancers, Advanced Drug Delivery Reviews, 56 (5): 603-618.

[14] Miyazaki, S. (2006) Nanoparticles as carriers for enhanced skin penetration, in E. W. Smith and H. I. Maibach, eds., Percutaneous Penetration Enhancers: Boca Raton, FL, CRC Press, p. 117-124.

[15] Vauthier, C.*, et al.* (2003) Poly(alkylcyanoacrylates) as biodegradable materials for biomedical applications, Advanced Drug Delivery Reviews, 55 (4): 519-548.

[16] Hans, M. L. and Lowman, A. M. (2002) Biodegradable nanoparticles for drug delivery and targeting, Current Opinion in Solid State & Materials Science, 6 (4): 319-327.

[17] Cui, Z. (2001) Chitosan-based nanoparticles for topical genetic immunization, Journal of Controlled Release, 75 (3): 409-419.

[18] Mu, L. and Feng, S. S. (2003) A novel controlled release formulation for the anticancer drug paclitaxel (Taxol(R)): PLGA nanoparticles containing vitamin E TPGS, Journal of Controlled Release, 86 (1): 33-48.

[19] de Jalon, E. G.*, et al.* (2001) Topical application of acyclovir-loaded microparticles: quantification of the drug in porcine skin layers, Journal of Controlled Release, 75 (1-2): 191-197.

[20] Shim, J.*, et al.* (2004) Transdermal delivery of minoxidil with block copolymer nanoparticles, Journal of Controlled Release, 97 (3): 477-484.

[21] Lombardi Borgia, S.*, et al.* (2005) Lipid nanoparticles for skin penetration enhancement - correlation to drug localization within the particle matrix as determined by fluorescence and paraelectric spectroscopy, Journal of Controlled Release, 110 (1): 151-163.

[22] Mei, Z.*, et al.* (2003) Solid lipid nanoparticle and microemulsion for topical delivery of triptolide, European Journal of Pharmaceutics and Biopharmaceutics, 56 (2): 189-196.

[23] Ricci, M.*, et al.* (2005) Evaluation of indomethacin percutaneous absorption from nanostructured lipid carriers (NLC): in vitro and in vivo studies, Journal of Pharmaceutical Sciences, 94 (5): 1149-1159.

[24] Souto, E. B.*, et al.* (2004) Development of a controlled release formulation based on SLN and NLC for topical clotrimazole delivery, International Journal of Pharmaceutics, 278 (1): 71-77.

[25] Müller, R. H.*, et al.* (2002) Solid lipid nanoparticles (SLN) and nanostructured lipid carriers (NLC) in cosmetic and dermatological preparations, Advanced Drug Delivery Reviews, 54 (Suppl 1): S131-S155.

[26] Müller, R. H.*, et al.* (2000) Solid lipid nanoparticles (SLN) for controlled drug delivery - a review of the state of the art, European Journal of Pharmaceutics and Biopharmaceutics, 50 (1): 161-177.

[27] Santos Maia, C.*, et al.* (2000) Solid lipid nanoparticles as drug carriers for topical glucocorticoids, International Journal of Pharmaceutics, 196 (2): 165-167.

[28] Wissing, S. A. and Müller, R. H. (2001) A novel sunscreen system based on tocopherol acetate incorporated into solid lipid nanoparticles, International Journal of Cosmetic Science, 23 (4): 233-243.

[29] Jenning, V.*, et al.* (2000) Vitamin A loaded solid lipid nanoparticles for topical use: occlusive properties and drug targeting to the upper skin, European Journal of Pharmaceutics and Biopharmaceutics, 49 (3): 211-218.

[30] Jenning, V.*, et al.* (2000) Vitamin A-loaded solid lipid nanoparticles for topical use: drug release properties, Journal of Controlled Release, 66 (2-3): 115-126.

[31] Müller, R. H.*, et al.* (1997) Cytotoxicity of solid lipid nanoparticles as a function of the lipid matrix and the surfactant, Pharmaceutical Research, 14 (4): 458-462.

[32] Wissing, S. A. and Muller, R. H. (2002) Solid lipid nanoparticles as carrier for sunscreens: in vitro release and in vivo skin penetration, Journal of Controlled Release, 81 (3): 225-233.

[33] Brannon-Peppas, L. (1995) Recent advances on the use of biodegradable microparticles and nanoparticles in controlled drug delivery, International Journal of Pharmaceutics, 116 (1): 1-9.

[34] Panyam, J. and Labhasetwar, V. (2003) Biodegradable nanoparticles for drug and gene delivery to cells and tissue, Advanced Drug Delivery Reviews, 55 (3): 329-347.

[35] Yoo, H. S.*, et al.* (1999) Biodegradable Nanoparticles Containing Doxorubicin-PLGA Conjugate for Sustained Release, Pharmaceutical Research, 16 (7): 1114-1118.

[36] de Jalon, E. G.*, et al.* (2001) PLGA microparticles: possible vehicles for topical drug delivery, International Journal of Pharmaceutics, 226 (1-2): 181-184.

[37] Wissing, S. A.*, et al.* (2001) Investigations on the occlusive properties of solid lipid nanoparticles (SLN), Journal of Cosmetic Science, 52 (5): 313-324.

[38] Rolland, A.*, et al.* (1993) Site-specific drug delivery to pilosebaceous structures using polymeric microspheres Pharmaceutical Research, 10 (12): 1738-1744.

[39] Lauer, A. C.*, et al.* (1995) Transfollicular drug delivery, Pharmaceutical Research, 12 (2): 179-186.

[40] Alvarez-Roman, R.*, et al.* (2004) Skin penetration and distribution of polymeric nanoparticles, Journal of Controlled Release, 99 (1): 53-62.

[41] Toll, R.*, et al.* (2004) Penetration profile of microspheres in follicular targeting of terminal hair follicles, Journal of Investigative Dermatology, 123 (1): 168-176.

[42] Lademann, J.*, et al.* (2001) Investigation of follicular penetration of topically applied substances, Skin Pharmacology and Applied Skin Physiology, 14 (Suppl 1): 17-22.

[43] Lademann, J*., et al.* (2006) Hair Follicles - A long-term reservoir for drug delivery, Skin Pharmacology and Physiology, 19 (4): 232-236.

[44] Lademann, J*., et al.* (1999) Penetration of Titanium Dioxide Microparticles in a Sunscreen Formulation into the Horny Layer and the Follicular Orifice, Skin Pharmacology and Applied Skin Physiology, 12 (5): 247-256.

[45] Schaefer, H. and Lademann, J. (2001) The Role of Follicular Penetration, Skin Pharmacology and Applied Skin Physiology, 14 (Suppl 1): 23 - 27.

[46] Schenke-Layland, K*., et al.* (2006) Two-photon microscopes and in vivo multiphoton tomographs -- Powerful diagnostic tools for tissue engineering and drug delivery, Advanced Drug Delivery Reviews, 58 (7): 878-896.

[47] Stracke, F*., et al.* (2006) Multiphoton microscopy for the investigation of dermal penetration of nanoparticle-borne drugs, Journal of Investigative Dermatology, 126 (10): 2224-2233.

[48] Oberdörster, G*., et al.* (2005) Nanotoxicology: An emerging discipline evolving from studies of ultrafine particles, Environmental Health Perspectives, 113 (7): 823 - 839.

[49] Menzel, F*., et al.* (2004) Investigation of percutaneous uptake of ultrafine TIO_2 particles at the high energy ion nanoprobe LIPISION, Nuclear Instruments and Methods in Physics Research Section B: Beam Interactions with Materials and Atoms, 219-220 82-86.

[50] Gamer, A. O*., et al.* (2006) The in vitro absorption of microfine zinc oxide and titanium dioxide through porcine skin, Toxicology in Vitro, 20 (3): 301-307.

[51] Hoet, P. H. M*., et al.* (2004) Nanoparticles - known and unknown health risks, Journal of Nanobiotechnology, 2 12.

[52] Abignente, E. and De Caprariis, P. (1982) Flufenamic Acid: Analytical Profiles of Drug Substances, v. 11, Academic Press, Inc., p. 313-346.

[53] Moffat, A. C. (1986) Clarke's Isolation and Identification of Drugs: London, Pharmaceutical Press.

[54] Wagner, H*., et al.* (2000) Drug distribution in human skin using two different in vitro test systems: comparison with in vivo data, Pharmaceutical Research, 17 (12): 1475-1481.

[55] OECD (2004), OECD guideline for testing of chemicals. Skin absorption: in vitro method, Nr. 428, Organisation for Economic Co-operation and Development, 13. April 2004

[56] Brain, K. R*., et al.* (2002) Methods for studying percutanous absorption, in K. A. Walters, ed., Dermatological and Transdermal Formulations: Drugs and the Pharmaceutical Sciences, v. 119: New York, Marcel Dekker, Inc., p. 197 - 269.

[57] Hailer, M. (1981) Freisetzung von Salicylsäure aus Suspensionssalben: Liberation im Membranmodell im Vergleich zur Wirkstoffabgabe an excidierte Haut, Doctoral Thesis, Department of Biopharmaceutics and Pharmaceutical Technology, Saarland University

[58] Blasius, S. (1985) Sorptionsvertmittler - Einfluß auf die Liberation von Indometacin aus Salben und auf die Arzneistoffaufnahme durch excidierte Haut, Doctoral Thesis, Department of Biopharmaceutics and Pharmaceutical Technology, Saarland University

[59] Wild, T. (1988) Einfluß der physikochemischen Eigenschaften von Arzneistoffen und Vehikeln aud die Permeabilität der menschlischen Hornschicht, Doctoral Thesis, Department of Biopharmaceutics and Pharmaceutical Technology, Saarland University

[60] Theobald, F. (1998) In-vitro-Methoden zur biopharmazeutischen Qualitätsprüfung von Dermatika unter Berücksichtung der Lipidzusammensetzung der Stratum corneum, Doctoral Thesis, Department of Biopharmaceutics and Pharmaceutical Technology, Saarland University

[61] Wagner, H. (2001) Charakterisierung des Arzneistofftransportes in Humanhaut unter in-vitro und in-vivo Bedingungen sowie unter Berücksichtigung des Einflusses zweier in-vitro Testsysteme, Doctoral Thesis, Department of Biopharmaceutics and Pharmaceutical Technology, Saarland University

[62] Roberts, M. S. and Anissimov, Y. G. (2005) Mathematical models in percutaneous absorption, in R. L. Bronaugh and H. I. Maibach, eds., Percutaneous Absorption, v. 155: Boca Raton, FL, Taylor & Francis Group, LLC., p. 1-44.

[63] Muhammad, F. and Riviere, J. E. (2006) In Vivo Models, in J. E. Riviere, ed., Dermal Absorption in Toxicology and Pharmacology: Raleigh, North Carolina, CRC Press, Taylor & Francis Group, p. 49 - 70.

[64] Davies, M. I. (1999) A review of microdialysis sampling for pharmacokinetic applications, Analytica Chimica Acta, 379 (3): 227-249.

[65] Kehr, J. (1993) A survey on quantitative microdialysis: theoretical models and practical applications, Journal of Neuroscience Methods, 48 (3): 251-261.

[66] Elmquist, W. F. and Sawchuck, R. J. (1997) Application of microdialysis in pharmacokinetic studies, Pharmaceutical Research, 14 (3): 267-288.

[67] Kreilgaard, M. (2002) Assessment of cutaneous drug delivery using microdialysis, Advanced Drug Delivery Reviews, 54 (Suppl. 1): S99-S121.

[68] Mathy, F.-X., *et al.* (2003) In vivo Tolerance Assessment of Skin after Insertion of Subcutaneous and Cutaneous Microdialysis Probes in the Rat., Skin Pharmacology and Applied Skin Physiology, 16 (1): 18-27.

[69] Mathy, F.-X., *et al.* (2005) Study of percutaneous penetration of flubiprofen by cutaneous and subcutaneous microdialysis after iontophoretic delivery in rat, Journal of Pharmaceutical Sciences, 94 (1): 144-152.

[70] Bielecka-Grzela, S. and Klimowicz, A. (2003) Application of cutaneous microdialysis to evaluate metronidazole and its main metabolite concentrations in the skin after a single oral dose, Journal of Clinical Pharmacy and Therapeutics, 28 (6): 465-469.

[71] Simonsen, L., *et al.* (2004) Differentiated in vivo skin penetration of salicylic compounds in hairless rats measured by cutaneous microdialysis, European Journal of Pharmaceutical Sciences, 21 (2-3): 379-388.

[72] Leveque, N*., et al.* (2004) Comparison of Franz cells and microdialysis for assessing salicylic acid penetration through human skin, International Journal of Pharmaceutics, 269 (2): 323-328.

[73] Kopacz, D. J*., et al.* (2003) A model to evaluate the pharmacokinetic and pharmacodynamic variables of extended-release products using in vivo tissue microdialysis in humans: Bupivacaine-loaded microcapsules, Anesthesia and Analgesia, 97 (1): 124-131.

[74] EPA, Dermal exposure assessment: principles and applications, US Environmental Protection Agency, 1992

[75] Hadgraft, J. (2001) Skin, the final frontier, International Journal of Pharmaceutics, 224 (1-2): 1-18.

[76] Barry, B. W. (1983) Dermatological Formulations. Percutaneous absorption, Drugs and the Pharmaceutical Sciences, v. 18: New York and Basel, Marcel Dekker, Inc.

[77] Wagner, H*., et al.* (2004) Effects of various vehicles on the penetration of flufenamic acid into human skin, European Journal of Pharmaceutics and Biopharmaceutics, 58 (1): 121-129.

[78] Kohli, A. K. and Alpar, H. O. (2004) Potential use of nanoparticles for transcutaneous vaccine delivery: effect of particle size and charge, International Journal of Pharmaceutics, 275 (1-2): 13-17.

[79] Lademann, J*., et al.* (2004) Penetration von Mikropartikeln in de menschliche Haut, Der Hautarzt, 55 1117-1119.

[80] Soppimath, K. S*., et al.* (2001) Biodegradable polymeric nanoparticles as drug delivery devices, Journal of Controlled Release, 70 (1-2): 1-20.

[81] Kumar, M. N. V. R*., et al.* (2003) Polymeric nanoparticles for drug and gene delivery, in H. S. Nalwa, ed., Encyclopedia of Nanoscience and Nanotechnology, v. X, American Scientific Publishers, p. 1-19.

[82] Dick, I. P. and Scott, R. C. (1992) Pig ear skin as an in vitro model for human skin permeability, Journal of Pharmacy and Pharmacology, 44 (8): 640-645.

[83] König, K. and Riemann, I. (2003) High-resolution multiphoton tomography of human skin with subcellular spatial resolution and picosecond time resolution, Journal of Biomedical Optics, 8 (3): 432-439.

[84] Bronaugh, R. L.*, et al.* (1986) Methods of in vitro percutaneous absorption studies VII: Use of excised human skin, Journal of Pharmaceutical Sciences, 75 (11): 1094-1097.

[85] Koenig, K. and Riemann, I. (2003) High-resolution multiphoton tomography of human skin with subcellular spatial resolution and picosecond time resolution, Journal of Biomedical Optics, 8 (3): 432-439.

[86] Fu, K.*, et al.* (2000) Visual Evidence of Acidic Environment Within Degrading Poly(lactic-co-glycolic acid) (PLGA) Microspheres, Pharmaceutical Research, 17 (1): 100-106.

[87] Anderson, J. M. and Shive, M. S. (1997) Biodegradation and biocompatibility of PLA and PLGA microspheres, Advanced Drug Delivery Reviews, 28 (1): 5-24.

[88] Belbella, A.*, et al.* (1996) In vitro degradation of nanospheres from poly(D,L-lactides) of different molecular weights and polydispersities, International Journal of Pharmaceutics, 129 (1-2): 95-102.

[89] Allémann, E.*, et al.* (1993) In Vitro Extended-Release Properties of Drug-Loaded Poly(DL-Lactic Acid) Nanoparticles Produced by a Salting-Out Procedure, Pharmaceutical Research, 10 (12): 1732-1737.

[90] Geigy, D. (1975) Wissenschaftliche Tabellen: Stuttgart, Sonderausgabe Georg Tieme Verlag.

[91] Netzlaff, F.*, et al.* (2005) The human epidermis models EpiSkin[(R)], SkinEthic[(R)] and EpiDerm[(R)]: An evaluation of morphology and their suitability for testing phototoxicity, irritancy, corrosivity, and substance transport, European Journal of Pharmaceutics and Biopharmaceutics, 60 (2): 167-178.

[92] Schmook, F. P*., et al.* (2001) Comparison of human skin or epidermis models with human and animal skin in in-vitro percutaneous absorption, International Journal of Pharmaceutics, 215 (1-2): 51-56.

[93] Schafer-Korting, M*., et al.* (2006) Reconstructed human epidermis for skin absorption testing: results of the German prevalidation study, Alternatives to laboratory animals, 34 (3): 283-294.

[94] Dunne, M*., et al.* (2000) Influence of particle size and dissolution conditions on the degradation properties of polylactide-co-glycolide particles, Biomaterials, 21 (16): 1659-1668.

[95] Siepmann, J*., et al.* (2005) How autocatalysis accelerates drug release from PLGA-based microparticles: a quantitative treatment, Biomacromolecules, 6 2312-2319.

[96] Hasirci, V*., et al.* (2001) Versatility of biodegradable biopolymers: degradability and an in vivo application, Journal of Biotechnology, 86 (2): 135-150.

[97] Cotellessa, C*., et al.* (1995) Glycolic acid and its use in dermatology, Journal of the European Academy of Dermatology and Venereology, 5 (3): 215-217.

[98] Sebastiani, P*., et al.* (2005) Effect of lactic acid and iontophoresis on drug permeation across rabbit ear skin, International Journal of Pharmaceutics, 292 (1-2): 119-126.

[99] Panyam, J*., et al.* (2003) Polymer degradation and in vitro release of a model protein from poly(D,L-lactide-co-glycolide) nano- and microparticles, Journal of Controlled Release, 92 (1-2): 173-187.

[100] McCleverty, D*., et al.* (2006) Microdialysis sampling and the clinical determination of topical dermal bioequivalence, International Journal of Pharmaceutics, 308 (1-2): 1-7.

[101] Sharp, P. E. and La Regina, M. C. (1998) The Laboratory Rat: Boca Raton, FL, CRC Press LLC.

[102] Biel, S. S.*, et al.* (2003) From tissue to cellular ultrastructure: Closing the gap between micro- and nanostructural imaging, Journal of Microscopy, 212 (1): 91-99.

LIST OF USED ABBREVIATIONS

AFM	Atomic force microscopy
CLSM	Confocal laser scanning microscopy
DDS	Drug delivery system
DF-NP	Drug-free nanoparticles
DMSO	Dimethylsulphoxide
DSL	Deep skin layers
FD-C	Franz diffusion cell
FFA	Flufenamic acid
HG	Hydrogel
HPLC	High-performance liquid chromatography
NLC	Nanostructured lipid carriers
NP	Nanoparticles
PLGA	Poly(lactide-*co*-glycolide)
PVA	Polyvinylalcohol
SB-M	Saarbrücken model
SC	Stratum corneum
SLN	Solid lipid nanoparticles

FIGURE INDEX

TABLE INDEX

SEMINARS AND CONFERENCES PARTICIPATION

Year	Participation	Details
2004	**A, S**	5th International Conference and Workshop on Cell culture and In-vitro Models for Drug Absorption and Delivery, Saarland University, Saarbrücken - Germany, February 25th – March 5th, 2004
	A	European IP – Galenos Course: "*Skin Barrier Function: Pharmaceutic and Cosmetic Applications*", Université Claude Bernard, Lyon – France, September 12 – 23, 2004.
	A, P	*2004 AAPS Annual Meeting and Exposition*, Baltimore (Maryland) – U.S.A., November 7 – 11, 2004.
2005	**A, P**	European IP – Galenos Course attendance: "*Cyclodextrins and their use in life sciences*". University of Lisbon, Lisbon – Portugal, September 5th -14th, 2005.
	A, S	"*Drug delivery to the skin*", Universidad de Concepción, Concepción – Chile, November 15th – 17th, 2005.
2006	**A, P, S**	6th International Conference and Workshop on Cell Culture and In-Vitro Models for Drug Absorption and Delivery, Saarland University, Saarbrücken – Germany. March 1st – 10th, 2006.
	A, P	10th Perspectives in Percutaneous Penetration Conference, La Grande Motte – France, April 18th – 22nd, 2006
	A, P	33rd Annual Meeting and Exposition of the Controlled Release Society, Vienna – Austria, July 22nd -26th, 2006

Keys: A = Attendance; S = Speaker; P = Poster presentation

LIST OF PUBLICATIONS

Publications in peer-reviewed journals

1. ***Influence of nanoencapsulation on human skin transport of flufenamic acid,*** **J. Luengo**, B. Weiss, M. Schneider, A. Ehlers, F. Stracke, K. König, K-H. Kostka, C-M. Lehr, U.F. Schaefer, Skin Pharmacology and Physiology, 19 (4):190 - 197, 2006

2. ***Nanoparticles – an efficient carrier for drug delivery into the hair follicles***, J. Lademann, H. Richter, A. Teichmann, N. Ottberg, U. Blume-Peytavi, **J. Luengo**, B. Weiss, U.F. Schaefer, C-M. Lehr, R. Wepf, W. Sterry, European Journal of Pharmaceutics and Biopharmaceutics, 66 (2): 159 – 164, 2007

3. ***Human skin permeation enhancement using PLGA nanoparticles is mediated by local pH changes***, **J. Luengo**, M. Schneider, K-H Kostka, A. Schneider, C-M Lehr, UF Schaefer, Journal of Controlled Release, submitted

Book Chapter

Models for skin absorption and skin toxicity testing, U.F. Schaefer, S. Hansen, M.Schneider, **J. Luengo** C-M. Lehr, in C. Ehrhard and K.J. Kim (Eds.), *Preclinical Biopharmaceutics - in situ, in vitro, and in silico tools for drug absorption studies,* Springer (submitted)

Conference presentations

❖ "*Influence of PLGA-nanoparticles on human skin penetration and permeation of flufenamic acid in vitro*" (<u>**J. Luengo**</u>, B. Weiss, C-M. Lehr, U. Schaefer), 2004 AAPS Annual Meeting and Exposition, Baltimore – Maryland, U.S.A., November 10, 2004.

❖ "*Effect on the human penetration of a highly lipophilic drug incorporated into PLGA nanoparticles*" (<u>**J. Luengo**</u>, B. Weiss, M. Schneider, A. Ehlers, F. Stracke, K-H. Kostka, C-M. Lehr, U.F. Schäfer), European IP – Galenos Course, Lisbon – Portugal, September 5th -14th, 2005.

❖ "*Interaction of human skin with biodegradable fluorescent nanoparticles*", (<u>M. Schneider</u>, **J. Luengo**, B. Weiss, F. Stracke, C-M. Lehr, U.F. Schäfer), AAPS Annual Meeting and Exposition, Nashville, TN – U.S.A., November 6th – 10th, 2005

❖ "*Transport of flufenamic acid incorporated into PLGA nanoparticles through human skin using infinite and finite dose regime*" (<u>**J. Luengo**</u>, K-H. Kostka, C-M. Lehr, U.F. Schäfer). 6th Int. Conference and Workshop on Cell Culture and In-Vitro Models for Drug Absorption and Delivery, Saarbrücken – Germany. March 1st – 10th, 2006

❖ "*Skin transport of flufenamic acid incorporated into PLGA nanoparticles. Infinite and finite dose effect*" (<u>**J. Luengo**</u>, K-H. Kostka, C-M. Lehr, U.F. Schaefer), 10th Perspectives in Percutaneous Penetration Conference, *La Grande Motte – France, April 18th – 22nd, 2006*

❖ "*Investigation of dermal diffusion processes in the presence of nanoparticles with multiphoton microscopy*" (M. Schneider, F. Stracke, K. König, **J.Luengo**, C-M. Lehr, U.F. Schaefer) 10th Perspectives in Percutaneous Penetration Conference, La Grande Motte – France, April 18th – 22nd, 2006.

❖ "*Improvement of skin permeation of flufenamic acid by PLGA nanoparticles across heat separated and reconstituted epidermis in vitro*" (**J. Luengo**, K-H. Kostka, C-M. Lehr, U.F. Schaefer), 33rd Annual Meeting and Exposition of the Controlled Release Society, Vienna – Austria, July 22nd -26th, 2006

❖ *"Non-invasive Investigation of the Fate of Nanoparticles and their Payload Diffusing into Human Skin"*, (M. Schneider , B. Weiss, **J. Luengo**, K. König, C-M. Lehr, U.F. Schaefer, F. Stracke), 33rd Annual Meeting and Exposition of the Controlled Release Society, Vienna – Austria, July 22nd -26th, 2006

ACKNOWLEDGMENTS

In the development of this research project…

I want to thank **Prof. Dr. Claus-Michael Lehr** by the invaluable opportunity to belong to the institute graduate staff that enriched my scientific career, as well as, my personal life, giving me the chance to know new scientists, new cultures and new friends.

Specially thank **Dr. Ulrich Schäfer** by his exigent supervision and direction of the scientific work. To him and Mony, thanks by your friendly care and words.

In the imaging: thanks to **Dr. Marc Schneider** for the collaboration on the CLSM and **Mrs. Noha Nafee** on the AFM.

Thanks to **Dr. Karl-Heinz Kostka** (Karitaskrankenhaus, Lebach) for the human skin provision, vital on the experimental performance of this thesis.

To **Mr. Norbert Ochs** (Department of Physical Chemistry) by the Teflon application devices manufacture required during the *in vivo* microdialysis experiments.

Prof. **Dr. Carlos von Plessing** and **Prof. Dr. Jacqueline Sepúlveda**, members respectively of the Departamento de Farmacia and Departamento de Farmacología, Universidad de Concepción, by their collaboration in the *in vivo* experimental setup, as well as, by their friendship and guide in different aspects of my life.

Dr. Rodrigo Klaassen and **Dr. Francisco Mucientes**, members of the Departamento de Patología of Universidad de Concepción, by their histological analysis of skin samples obtained during the microdialysis experiments.

Acknowledge, **Universidad de Concepción** and **Proyecto MECESUP UCO 0202 (Ministerio de Educación, Gobierno de Chile)**, by their financial support.

In the personal aspects of my life...

I want to thank the friendly and warm reception of all the secretaries: **Edel, Gisela and Isabelle**, in chronological order. Especially I want to thank Edel, for her friendship

and guide since the first day in Germany. In the same way a special thank to **Karin**, for her infinite patience with my "I have a question…" (When really where 1000 of questions) and the help with the infinity of papers from here and there (most of them in German) which, until the end, I never understood.

To my room-mates: **Samah** and **Noha**… thanks for let me know your culture and lifestyle… your presence opened a door to a world I would have never known in my own country… thanks for your warm friendship and opinions exchange.

To **Ruy**, thanks for the unforgettable trips and photographs shared, and because you gave me the starting point speaking German.

To my spanish-speaking friends: por todos los momentos compartidos, por apoyarme en los momentos de tristeza, por compartir mis alegrías y sobre todo por el relajo de poder hablar en español. A **Mayra**, **María**, **Natalia**, **Alba**, **Ana** y a todas aquellas que integraron la bien llamada **"terapia española"**. Muchas Gracias!. En forma muy especial, agradecer a **Paula y Frank**, quienes me apoyaron y estuvieron presentes en la mayor parte de este arduo camino, no saben cuan valioso es tener amigos como ustedes, cuando hizo falta el amor de la familia y de los amigos que estaban lejos, cuando necesité traducciones varias, cuando había que discutir algo científico, o simplemente para vitrinear, tomarse un café o salir a conocer algún lugar, siempre estuvieron conmigo, por eso: Gracias de todo corazón!.

Thanks to my friends from the church. Especially to **Ute**: Thanks a lot! You have been like my mother in Germany; to **"Radkito" and wife** for your friendship; to **Edilson** for the unforgettable trips, photos and anecdotes shared; to **Gaby and her mother** for the always-smiling greeting; to **Sonja and Mathias** for the Saturday-afternoons together.

I know I cannot mention all people I have known and all people that have been important during this time studying Germany, but to all of them:

Thanks!

CURRICULUM VITAE

PERSONAL INFORMATION

Name	:	Javiana Elizabeth Luengo Contreras
Nationality	:	Chilean
Marital Status	:	Single, no children
Date of birth	:	09 – 03 – 1976
Place of Birth	:	Concepción, Chile

WORK EXPERIENCE

Since April 2000	:	Junior lecturer.
Employer	:	Universidad de Concepción Barrio Universitario s/n, Concepción, Chile.
Main activities and responsibilities	:	Theoretical and practical teaching on the fields of: Pharmaceutical Technology, Biopharmaceutics, Pharmacokinetics and Cosmetics.

EDUCATION AND TRAINING

Dates: March 1993 – March 2000

Name and type of organization providing education and training:

Facultad de Farmacia, Universidad de Concepción, Concepción, Chile

Principal subjects / occupational skills covered:

♦ **Research project entitled:** "Obtención de un preparado farmacéutico de aciclovir complejado con ciclodextrina: estudio preliminar" (Obtention of a pharmaceutical formulation of acyclovir complexed with cyclodextrin: preliminary study)

♦ **Project involved:**

o Development and characterisation an acyclovir - β-cyclodextrin complex.

o Manufacture and control of microdialysis concentric probes.

o Comparative pharmacokinetic study of acyclovir as: free drug, complexed with β-cyclodextrin and a mixture of them, using endovenous microdialysis in laboratory animals.

Title of qualification awarded:

Bachelor in Sciences (Field: Pharmaceutics)
Pharmacist

Grade: 83,2 / 100 (Approved with distinction)

Dates : May 2003 – (Spring 2007, expected)

Name and type of organization providing education and training:

Department of Biopharmaceutics and Pharmaceutical Technology, Saarland University, Saarbrücken, Germany

Principal subjects / occupational skills covered:

- ♦ **Research project entitled:** Human skin drug delivery using biodegradable PLGA-nanoparticles
- ♦ **Project involved:**
  - o Development of analytical techniques for drug determination in biological matrices.
  - o Skin and derivatives preparation techniques.
  - o Skin permeation and penetration determination methods.
  - o Biodegradable nanoparticles preparation using solvent evaporation methods.
  - o Nanoparticles characterisation using photon correlation spectroscopy.
  - o Differential scanning calorimetry measurements.
  - o *In vivo* dermal bioavailability using microdialysis in laboratory animals.

Title of qualification awarded: Doktor rerum naturalium (Dr. rer. nat.) equivalent to Ph.D.

Finnancial support: Personal fellowship granted by Universidad de Concepción – Chile and Proyecto MECESUP UCO 0202 – Ministerio de Educación – Gobierno de Chile.

PERSONAL SKILLS AND COMPETENCES

Mother tongue	Spanish	
Other languages	**English**	**German**
❖ Reading skills	Fluent	Basic
❖ Writing skills	Fluent	Basic
❖ Verbal skills	Fluent	Basic

TECHNICAL SKILLS AND COMPETENCES

Software skills

Microsoft Office: Word, Excel, Powerpoint, Frontpage; Corel Graphics, EndNote, SigmaPlot, SigmaStat, Adobe Acrobat, for projects, reports, graphs and presentations.

Chromeleon and LaChrom D-7000, for HPLC management

Scientific skills

High performance liquid chromatography (HPLC)

Differencial scanning calorimetry (DSC)

UV/Vis Spectrophotometry

Franz diffusion cells and Saarbrücken model for diffusion, skin permeation and penetration experiments

Microdialysis.